General Disclaimer

One or more of the Following Statements may affect this Document

- This document has been reproduced from the best copy furnished by the organizational source. It is being released in the interest of making available as much information as possible.

- This document may contain data, which exceeds the sheet parameters. It was furnished in this condition by the organizational source and is the best copy available.

- This document may contain tone-on-tone or color graphs, charts and/or pictures, which have been reproduced in black and white.

- This document is paginated as submitted by the original source.

- Portions of this document are not fully legible due to the historical nature of some of the material. However, it is the best reproduction available from the original submission.

Final Report

EFFECT OF ENVIRONMENT ON THERMAL CONTROL COATINGS

Prepared for:

CALIFORNIA INSTITUTE OF TECHNOLOGY
JET PROPULSION LABORATORY
4800 OAK GROVE DRIVE
PASADENA, CALIFORNIA 91103

JPL CONTRACT 951522
Subcontract under NASA Contract NAS7-100
Task Order RD-29

SRI
STANFORD RESEARCH INSTITUTE
Menlo Park, California 94025 · U.S.A.

STANFORD RESEARCH INSTITUTE
Menlo Park, California 94025 · U S A

Final Report *October 15, 1969*

EFFECT OF ENVIRONMENT ON THERMAL CONTROL COATINGS

By: S. R. MORRISON
K. M. SANCIER

Prepared for:

CALIFORNIA INSTITUTE OF TECHNOLOGY
JET PROPULSION LABORATORY
4800 OAK GROVE DRIVE
PASADENA, CALIFORNIA 91103

JPL CONTRACT 951522
Subcontract under NASA Contract NAS7-100
Task Order RD-29

SRI Project PAD-6146

This work was performed for the Jet Propulsion Laboratory, California Institute of Technology, sponsored by the National Aeronautics and Space Administration under Contract NAS7-100.

Copy No. 19

TABLE OF CONTENTS

LIST OF PUBLICATIONS BASED ON RESEARCH UNDER THIS CONTRACT

1. "Mechanism of Cathodic Processes on the Semiconductor Zinc Oxide," T. Freund and S. Roy Morrison, Surface Science 9, 119 (1968).

2. "Electron Capture by Ions at the ZnO/Solution Interface," S. Roy Morrison, Surface Science 15, 363 (1969).

3. "Electron Injection into Zinc Oxide," Thomas Freund, J. Phys. Chem. 73, 468 (1969).

4. "Iron Cyanide as a Surface State to Prevent ZnO Photolysis in Vacuum," S. Roy Morrison, J. Vacuum Science and Tech. (in press, to appear about Jan. 1970).

5. "Ionization Energy of Donors in ZnO Powder, Determined by Extended ESR Measurements," K. M. Sancier (to be submitted to J. Phys. Chem.).

6. "Surface Recombination Centers as Protection against Vacuum Photolysis of Thermal Control Coatings," S. Roy Morrison and K. M. Sancier (to be submitted to Progress in Astronautics and Aeronautics).

7. "ESR Measurements of Vacuum Photolysis of ZnO Powders," K. M. Sancier (to be submitted to Surface Science).

SUMMARY OF RESEARCH PROGRAM

Degradation of thermal control coatings under combined conditions of ultraviolet radiation and vacuum is initiated by the photoproduced holes and electrons, either of which can undergo chemical reaction. Such chemical reactions change the structure of the coating, leading eventually to coloration. The approach we have used to prevent optical degradation is to find surface additives that act as recombination centers, alternately capturing the holes and electrons and thus removing the photoproduced carriers with no net chemical change. The approach has been very encouraging in the research phase. For example, single crystal measurements show improvement up to a factor of 10^6 in rate of conductivity degradation, and powder measurements show photodamage protection from 10^{-2} monolayers of additive.

A summary of the overall program is presented in this portion of the report. The details of the research program are presented in later sections in the format of technical articles which, for the most part, have been published or will soon be submitted for publication.

1. Electron and Hole Capture Cross Section

The fundamental portion of the investigation was the development of background knowledge for prediction of those chemical species which in the reduced form should capture holes and in the oxidized form should capture electrons. These studies have been brought to a satisfactory completion by use of the aqueous electrochemical technique. With the ZnO as an electrode, the cathodic current is directly proportional to the electron capture cross section of surface species. Various species were tested in the form of ions in the electrolyte. It was found that there was a maximum in electron capture cross section for species with a surface state energy just below the bottom of the conduction band. The capture of holes by reducing agents (again introduced as ions in solution) was tested by a phenomenon we have termed "current doubling", observed in the following manner. With an indifferent electrolyte, the anodic current is solely due to photoproduced holes which reach the surface.

However, with many two-equivalent species, the anodic current almost doubles because the unstable intermediate injects electrons into the conduction band. That is, captured holes will oxidize the ion in a one-equivalent process, but with a two-equivalent ion a highly unstable intermediate is formed. It decomposes spontaneously, injecting an electron to provide the second equivalent of oxidation. Thus for each hole reaching the surface, an electron is injected, and the current doubles. The phenomenon of current doubling can be used not only to determine when a species is oxidized in a two-equivalent process, but also to compare the hole capture cross section of one-equivalent and two-equivalent reducing agents. The method of comparison consisted of a titration in which the hole capture cross section of a series of one-equivalent reducing agents was compared, and it was concluded that for maximum hole capture cross section, the energy level of the surface state should be near the bottom of the conduction band.

Consideration of the phenomenon of current doubling leads to the conclusion that one-equivalent species are required for electron-hole recombination centers, because a two-equivalent species cannot have a high electron capture cross section and will almost always lead to an irreversible chemical change. Furthermore, a candidate for a recombination center should have an energy level a few tenths of an electron volt below the conduction band edge.

In our studies of ZnO, several additive species potentially suitable as recombination centers were identified (all one-equivalent species with redox potentials, and hence surface energy levels, in a certain range). However, of the species actually tested, the redox couple ferro/ferricyanide stood out as having optimum properties with respect to stability, ease of handling, and high capture cross sections.

The detailed report on electron capture cross section appears in Section A, and that on hole capture cross section in Section B.

2. Tests of the Additive Iron Cyanide as a Surface State to Prevent Degradation of ZnO

Tests of the effectiveness of the additive couple ferro/ferricyanide have been made on ZnO using two accelerated test procedures.

In one test procedure vacuum photolysis of ZnO is monitored by measurement of the increase in dark conductance of ZnO crystals. This measurement permitted quantitative analysis of the action of the additive, and it was found that the rate of photolysis was decreased by as much as 5 orders of magnitude with a monolayer of a 1:1 mixture of ferro/ferricyanide additive on the surface. The results indicated that the initial behavior is complicated by the presence of adsorbed oxygen. This oxygen is apparently photodesorbed during the first hours of illumination in vacuum, and afterwards quantitative interprecation of the photoeffects due to the additive becomes possible. The analysis at this stage indicates that the iron cyanide behaves as a simple recombination center, as desired. From both experimental observations and theory it is clear that a mixture of both oxidation states must be present, and that the degradation rate varies inversely as the square of the total additive concentration.

According to the second test procedure, vacuum photolysis is monitored by electron spin resonance (ESR) of a signal at g = 1.96 associated indirectly with donors in ZnO. The ESR technique was chosen because it is applicable to powdered ZnO. It was shown for the test conditions that if the ferro/ferricyanide concentration exceeded about 10^{-2} monolayers, no change in the ESR spectra occurred upon uv illumination in vacuum. An attempt was made to determine the optimum ferro/ferricyanide ratio, but there is enough uncertainty in the data that further studies seem to be warranted. The results of the ESR study on powders is at least in qualitative agreement with those on single crystals. Preliminary measurements using an electron beam for irradiation indicate that iron cyanide may protect ZnO against particulate as well as uv damage. The ESR study also provided some detailed information about the probable nature of the photodamage centers. For example, uv irradiation produces two resonance centers, which exhibit behavior to oxygen suggest-

ing they may be associated with the optical damage centers giving rise to visible and infrared absorption. Also, from a temperature study we tentatively conclude that some of the paramagnetic centers produced by photodamage are in the conduction band and some may be associated with excess zinc arising from ZnO photolysis. Finally, the ESR measurements show that when dislocations are introduced in ZnO the characteristic resonances show greater susceptibility to photoirradiation. Further work is needed to determine the correlation between the ESR resonance centers and the optical centers, and to determine whether surface additives will decrease the photodamage susceptibility of pigments with dislocations.

The detailed report on photodamage measured by electrical conductance appears in Section C and that on photodamage measured by ESR in Section D. The report on the ionization energy of donors in ZnO appears in Section E.

3. Studies of Materials other than ZnO

Materials other than ZnO were examined, in particular ZrO_2 and La_2O_3, with unsatisfactory results. With the electrochemical technique our fundamental studies indicated that it was necessary to determine only one parameter for each pigment, in order to suggest a redox couple suitable as a recombination center. This one parameter is the effective redox potential (energy level) of the conduction band edge of the semiconductor pigment. We attempted to measure this parameter by a study of electron injection from strong one-equivalent reducing agents into the conduction band. By noting the redox couple (potential) where electron injection was no longer possible, we determined the parameter of interest. Such a measurement was entirely successful in ZnO studies. Unfortunately, the results obtained with a series of species on ZrO_2 could not be interpreted; injection apparently depends on parameters we did not have under control. Thus it was concluded that another technique must be used to determine the effective redox potential of the conduction band for ZrO_2.

Studies of ZrO_2 and La_2O_3 by the ESR technique were only prelimi-

nary. The ESR spectrum was slightly sensitive to illumination of ZrO_2, but the weak photoproduced resonance may as well have been due to an impurity as to photolysis of ZrO_2. The detailed report on studies of pigments other than ZnO appears in Section F.

DISCUSSION AND RECOMMENDED FUTURE WORK

1. General Applicability of the Recombination Center Concept

From the research performed under this contract it is concluded that suitable surface additives, acting as electron-hole recombination centers, can prevent degradation of thermal control coatings by preventing irreversible chemical reactions at the surface of the pigment grains. Present theories indicate the surface additive will be effective if it has the following properties: (a) it must be nonvolatile and chemically inert toward its environment and toward photolysis, (b) it must exist in two stable oxidation states separated by one electron, (c) the energy level occupied by this electron should be just below the bottom of the conduction band of the pigment (in order that both the hole and electron capture cross sections be high), (d) the additive must be present in both oxidation states, and (e) it must uniformly cover the surface of each grain of pigment material.

There is no indication that the effectiveness of the surface additive approach should be limited to ZnO, or even to similar materials. If both hole and electron come to the surface, as in ZnO, the additive should act as a recombination center. If excitons are produced by the light and come to the surface, the action should be the same. If only one carrier reaches the surface, it should be captured in a stable energy level, and an electrostatic potential will build up to stop further flow of this carrier. In cases where the hole or electron tends to react with the paint vehicle, rather than to decompose the pigment, the recombination center approach should also be effective in protecting the vehicle.

Although surface recombination centers are most effective for preventing surface reactions, such centers may also be effective in re-

ducing coloration from reactions arising totally in the bulk, for example, color centers arising from movement of surface-produced electrons or holes to deep bulk-trapping centers (such as F-centers or dislocations). If a very effective recombination center is provided at the surface, the probability of activating bulk color centers will be reduced because the density of mobile carriers in the bulk will be reduced.

In summary, from a theoretical viewpoint the surface additive approach appears sound, and from an experimental viewpoint, the present research has shown that many of the theoretical expectations are met. In fact, for ZnO it is clear that the additive tested, iron cyanide, prevents photolysis of the ZnO at very low surface concentrations. The measurements are consistent with a model that should be common to many pigments, and there is as yet no indication of restrictions.

2. Future Development Required to Exploit the Recombination Center Concept

Future work to exploit this development in coating technology will have to include many aspects.

(a) With ZnO as the pigment, the couple ferro/ferricyanide seems satisfactory, but other additives may be superior. If extensive use of ZnO is anticipated, examination of improved additives should perhaps be considered.

(b) Additive deposition techniques should be investigated further. Theory tells us that approximately each Debye area (about $10^{-10}cm^2$) will act independently. Thus the additive must be deposited very uniformly to ensure that the area is effectively covered. If improvement of photostability (lowering of degradation rate) by a factor of 100 is required, then at most 1% of the Debye areas can be left insufficiently unprotected. This puts a severe requirement on the technique of additive deposition if we wish to minimize the gross amount of additive used. Further complications with the additive couple can occur if the couple is highly soluble in some solvents, which may leach the additive off the surface.

(c) The stability of typical additive candidates in various chemical environments should be explored. The action of oxygen on ferrocyanide, for example, has been shown (Section C) to be very different when the ferrocyanide is deposited on the ZnO surface than when it is a free species. Information regarding such stability is necessary both to specify the permissible environments and pretreatments for coatings with additives, and to aid in the determination of additives that will be chemically inert in ordinary atmospheric conditions (oxygen, water vapor) particularly before exposure to the vacuum photolysis of outer space.

(d) The application of the recombination center concept to pigments other than ZnO should be pursued. Our attempts to apply the electrochemical technique to ZrO_2 and La_2O_3 were unsuccessful, not because the concept was incorrect, but because this technique to measure the conduction band edge was not fruitful. Two other methods are under present study: one is an electrostatic technique developed for ARO-Durham to measure surface energy levels (relative to the conduction band); the other is a powder conductance measurement presently being developed on SRI funds. From such measurements potentially suitable additives can be suggested; the testing of such additives to determine if they actually follow the theory would be the next step.

(e) The mechanisms of photodegradation may warrant further examination not only to provide support for the present approach to photo protection, but also to provide basic information for developing other approaches. Several clues arose during the present study that may indicate fruitful directions of research.

For example, the ESR of ZnO powder revealed two damage centers, which appear to be related to the two optical damage centers, in the visible and infrared. This correlation should be further explored in order to better understand the mechanism of the photodamage; furthermore, the ESR technique appears to be much more sensitive than that of spectral reflectance for measuring photodamage. Also the role of dislocations in photodamage, as examined briefly in our ESR studies, should be investigated further, and the ability of surface additives to control damage of

unstable pigments containing dislocations should be determined.

(f) Although not considered in this study, the problem of developing a compatible vehicle is related to the uniformity of the additive deposition. The additive must not only be inert with respect to the vehicle; it should probably be negligibly soluble in the vehicle. On the other hand, restrictions with respect to photolysis reactions between pigment and vehicle may be relaxed in the presence of the additive. The ESR technique is well suited for examination of pigment-vehicle combinations.

Although this research program has been valuable in suggesting a new concept in coating stabilization, there are still many important phases to be examined before the concept is understood in detail and exploited for its potential advantages in coating technology. It is our hope that the approach will prove to be of practical utility to prevent photolysis of coatings both in vacuum and in air. Thus we feel that a development program as described above would be well worth the investment.

SECTION A

ELECTRON CAPTURE BY IONS AT THE ZnO/SOLUTION INTERFACE*‡

S. ROY MORRISON
Solid-State Catalysis Laboratory
Stanford Research Institute
333 Ravenswood Avenue, Menlo Park, California 94025

ABSTRACT

The electron reactivity (electron capture rate) of one-equivalent oxidizing agents at the ZnO surface is determined by cathodic electrochemical reduction. Because in this system the Helmholtz potential is insensitive to the oxidizing agent used, the energy level of a particular species with respect to the ZnO conduction band is not considered a variable. Thus the electron capture by (reduction of) the species can be interpreted according to surface state capture theory. The energy levels are estimated by analysis of the redox potential of the species. A maximum in electron reactivity is found for energy levels just below the conduction band minimum, the reactivity decreasing rapidly for higher energy levels. There is some indication that the electron reactivity decreases for very low energy levels, in accordance with expectations if the process is controlled by a multi-phonon electron capture model.

*This research was supported by the Jet Propulsion Laboratory California Institute of Technology, sponsored by National Aeronautics and Space Administration under Contract NAS 7-100.

‡Published in Surface Science 15,363-379 (1969).

1. Introduction

In a recent publication[1]), the techniques and theory for cathodic reduction of ferricyanide ions at the surface of a single-crystal ZnO electrode have been presented. The present paper reports similar results on several other one-equivalent oxidizing agents, and attempts to correlate the electron reactivity of these species with their energy level in solution. The energy level is estimated from the redox potential of the ions in solution. Beck and Gerischer[2]) suggested the redox potential and the energy level should be related; it will be shown below that a quantitative relationship exists for one-equivalent redox systems.

The theory of electron capture by energy levels in a semiconductor has been thoroughly analyzed in the past years [3,4]). It has been shown that for simple phonon-aided processes, the electron capture cross section rapidly decreases the deeper the levels are below the conduction band, because more and more phonons are required to dissipate the energy. High electron capture cross sections for very deep energy levels are observed at times and interpreted[4]) in terms of a model involving capture of electrons in excited states with subsequent cascading of the electron to the deep ground state energy.

The theory of electron capture from a metal electrode by ions in solution, on the other hand, has been formalized quite differently. It is clear that in this case the energy levels of the active species will tend to move often toward the Fermi level in the solid, during the formation of the Helmholtz double layer[5]). This will also be expected with semiconductor electrodes if electron exchange associated with the active redox reaction determines the Helmholtz potential[5]).

In fact, because of the dominance of Helmholtz potential effects, and of the effects associated with chemical changes between filled and empty levels (reducing and oxidizing agents) the formulation of electrochemical theory in terms of energy levels has been inappropriate.

With the ZnO electrode, however, there is evidence[1]) that Helmholtz

double layer effects are not dominating, and for most species of interest the Helmholtz potential is not affected by the presence or absence of these species. It has also been shown[1,6] that for many common species, electron exchange is irreversible; that although the oxidizing agent of a redox couple can be reduced, electrons cannot be injected into the ZnO conduction band by the reducing agents. The latter effect can be interpreted as an indication that the filled energy level is far below the conduction band, and the former effect indicates why: the ZnO is not acting as a reversible electrode controlled by the redox couple.

If the Helmholtz potential of the ZnO does not change as the oxidizing agent is changed, then the energy of the conduction band edge in the ZnO with respect to the solution potential will be invariant, independant of the energy level of the oxidizing agent used. For example, if the energy of the conduction band edge is at -0.3 eV with respect to some arbitrary zero of energy, it will remain at -0.3 eV independant of the oxidizing agent used. Then if the oxidizing agent has an energy level at -0.1 eV, it will be above the conduction band edge by 0.2 eV, if it has an energy level at -0.5 eV, it will be below the conduction band edge by 0.2 eV.

Because of this behavior of the ZnO electrode, it would appear that the electron capture cross section of ions in solution may well be controlled by their energy level in a manner similar to electron capture by energy levels in the solid. It becomes possible to analyse in these terms the electron capture cross section of various species in solution, a possibility not realizable on a metal electrode because the Helmholtz double layer compensates for differences in energy level. The experimental test of such a model using a series of one-equivalent oxidizing agents is the purpose of this paper.

2. Method

To compare the capture cross section of various species with their calculated energy level, two requirements must be met. First, it must

be shown that the Helmholtz voltage on the ZnO does not change when the species of interest is added to the solution. Denoting the energy of the edge of the conduction band by E_c and the energy level of the oxidizing agent in solution by E_x, we have

$$\Delta E = E_c - E_x + eV_H + e\Delta V_H\,(X) \qquad (1)$$

where ΔE is the energy released by the electron transition, V_H is the Helmholtz potential with no active oxidizing agents in solution, and $\Delta V_H(X)$ the change in Helmholtz voltage when X is added. As it is the objective to show that σ, the capture cross section, varies with ΔE in a manner consistent with solid-state theory, it is clear that $\Delta V_H(X)$ should be zero for all species X, in order to yield a simple interpretation.

Second it must be shown that the electron capture process can be described by the formulations of surface-state capture used in solid-state physics. This permits identification of the quantity σ, the capture cross section.

The methods used in this work have been described in an earlier communication[1]). To emphasize how the two requirements discussed above are met, a brief summary will be presented here.

Measurement is made of the voltage V of the ZnO vs. a saturated calomel reference electrode, of the cathodic current, and of the differential capacity between the ZnO and a Pt working electrode. It has been shown[7]) that with a ZnO electrode the capacity measured is the capacity of the depletion layer at the ZnO surface. With V_s the surface barrier, C the capacity, A the area of ZnO exposed to the solution, N_D the donor density, we have from the Schottky relation and the parallel plate capacity formula:

$$V_s - kT/q = \tfrac{1}{2}\, q\, N_D\, A^2\, \epsilon\epsilon_0\, (1/C^2) \qquad (2)$$

where the other symbols have their usual meaning.

The ZnO voltage is determined by V_s, the Helmholtz voltage, and other double-layer potentials in the circuit, the latter considered constant.

$$V = V_s + V_H + \Delta V_H(X) + \text{constant} \qquad (3)$$

If $d(1/C^2)/dV$ is constant, it is concluded that V_H and $\Delta V_H(X)$ are independant of V. Then we can simplify (2) and (3)

$$V - V_f(X) = \tfrac{1}{2}\, q\, N_D\, A^2\, \epsilon\epsilon_o\, (1/C^2) \qquad (4)$$

where V_f is the "flat band potential," the potential when $1/C^2$ is extrapolated to zero. If V_f is independant of the presence or concentration of the species X, the first requirement given above is met.

In order to conclude that the electron capture process can be described by the formulations of surface-state capture, it must be shown that the capture rate (= cathodic current J) must be first order in the electron density at the surface (n_s) and first order in the density of available levels ([X]).

The electron density at the surface is calculated from the density in the bulk [N_D, calculated from the slope of Eq. (4)], multiplied by the Boltzmann factor associated with the surface barrier:

$$n_s = N_D \exp\,(-eV_s/kT) \qquad (5)$$

where V_s is determined from (2).

If the current (at constant n_s) is found proportional to the concentration of X in solution, the assumption is made that the capture rate is proportional to [X]. This implies that the concentration (cm^{-2}) of available levels is proportional to the concentration (per cm^3) of ions in solution. It has been found that the criterion can usually be met at sufficiently low concentration.

When the requirements are found to be met, as was found for all of the results reported below, the results can be interpreted according to the normal theories of irreversible electron capture by surface states

$$J = q\,\sigma\,[X]\cdot\bar{c}\,n_s = q\,\sigma\,[X]\,\bar{c}\,N_D \exp(-eV_s/kT) \qquad (6)$$

with σ the capture cross section and $\bar{c}$ the mean electron velocity. In Eq. (6), J is measured, $\bar{c}$ is estimated (we use 10^7 cm/sec), and n_s is calculated from the capacity.

From Eq. (6), a value is calculated for $\sigma[X]$, the "electron reactivity" of the species X. In the measurements below, the values are normalized to $[X] = 10^{-2}M$, and the data for $\sigma[X]$ recorded for this molarity. The parameter of interest is σ, the capture cross section of the various ions, but this is not experimentally separated from [X] (the active surface concentration of the oxidizing agent when the solution concentration is $10^{-2}M$). In order then to compare σ for various species, the assumption must be made that the change in $\sigma[X]$ from species to species occurs primarily as a result of the change in σ. This assumption will be considered further under "Discussion."

The crystals, their etching, mounting, and the electrochemical cell used have been described in the earlier communication.[1])

The oxidizing agents studied were chosen so that reasonably well-defined one-equivalent reductions were possible. The list included $K_3Fe(CN)_6$, $(NH_4)_2IrCl_6$, $KMnO_4$, 1,10 Phenanthroline ferric perchlorate, $CuCl_2$, $Ce(HSO_4)_4$, $Ce(NH_4)_2(NO_3)_6$, VCl_3, and $Ag(NH_3)_2^+$ from $AgNO_3$ in ammonia. For the various pH values studied the buffers were phthalate (pH3.7), acetate (pH4.5 to 5.5), borate (pH8.7), ammonia (pH12), and H_2SO_4 or HNO_3 used to reach pH 1.5.

The iron phenanthroline solution was prepared by oxidation of the ferrous form, using PbO_2 in sulphuric acid and filtering. The other salts were dissolved from stock reagents.

3. Results

Typical results plotted according to Eq. (6) are shown for various species in fig. 1. The logarithm of current per unit area exposed is plotted against the surface barrier V_s as determined from capacity. For each curve the surface barrier shown is equal to the applied voltage plus the constant V_f, determined from a plot of $1/C^2$ vs. V [Eq. (4)]. This constant V_f varies considerably with pH, to a less extent with variations of donor density[6]) and slightly from unknown sources[1]). The results shown are those corresponding to 0.01M solutions where measurements were made at this concentration.

In all of the cases recorded in fig. 1 the current readings were observed with substantially positive V_s (bands bending up). With other measurements such as the measurements with Cu^{++} ions, or with no active ion in solution, high cathodic potentials such that $V_s \rightarrow 0$ were required in order to obtain measureable currents. In this region, where $V_s \rightarrow 0$, the value of V_s is not known; below about $V_s = 0.03$, $1/C^2$ is no longer linear in V, and estimation of the surface barrier is not reliable[7]). However, a maximum $\sigma[X]$ can be estimated.

In Table I below, results are tabulated for the various ions tested. The ion concentration tested and pH are listed, together with the ZnO crystal face exposed and donor density calculated (from $1/C^2$ vs. V). The constant V_f, the "flat band potential," is recorded for each case. It is observed to be insensitive to the oxidizing agent used, although it varies considerably with pH.

From the curves of fig. 1, the values for N_D, and the molarity of the solution, the values of the "electron reactivity," $\sigma[X]$ normalized to 0.01M, can be calculated from Eq. (6) and are listed in Table I for the various species. As V_f, and hence V_s, cannot be considered accurate to better than ±0.03 volts, the value of $\sigma[X]$ must be considered to be at best accurate to within perhaps a factor of 5 either way, so even the one figure given is not to be considered significant. For a given

Table I

Parameters for calculation of electron reactivity of various oxidizing agents

Oxidizing agent	Concentration (molarity)	pH	face	V_f (volts vs. calomel)	N_D (cm^{-3})	σX (extrap. to 0.01M)
Ce^{+4} (in HNO_3)	10^{-3}, 10^{-4}	1.5	(0001)	+.04	10^{17}	$< 10^{-12}$
Ce^{+4} (in H_2SO_4)	10^{-3}, 10^{-4}	1.5	(0001)	+.04	6×10^{18}	6×10^{-9}
Fe^{+3} (phenanthroline)	10^{-3}, 10^{-4}	1.5	(0001)	+.02	10^{17}	1×10^{-5}
MnO_4^-	10^{-4}, 10^{-3}, 10^{-2}	4.5	$(000\bar{1})$	-.20	7×10^{18}	2×10^{-5}
	10^{-4}, 10^{-3}	8.7	$(000\bar{1})$	-.38	1×10^{18}	7×10^{-4}
$IrCl_b^=$	10^{-3}, 10^{-2}	3.8	$(000\bar{1})$	-.17	1×10^{18}	1×10^{-3}
	10^{-3}, 10^{-2}	3.8	(0001)	-.25	3×10^{16}	6×10^{-3}
Fe^{+3} (cyanide)	10^{-3}, 10^{-2}	8.7	(0001)	-.55	8×10^{18}	3×10^{-6}
	10^{-4}, 10^{-3}	12	$(000\bar{1})$	-.5	4×10^{18}	3×10^{-7}
	10^{-4}, 10^{-3}, 10^{-2}	9	$(000\bar{1})$	-.45	4×10^{18}	1×10^{-7}
	10^{-4}, 10^{-3}, 10^{-2}	3.8	$(000\bar{1})$	-.20	2×10^{18}	8×10^{-6}
I_3^-	10^{-4}, 10^{-3}, 10^{-2}	3.8	(0001)	-.27	7×10^{18}	2×10^{-10}
	10^{-3}, 10^{-2}	3.8	$(000\bar{1})$	-.25	1×10^{17}	6×10^{-10}
$Ag(NH_3)_2^+$	10^{-2}, 10^{-1}	12	$(000\bar{1})$	-.6	1×10^{17}	1×10^{-5}
Cu^{++}	5×10^{-2}, 10^{-2}	3.7	(0001)	-.25	10^{19}	$< 10^{-12}$
V^{+3} (in HCl)	0.5	(0.5MHCl)	(0001)	+.12	1×10^{17}	$< 10^{-12}$

oxidizing agent, the value of $\sigma[X]$ was independant of concentration for the concentrations studied to well within this error. Another source of error in the calculation of $\sigma[X]$ arises because the slope of the line is not the 60 mV/decade required by Eq. (3), although always in the range 65 ± 5 mV/decade. It has been found by experience that as we have refined our techniques and improved the curves toward a 60 mV/decade slope, the low currents are seldom affected greatly. The error is normally accentuated at higher current. Thus for our calculations of $\sigma[X]$ where the slope is greater than 60 mV/decade, we have used the low current measurements.

The results indicate that perhaps there is a slightly higher electron reactivity $\sigma[X]$ on the (0001) side than on the $(000\bar{1})$ side. The influence of pH shows no particular pattern, $\sigma[X]$ increasing with pH with MnO_4^-, decreasing or passing through a minimum with $Fe(CN)_6^{-3}$.

The values of $\sigma[X]$ were in general fairly reproducible. Of the materials listed, the only one in which there appeared serious problems was the silver ion. The problems were attributed to metallic deposits during the reduction process. The current became very high if a high intergrated current was permitted to pass. By keeping the current low, and the elapsed time during the measurement short, the results appeared reproducible.

A similar problem, but much less serious, was found with permanganate. The results became erratic and deposits were found on the crystal, if extremely high current ($> 10\ \mu\ a/cm^2$) was employed extensively. This was ascribed to reduction to MnO_2 and was avoided by using only low current values.

4. Discussion

4.1 Method of Energy Level Calculation

In order to relate the capture cross section of ions at the ZnO surface to their energy level in solution, it is necessary to estimate

the relative energy levels of the various species. We will analyse electron transfer between the redox couple X^{+}/X^{++} and an inert metal electrode and from this analysis obtain an expression for the energy level in terms of the redox potential of the species.

Both the experimental and theoretical phases of this work are limited to clearly one-equivalent species, as two-equivalent species need two energy levels to describe the equilibrium[8]), so cannot be calculated from a single parameter, the electrode potential.

The broadening of energy levels, discussed in detail by Gerischer[9]), will not be considered. Broadening due to variations in hydration will certainly occur but will be limited in general to the kT range, which is of little interest here. It is felt that more energetic chemical processes such as hydrolysis or complex formation will cause multiple energy levels in general, rather than broadening of a single energy level. This will complicate the observed behavior of the species, but does not change the arguments to be presented for the calculation of each of the several energy levels.

When an electron is transferred from an electrode to an ion in solution, several distinct steps occur. There is electronic motion--the transfer itself, and the movement of neighboring electrons in response to the new electrostatic conditions. There is ionic motion such as hydration, hydrolysis, dimerization, and desorption (if the species is adsorbed). After each of these processes, the energy level of the electron will be different. The first problem, therefore, is to identify which energy level is important in determining the capture cross section. It will be the assumption of the present analysis that the energy level we wish to calculate is the energy level of the electron after electron motion only. The subsequent changes in the energy level of the electron due to chemical reaction of the newly reduced species will not affect the capture cross section. The designation of such a level as an important intermediate is consistent, for example with the Franck-Condon principle, where ionic motion takes place after the electronic transition is completed[10,11]). Standard electrochemical models do not, unfortunately, separate the reaction

into chemical steps, involving ion motion, and electronic steps, which involve only electron motion. It is necessary then to reformulate the expressions of electrochemistry with these two types of reaction steps explicitly separated.

If the dominant form of the oxidized species is denoted as $R \cdot X^{++}$, and the dominant form of the reduced species as $R'' \cdot X^{+}$, we can write the equilibrium redox reaction in a form explicitly separating an intermediate $R' \cdot X^{++}$:

$$R \cdot X^{++} \overset{\Delta G^{++}}{\rightleftharpoons} R' \cdot X^{++} \pm P_1 \tag{7}$$

$$e + R' \cdot X^{++} \rightleftharpoons R' \cdot X^{+} \tag{8}$$

$$R' \cdot X^{+} \overset{\Delta G^{+}}{\rightleftharpoons} R'' \cdot X^{+} + P_2 \tag{9}$$

Here the R's are molecules or ions associated with the reactants at various stages of the reaction. They could be water of hydration, protons, etc. The intermediate shown, $R' \cdot X^{++}$ is specified as the form of the oxidized reactant which we postulate exhibits the highest electron capture rate under cathodic conditions and whose energy level we wish to calculate. The species P are those absorbed or released from the reactant during the chemical rearrangements (7) or (9). The quantities ΔG are the free energy absorbed in the forward direction of reactions (7) or (9). Eq. (8) is intended to represent the electronic transition only between the energy levels in the solid and the energy level in solution. At equilibrium the principle of detailed balance[12]) requires that the forward rate equal the reverse rate for each of Eqs. (7) through (9).

Now with an inert metal electrode, the only species which crosses the phase boundary between the electrode and the solution are electrons. Thermodynamics then requires that the electrochemical potential for electrons be constant across the interface at equilibrium. Thus:

$$E_F = \mu_e \tag{10}$$

where E_F is the Fermi level in the solid, and μ_e is the Fermi level or electrochemical potential of electrons in solution. However, relation (10) only begins to have significance if we can define μ_e in terms of the type and concentration of chemicals in solution.

Consider ions near the metal electrode but on the solution side of the Helmholtz double layer. These species can for our purposes be viewed as surface states if they are near enough to the metal electrode to permit electron transfer even when there is no specific adsorption. Thus they can be described by the Fermi distribution utilizing the Fermi level of the metal:

$$[R\cdot X^{++}]/[R\cdot X^{+}] = \exp\left\{-\left(E_F - E_X{}^{++}\right)/RT\right\} \qquad (11)$$

where $E_X{}^{++}$ is the surface state energy level of the redox couple and Eq. (11) the Fermi distribution, describes the ratio of the unoccupied energy levels $[R\cdot X^{++}]$ to the occupied $[R\cdot X^{+}]$.

Now, if we neglect the Gouy layer, the species obeying (11) are at equilibrium in all respects with ions in the bulk solution. There is at equilibrium no difference in ratio of $[R\cdot X^{++}]/[R\cdot X^{+}]$ between species which are, say, 5A from the electrode and those which are 5 mm from the electrode. Thus Eqs. (11 and (10), represent a meaningful definition of electrochemical potential for bound electrons in the solution. The definition is probably quite satisfactory as a first approximation, but the effect of differences in the Gouy layer is not clear.*

With this relationship Eqs. (7) through (9) can be analyzed to yield $E_X{}^{++}$, the energy level of interest. We will use the relations from thermodynamics governing equlibrium:

$$\Delta G^{++} = - kT\ln \frac{[R'\cdot X^{++}]\cdot[P_1]^{\pm 1}}{[R\cdot X^{++}]} \qquad (12)$$

*A simple mathematical analysis of the distribution of ions in the Gouy layer[13]) leads to consistency with (11) throughout the region, viz. E_F (or μ_e) as defined is constant, with the concentration changes and $E_X{}^{++}$ changes compensating through the region of varying potential.

$$\Delta G^{+} = - kT\ln \frac{[R'' X^{+}]\cdot[P_2]^{\pm 1}}{[R'\cdot X^{+}]} \qquad (13)$$

and combining (10) through (13) to eliminate the species involving R′, we have

$$E_{R'\cdot X^{++}} = \mu_e - \Delta G^{++} - \Delta G^{+} - kT\ln \frac{[R''\cdot X^{+}]\cdot[P_1]^{\pm 1}\cdot[P_2]^{\pm 1}}{[R\cdot X^{++}]} \qquad (14)$$

If added reactants $R\cdot X^{++}$ and $R''X^{+}$ are at unit activity, and if the species P are at unit activity, we find the simple relation

$$E_{R'X^{++}} = \mu_e - \Delta G^{++} - \Delta G^{+} \qquad (15)$$

In Eq. (14) we have not yet defined a zero of energy. In the following we will define the zero of energy as the Fermi level (the electrochemical potential for electrons) at the reversible hydrogen electrode. With this zero, the value of μ_e to be used in Eq. (14) is from (10) the reversible electrode potential for the couple X^{++}/X^{+} relative to the standard hydrogen electrode, and the energy levels are measured relative to the hydrogen electrode reference energy.

The most convenient approach is in the estimation of the energy level $E_{R'X^{++}}$ to use Eq. (15) with the standard oxidation/reduction potential, using the tables for acid or base depending on whether P_1 and P_2 are written in terms of protons or hydroxide ions.

4.2 Energy of Hydration

To illustrate the calculation of the ΔG's it is of interest to consider the problem of hydration energy, using a simple Born approach to hydration.

The mechanism of electron capture requiring the lowest energy transition state is pre-polarization of the dielectric [Eq. (7)] followed by electron capture on the pre-solvated species [Eq. (8)]. The pre-polarization

energy can be estimated on the basis of the following simple model. Consider the ion, of charge Ze, as a sphere of radius r imbedded in a dielectric medium of dielectric constant ϵ. Just outside this sphere, on the "surface" of the dielectric, resides a surface charge associated with the dielectric polarization. This surface charge[14]) is $-Ze(1 - 1/\epsilon)$. If we draw an imaginary "outer sphere" of radius a which includes this charge, it is clear that the energy to be calculated is the energy to place one positive charge on the surface of this "outer sphere," with the corresponding negative charge remaining on the surface of the grounded electrode. Thus the charge associated with the "outer sphere" changes from Ze/ϵ to $(Ze/\epsilon + e)$. We will assume the value of ϵ for water to be on the order of 80, so $Z/\epsilon \ll 1$. The energy to pre-polarize the medium becomes approximately the energy to charge a neutral sphere of radius a by one positive electronic charge:

$$\Delta G_0^{++} = e/8\pi\epsilon\epsilon_0 a \text{ e. v.} \qquad (16)$$

where the ΔG_0^{++} symbol is used because the course of the reaction is along the lines of Eqs. (7) and (8). This is on the order of 0.05 eV for a about 2Å.

4.3 Correlation of Energy Levels with Electron Reactivity

To test the general features of the overall model, the energy level associated with the various species must be evaluated, then the measured electron reactivity from Table I compared with the energy level. As discussed in Section 4.1, the identification of energy levels in solution is somewhat arbitrary, for there is a possibility of many forms of each species, and one must assume which form is the kinetically active species.

We will make several assumptions and approximations in order to arrive at an estimate of the energy level. The first is that there is negligible specific adsorption of the active species. The second is that hydrolysis contributes negligibly to the energy for the species studied. The third is that the kinetically active species is the pre-hydrated species (as discussed in Section 5), so that hydration and similar electrostatic effects contribute

a small fairly constant energy correction and will be neglected. We will assume in general that the dominant species in solution (pre-hydrated) is the kinetically active species.

With these approximations it turns out from the analysis above that the calculated energy level for a species is below the standard hydrogen electrode Fermi energy by an amount equal to the standard redox potential of the species. We have used for the redox potential the values given by Latimer[15]). It is clearly possible for some ions to make the small adjustments suggested by theory for hydration and hydrolysis, but the accuracy of the electron reactivity results do not warrant it at this time.

For some of the species used, more complex considerations must be evaluated. The $Ag(NH_3)_2^+$ ion is an example. In this case we have at least two possible routes for the reduction:

$$Ag(NH_3)_2^+ + e \rightarrow Ag(NH_3)_2 \qquad (17a)$$

$$Ag(NH_3)_2 \overset{\Delta G_1}{=} Ag + 2NH_3 \qquad (17b)$$

or

$$Ag(NH_3)_2^+ \overset{\Delta G_2}{=} Ag^+ + 2NH_3 \qquad (18a)$$

$$Ag^+ + e \rightarrow Ag \qquad (18b)$$

The decision regarding which route is kinetically active is somewhat arbitrary. If we assume Eq. (17) is the dominant route, an estimate for ΔG_1 must be made to determine the energy level. We will assume neglibible energy release in Eq. (17b), as the reaction corresponds simply to the desorption of the ammonia, so $\Delta G_1 \sim 0$. Then the energy level for $Ag(NH_3)_2^+$ becomes the redox potential of this species in one molar NH_3. If, on the other hand, Eq. (18) is kinetically active, the simplest approach is to use the standard redox potential of silver reduction (18b), and determine the concentration of silver by the equilibrium constant of (18a), $K = 10^{-7}$.

The energy level is thus -0.69 eV, but the concentration of free silver used in estimation of $\sigma[X]$ is too high by a factor of 10^7 (the solution studied was 1 molar in NH_3). With this correction, $\sigma[X]$ when normalized must be the order of 10^2 to account for the observed reduction. This is anomalously high compared to the values for other ions and we therefore assume that Eq. (17) represents the dominant reduction route.

Similar reasoning was used in the case of I_3^-, which was found to have $\sigma[X] = 5 \times 10^{-10}$. The only route for the reduction with only one energy level involved would be first the dissociation of the ion yielding neutral iodine atoms and then the reduction of these species. Estimating the effective concentration of neutral iodine atoms, which would be very low, the value for $\sigma[X]$ normalized to 10^{-2}M in I would be anomalously high. Thus it was assumed that the iodine was reduced by a two-equivalent process, and the results therefore are not comparable to the simple model. Alternatively, strong adsorption of iodine on the ZnO surface could account for the results.

In fig. 2 is shown the electron reactivity at 10^{-2} molar, $\sigma[X]$, as a function of the standard redox potential, for the various species tested, excluding I_3^-. Solid lines with a slope of 60 mV/decade have been included for later reference.

4.4 Model

In this section we attempt to reconcile the curve of Fig 2 with a simple model.

It has been shown in this laboratory[16]) that the vanadous and chromous ions which have a positive redox potential inject electrons into the ZnO conduction band, indicating an energy level above the conduction band minimum. It has also been shown[17]) that at times $Fe(CN)_6^{-4}$ will inject electrons, but the results have not been reproducible and the critical conditions for injection have not been identified. At the gas/solid interface, it has been shown that H atoms inject electrons[18]) into the ZnO conduction band, that Sn^0 or Sn^{+2} inject [19]), and that on the $(000\bar{1})$ plane, $Fe(CN)_6^{-4}$ has an energy level about 0.15 e.v. below the conduction band[19]).

From these indications, it would appear that the bottom of the ZnO conduction band must be located in the region of the energy level of $Fe(CN)_6^{-4}$, perhaps a few tenths of an e.v. above it. As most of the evidence arises from measurements in solution, the estimate should be valid with the Helmholtz double layer present. Thus we may expect the ZnO conduction band edge to be at $-0.2 \pm .1$ eV on the E^0 scale of Fig. 2. Now capture by energy levels substantially above the conduction band edge should be unfavorable, so we expect a decrease in apparent cross section for species more electropositive than $Fe(CN)_6^{-3}$. The decrease may be a factor of 10 for each 60 mV increase in energy level. A simplified model shows how this factor could arise. For those levels near or above the edge of the conduction band, we can assume that the charge on the levels are in equilibrium with the surface density of conduction electrons n_s[20]. That is, the exchange current between the conduction band and the active species is assumed to be higher than the net cathodic current when the level is near or above the conduction band. Then the ion current will be proportional to the concentration of reduced species $[X^-]$, given from Fermi statistics:

$$J \propto [X^-] = (n_s/N_c)[X] \exp\left\{-(E_t - E_c)/kT\right\} \qquad (19)$$

with N_c the effective density of states in the conduction band ($n_s \ll N_c$), and E_t and E_c the surface state and conduction band energies respectively. The Tafel dependence of current on voltage arises as usual through the dependence of n_s upon V. By comparison of (19) with (6), there will be an apparent decrease of $\sigma[X]$ as E_t increases above E_c, with a decrease of one order of magnitude per 60 mV increase in $E_t - E_c$. This model illustrates how a high energy level could decrease the effective σ by re-injection, but is simplified, as it assumes a high electronic exchange current and ignores the difference in energy level between the oxidized and reduced species.

Capture of electrons by species with an energy level below that of $Fe(CN)_6^{-3}$ (viz. below the conduction band edge) should be favorable, but one cannot predict whether the capture cross section for stronger oxidizing agents should pass through a peak and decrease (as would be predicted by a phonon-aided capture process[3]) or should be maintained at a high but erratic value (as would be predicted by a cascade-aided process[4]).

It is observed in Fig 2 that the value of $\sigma[X]$ decreases rapidly for redox potential more positive than $Fe(CN_6)^{-3}$. This then provides further evidence that the energy level of the ZnO conduction band is close to the $Fe(CN_6)^{-3}$ level.

The apparent decrease in electron reactivity for E^0 more negative than -1.0 may be suggestive of a multi-phonon electron capture process. However, there is too little data in this region of redox potential to establish confidence in this observation.

The ceric results are of interest not only because of the indication of low capture cross section, but also because two forms of ceric ion were studied: one the highly complexed form[21]) as found in sulphate solutions; the other, ceric ions in nitrate, where minimal complex formation is expected[15]). The ceric nitrate result is included in fig. 2. The sulphate result cannot be included in the figure because we do not know which complex is kinetically active. It is of interest, however, that the complexed form shows a $\sigma[X]$ much greater than the uncomplexed form. This observation is consistent with the present model because the complexing of the ceric may produce a higher energy level. If one of the complexes has an energy level in the region of the maximum of fig. 2, the product of its high cross section and the low concentration of the complex may lead to $\sigma[X]$ of observed order of magnitude.

The data of fig. 2 are consistent with the assumption of little specific adsorption. If we make the approximation that the maximum cross section expected is on the order of $10^{-15}cm^2$, the ionic cross section, and that ions within the order of 20A of the surface can be reduced, then with the $6 \times 10^{18}cm^{-3}$ ions available at $10^{-2}M$, the maximum $\sigma[X]$ that should be measured is 10^{-3}. This estimated value compares well with the maximum value actually observed. If the assumption is correct that there is little specific adsorption, then the values for σ become more meaningful.

However, the apparent agreement should not be interpreted as evidence for a particular theory for the capture mechanism. The numbers used are values expected approximately from a tunnelling model, where the barrier for tunnelling is negligable below some small distance (we assummed 20A). However, similar orders of magnitude might be found if the electrons transfer by an anion bridge, for example.

A comment should be made with respect to the effect of pH. The energy level of the unfilled state with respect to the conduction band is not only determined by the properties of the ion, but also the double layer potential across the Helmholtz region. Our attempt to relate σ to the energy level is based on the assumption (supported by some evidence) that the latter is constant, independent of the ion under study. However, clearly the Helmholtz potential is dependent on pH. Thus the variation of $\sigma[X]$ with pH, observed with ferrocyanide and permanganate, could thus occur due to a change in the energy level of the conduction band relative to the zero in solution because of a Helmholtz potential change at the electrode. Alternately it could be associated with hydrolysis of the ion under study, changing its energy level or changing the concentration of the kinetically active species. It would be premature to attempt an interpretation of the behavior at this time.

5. Conclusions

The suggestion that there should be a relation between electron reactivity of ions in solution and electron capture theories of semiconductor physics appears to be qualitatively justified. The energy level, as estimated from the redox potential, must be slightly below the semiconductor conduction band minimum for maximum capture cross section. There is some indication that if the level becomes too deep, the capture cross section diminishes.

If this model is correct it suggests some interesting implications about selectivity in reduction of ions at such a semiconductor surface with a non-varying Helmholtz voltage. Two-equivalent reductions would almost inevitably be slow, as one of the energy levels normally would be far from the region of maximum cross section. (Experimentally we have found no clearly two-equivalent ions, out of perhaps 5 or 6 studied, with

$\sigma[X]$ greater than 10^{-9}.) The relative electron reactivity of various species will be far different from that found at a metal electrode, where the semiconductor rules do not apply (here filled energy levels in the solid are available at all energies below the Fermi level). Thus some interesting new electrochemical synthesis may be possible with semiconductor electrodes.

Presumably similar concepts may be expected to apply regarding hole capture (oxidation) at the surface of p-type semiconductor electrodes. However many p-type semiconductors with a wide band-gap involve oxide ions as the anion, and as these are easily oxidized themselves, they can complicate the behavior.

I would like to acknowledge the valuable discussions and suggestions of Dr. T. Freund during the course of this research. From his observations, the data used for the reduction of V^{+3} was obtained.

References

1) T. Freund and S. R. Morrison, Surface Sci. 9 (1968) 119.

2) F. Beck and H. Gerischer, Z. f. Electrochemie 63 (1959) 943.

3) C. Herring and M. Lax, Photoconductivity Conference Ed. R. G. Breckenridge, John Wiley & Sons, New York, 1954, pp. 81, 111.

4) M. Lax, Phys. Rev. 119 (1960) 1502.

5) H. Gerischer, The Surface Chemistry of Metals and Semiconductors Ed. H. Gatos, John Wiley & Sons, New York, 1960, p. 177.

6) S. R. Morrison and T. Freund, J. Chem. Phys. 47 (1967) 1543.

7) J. F. Dewald, J. Phys. Chem. Solids 14 (1960) 155.

8) S. R. Morrison, Surface Sci. 10 (1968) 459.

9) H. Gerischer, "The Surface Chemistry of Metals and Semiconductors," ed. H. C. Gatos, John Wiley & Sons, New York, 1959, p. 177.

10) W. F. Libby, J. Phys. Chem. 56 (1952) 863.

11) R. A. Marcus, Can. J. Chem. 37 (1959) 155.

12) J. Blakemore, "Semiconductor Statistics," Pergamon Press, New York, 1962.

13) P. Delahay, "Double Layer and Electrode Kinetics," Interscience, New York, 1965.

14) L. Page and N. I. Adams, "Principles of Electricity," Van Nostrand, New York, 1947.

15) W. M. Latimer, Oxidation Potentials, Prentice-Hall, New York, 1952.

16) T. Freund, reported at Catalysis Conference, Moscow, 1968.

17) W. Gomes, unpublished data.

18) F. Haberrecker, E. Mollwo, H. Schreiber, H. Hoinkes, H. Nahr, P. Lindner, and H. Wilsch, Nuclear Instrum. Methods, 57 (1967) 22.

19) S. R. Morrison, Surface Sci., 13 (1969) 85.

20) W. H. Brattain and J. Bardeen, B.S.T.J. 32 (1953) 1.

21) "Stability Constants of Metal-Ion Complexes" compiled by L. G. Sillen and A. E. Martell for the Chemical Society, London, Metcalf and Cooper Ltd., London, 1964.

List of Figures

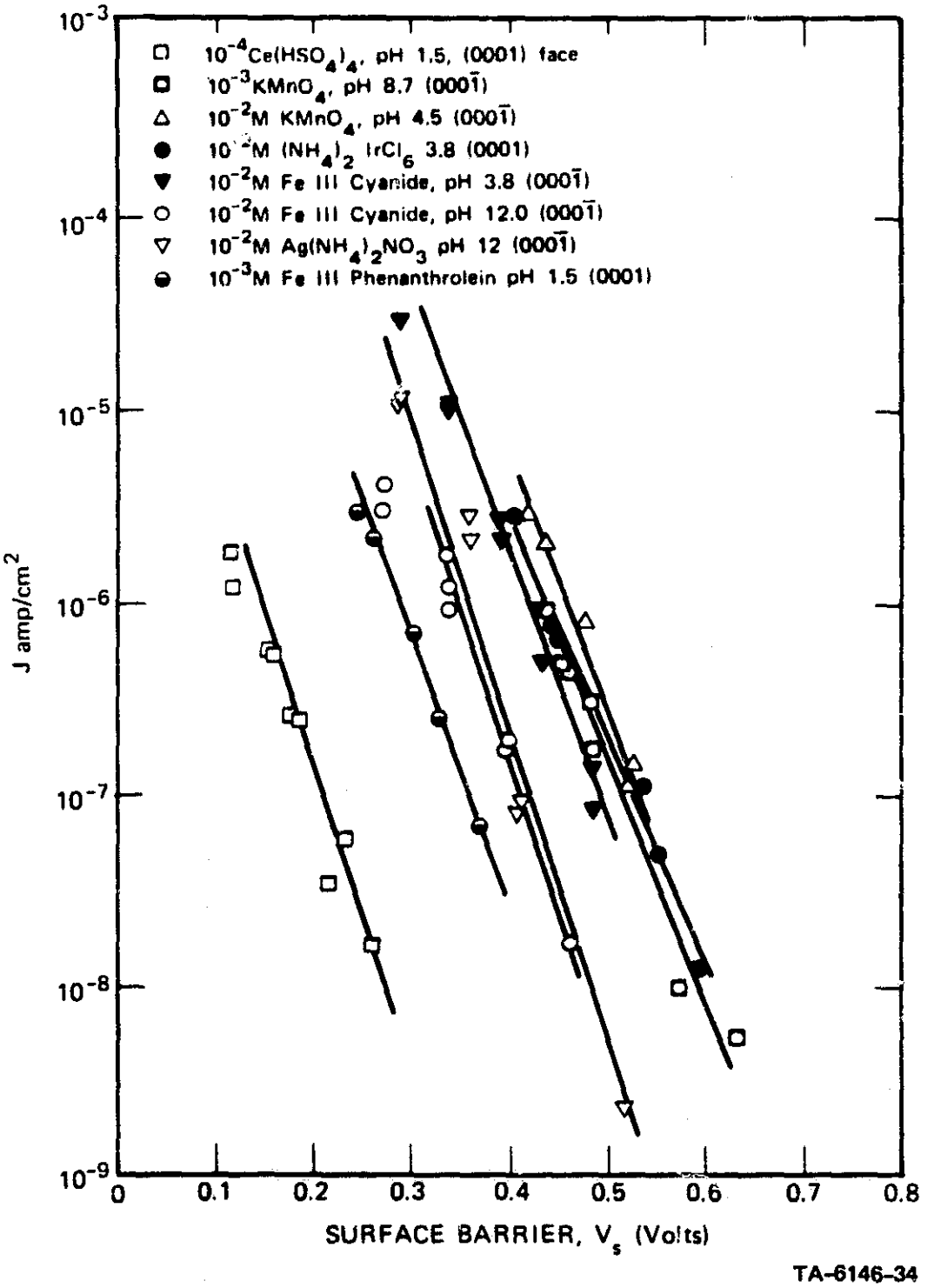

FIGURE 1 THE VARIATION IN CATHODIC CURRENT WITH THE SURFACE BARRIER, FOR VARIOUS ONE-EQUIVALENT OXIDIZING AGENTS

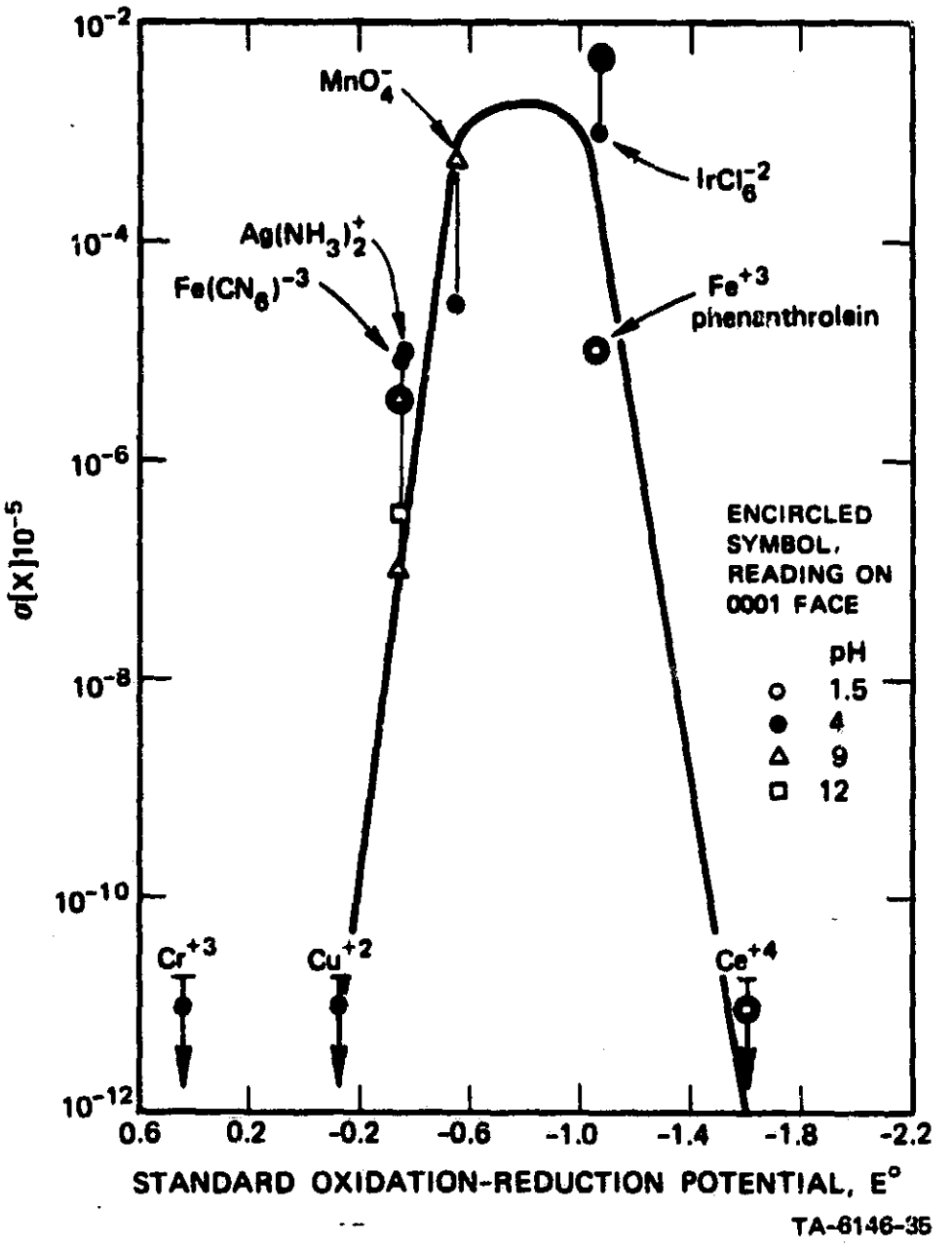

FIGURE 2 THE VARIATION IN ELECTRON REACTIVITY AS A FUNCTION OF THE REDOX POTENTIAL (THE ENERGY LEVEL) FOR VARIOUS ONE-EQUIVALENT OXIDIZING AGENTS

SECTION B

ANODIC PROCESSES ON ZnO *

1. Electron Injection into Zinc Oxide[1]

Sir: Various surface properties of the wide band-gap semiconductor ZnO have been of considerable interest including dark catalysis[2] and photocatalysis,[3] adsorption,[4] charge transfer adsorption,[5] spin resonance,[6] and oxidation-reduction processes.[7] Zinc oxide single crystals are very

---

(1) Part of the research was performed for the Jet Propulsion Laboratory, California Institute of Technology, sponsored by the National Aeronautics and Space Administration under Contract NAS 7-100 and part of the research was supported by Stanford Research Institute.

(2) G. Natta in "Catalysis" Vol. 3, P. H. Emmett, Ed., Reinhold Publishing Corp., New York, 1955.

(3) M. C. Markam, J. C. Kuriacose, J. DeMarco, and C. Giaquinto, J. Phys. Chem., 66, 932 (1962); T. S. Nagarjunan and J. G. Calvert, J. Phys. Chem., 68, [illegible] (1964); T. Freund, J. Catal., 3, 289 (1964); J. G. Calvert, K. Theurer, G. T. Rankin, and W. M. MacNevin, J. Amer. Chem. Soc., 76, 2575 (1954); S. R. Morrison and T. Freund, J. Chem. Phys., 47, 1543 (1967).

(4) V. Kesavulu and H. A. Taylor, J. Phys. Chem., 66, 54 (1962); M. J. D. Low, J. Amer. Chem. Soc., 87, 7 (1965).

(5) H. Saltsburg and D. P. Snowden, J. Phys. Chem., 68, 2734 (1964).

(6) R. J. Kokes, J. Phys. Chem., 60, 99 (1962); K. S. Sancier and T. Freund, J. Catal. 3, 293 (1964).

(7) G. Oster and M. Yamamoto, J. Phys. Chem., 70, 3033 (1966).

* Published in J. Phys. Chem. 73, 468-9 (1969).

suitable for the investigation of charge transfer processes because of their behavior as an electrode[8] and their commercial availability.[9] Electron injection into wide band-gap semiconductors from aqueous solutions of stable substances seems to be unknown.[10] Previously the author and co-workers have reported[11] electron injection at room temperature from radical-type sorbed species that were generated by the hole oxidation of multi-equivalent reducing agents.

We wish to report that we have found that the property of electron injection can be correlated with the oxidation potential of the substance. Specifically, reductants with high oxidation potentials (Latimer's[12] convention, the more positive the oxidation potential the stronger the reducing agent) inject electrons while those with low potentials do not inject. We found that aquo chromium(III), $E^0 = 0.4$; aquo europium(II), $E^0 = 0.4$; aquo vanadium(II), $E^0 = 0.3$; ethylendiamine cobalt(II), $E^0 = 0.3$; dithionite ion, $E^0 = 0.1$; aquo titanium(III), $E^0 = -0.1$ inject in contrast to the weaker reducing agents such as hexammine cobalt(II), $E^0 = -0.1$; ethylenediaminetetraacetic acid iron(II), $E^0 = -0.1$; hexacyano

---

(8) J. F. Dewald, Bell Systems Tech. J., 39, 615 (1960); W. P. Gomes, T. Freund, and S. R. Morrison, J. Electrochem. Soc., 115, 818 (1968); T. Freund and S. R. Morrison, Surface Sci., 8, 119 (1968).

(9) Minnesota Minning and Manufacturing Co., St. Paul, Minnesota.

(10) P. J. Boddy, J. Electrochem. Soc., 115, 199 (1968); P. J. Boddy, D. Kahng and Y. S. Chen, Electrochim. Acta. (to be published).

(11) T. Freund, W. P. Gomes and S. R. Morrison, IV International Congress on Catalysis, Moscow, June 1968.

(12) Standard acid potentials for unit activity reductant, oxidant, and hydrogen ion.

iron(II),[13] $E^0 = -0.4$; aquo iron(II) $E^0 = -0.7$; orthophenanthroline iron(II), $E^0 = -1.1$; aquo manganese(II), $E^0 = -1.5$. Clearly a high oxidation potential is not sufficient since the eight-equivalent reducing agent borohydride ion ($E^0 = 0.5$)[14] and the two-equivalent formic acid ($E^0 = 0.2$) do not inject. It is also clear that one-equivalency is not a requirement for electron injection since $S_2O_4^{-2}$, $E^0 = 0.1$, injects. Borohydride ion does not inject electrons into other semiconductors[10] including $KTaO_3$, TiO_2, and Ta_2O_5. The correlation with oxidation potential may be expected to fail for multi-equivalent reductants since the oxidation potential for the oxidation of the first equivalent of a multi-equivalent reductant may be very low. The lack of reducing activity of borohydride ion is not surprising since its reactions[15] with aqueous oxidants are often slow.

Electron injection, Eq. (1), can be distinguished from the other possible mechanism for an anodic current i.e., hole capture, Eq. (2):

$$M \rightarrow M^+ + e \qquad (1)$$

$$p + M \rightarrow M^+ \qquad (2)$$

M is a reducing agent, e is an electron in the conduction band, and p is a hole in the valence band. For a wide band gap n-type semiconductor, such as ZnO, an anodic current in the dark can be taken as evidence of electron injection since holes are virtually absent without band-gap illumination. In terms of the band model, electron injection will occur from an adsorbed species when its electronic energy level is above the

---

(13) T. Freund and S. R. Morrison, Surface Sci., 9, 119 (1968).

(14) W. H. Stockmayer, D. W. Rice, and C. C. Stephenson, J. Amer. Chem. Soc., 77, 1980 (1955).

(15) T. Freund, J. Inorg. and Nucl. Chem., 9, 246 (1959); J. Amer. Chem. Soc., 84, 873 and 2678 (1962).

the bottom of conduction band at the surface or when the temperature is sufficiently high to provide the activation energy for the transition of an electron from the surface level to the bottom of the conduction band.

The results of preliminary experiments, given below, are consistent with the assignment of electronic energy levels for injecting reductants at fixed energies that are about equal to or above the bottom of the ZnO conduction band at the surface. The increase of the injection current with stirring indicated that the electron transfer step is fast compared to mass transport in solution; such a result is consistent with a small or zero energy barrier for the transition of an electron from the reductant level to the bottom of the conduction band at the surface. The lack of dependence of the injection current on applied voltage and the lack of dependence of the Helmholtz voltage (determined from capacitance-voltage measurements) on reductant concentration are consistent with fixed levels since movement of adsorbate levels might be expected to change the current. The lack of dependence of current on the concentration of the oxidized form of the reductant and the increase of injection current with increasing concentration of reductant are consistent with the postulated location of adsorbate levels since high empty levels would not be expected to capture electrons and the current should increase with an increasing number of filled levels.

Solid State Catalysis Laboratory
Stanford Research Institute
Menlo Park, California 94025

Thomas Freund

2. Hole Capture Cross Section

The measurement of relative hole capture cross section by the reduced form of a one-equivalent species is made by a comparison with a two-equivalent species.[1,3,4] The two-equivalent species injects an electron following hole capture; the one-equivalent does not. The electron injection results in an anodic current increase. Thus if a solution contains a two-equivalent ion (a "doubling" agent), and a one-equivalent species is slowly added, then the current will decrease because the one-equivalent species captures a larger and larger fraction of the holes. By experimental analysis, one can then determine the hole capture cross section of the one-equivalent species relative to the two-equivalent species.

To compare a series of one-equivalent species, as is required in this program, one simply compares each species in the series to the same two-equivalent ion.

Details of the method are given in references 1, 3, and 4. Details of the theory are presented in reference 4.

Our recent results of relative hole capture cross section vs. redox potential of the additive are summarized in Fig. 1. The redox potentials were taken from Latimer.[5] We use the redox potential to characterize the properties of the various species on the same basis as was described earlier. Each curve in Fig. 1 represents a different doubling agent. The various curves should not be the same because the capture cross section of the various doubling agents is not the same. However, the slopes should be the same, but are not. This indicates problems in either the theory or the measurement procedure.

The important qualitative feature of Fig. 1 is the apparent increase in capture cross section, σ_p, as the redox potential of the additive approaches the "redox potential" of the ZnO conduction band, about -0.1 eV. Measurements at higher redox potential cannot be made because such species spontaneously inject electrons. (This is one of the reasons that -0.1 eV is considered the conduction band potential; an energy level above the conduction band edge is expected to

spontaneously inject electrons.)

In practical application, then, the optimum level for hole capture is apparently close to the conduction band edge. In studies of other oxide pigments we will use this criterion.

Theoretically, the observed increase in σ_p with higher redox potential (energy level) is best interpreted in terms of electron transfer from one localized surface level to another. Thus, we assume that the (photo-produced) hole is first captured by a surface state, viz., becomes localized on a specific oxygen ion at the surface. Then the electron from the reduced form of the additive makes the transition from its localized level to the surface state occupied by the hole. It is often found for electron transfer from one molecule to another that the probability increases with the difference in energy. The transfer is best described using the reaction coordinate approach where the rate may decrease as the energy difference increases (see, for example, Delahay[6]). This behavior is in direct contrast to that expected if the process were free hole capture, in which case, as was described above in the discussion of free electron capture, one would have expected the cross section to decrease with higher energy level (or redox potential).

If the two-step model of hole capture is correct, it should be possible to apply it to other oxide materials (where the surface states may be similar to ZnO). It is expected, therefore, that one needs a level a few tenths of an electron volt below the conduction band edge for efficient hole and electron capture.

C. Tabulated Results

A summary of the values of the capture cross sections for holes and electrons for substances that may undergo one-equivalent oxidation-reduction processes is given in Table I, parts 1 and 2. The vertical arrangement follows an order of decreasing redox potentials (column IV). Column I lists the chemical element with its probable oxidation states. Column II gives the values of the product of the electron capture cross section, σ_e, and the surface concentration of the capturing species, [X],

Table I, Part 1

CAPTURE CROSS SECTIONS

I Element, Oxidation States	II Electron Capture[a], $\log_{10} \sigma_e [X]$	III Hole Capture[b], $\log \sigma/\sigma_D$ D = Sn(II)	D = CH_3OH	IV Redox Potential[c], E_o
V (II/III)	<-12	Injects electrons		+0.25
Co (II/III)	<-14 <-10		4.5 3.4 3.2	-0.1
S (IV/V)			0.8[d]	?
S (IV/V)			0.7[d]	?
S (IV/V)		-0.8[d] -1.1[d]	0.5[d]	-0.17
Cu (I/II)	<12			-0.15
Fe (II/III)	-5.7 -6.7 -7.0 -5.1	-0.8	2.7 3.1 3.4	-0.36
Ag (0/I)	-5.0			-0.37
I (0/-I)	-9.7 -9.2		1.1	-0.5
Mn (VI/VII)	-4.7 -3.2			-0.5
Mn (II/III)		-2.3 -1.5 -1.9 -1.5	D = As(III)	-1.5
Ir (III/IV)	-3.0 -2.2	-2 -2.2 -1.4 -1.4		-1.0
Fe (II/III)	-5.0	+0.2 -0.01		-1.1
Br (0/-I)			-0.9	-1.1
Ce (III/IV)	<-12 -8.2	-3.0 -3.3		-1.6 -1.4
Cl (0/-I)		<<-3	<<-3	-1.4

(a) σ_e, electron capture cross section; [X], surface concentration in numbers per unit area (J normalized to a solution concentration of 0.01 molar--see Eq. 1). (b) σ, hole capture cross section of element; σ_D, hole capture cross section of current-doubling agent D. (c) E_o, redox potential under standard conditions given in W. Latimer, Oxidation Potentials, 2nd ed., Prentice Hall, 1952, (d) maybe a two-equivalent process involving capture of two holes.

Table I, Part 2

EXPERIMENTAL DETAILS FOR CAPTURE CROSS SECTIONS

I	V Electron Capture Details				VI Hole Capture Details		
Element, Oxidation States	Form of ion	pH	log N_D^b	pF^e	Form of ion	pH	pD_1^f
V (II/III)	HCl^b	0.3	17^c	0.3	HCl^a		
Co (II/III)	$Co(NH_3)_3^{+3}$	4.0 10.3	17.7^c 17.9^d	1.4 1	$Co(NH_3)_6^{+2}$	10.3^d 10.3^d 10.3^d	0.0 -0.1 -0.1
S (IV/V)					$C_6H_5SO_2^-$	12.5^d	0.0
S (IV/V)					$CH_3C_6H_5SO_2^-$	12.5^d	-0.1
S (IV/V)					SO_3^{-2}	1^c 1^c 12.5^c	3.5 3.5 0.5,0
Cu (I/II)	Cu^{+2}	3.7	19^c	1.3			
Fe (II/III)	$Fe(CN)_6^{-3}$	8.7 12 9 3.8	18.9^c 18.6^d 18.6^d 18.3^d	2,3 3,4 2,3,4 2,3,4	$Fe(CN)_6^{-4}$	12.5^d 12.5^d 12.5^d 1^c	-0.2 -0.4 -0.7 3.2
Ag (0/I)	$Ag(NH_3)_2^+$	12	17.0^d	1,2			
I (0/-I)	I_3^-	3.8 3.8	16.8^c 17.0^d	2,3,4 2,3	I^-	12.5^d	0.5,0
Mn (VI/VII)	MnO_4^-	4.5 8.7	18.8^d 18.0^d	2,3,4 3,4			
Mn (II/III)					OAc^{-a}	4^d 4^d 4^d 4^d	1.3 2.4 2.5 2.5
Ir (III/IV)	$IrCl_6^{-2}$	3.8 3.8	18.0^d 16.5^d	2,3 2,3	$IrCl_6^{-3}$	1^c 1^c 1^c	3.5 3.3 -- 3.2
Fe (II/III)	$Fe(phen)_3^{+3}$	1.5	17^c	3,4	$Fe(phen)_3^{+2}$	1^c	4.7 3.5
Br (0/-I)					Br^-	12.5^d	0.5,0
Ce (III/IV)	NO_3^{-b} SO_4^{-2} b	1.5 1.5	17^c 18.8^c	3,4 3,4	NO_3^{-a}	1^c 1^c	3.7 3.7
Cl (0/-I)						$1,4,9,13.5^c$	-1

(a) possible complexing agent; (b) N_D, donor density in numbers per cubic centimeter; (c) (0001) crystal face; (d) (0000) crystal face; (e) pF, - $\log_{10}$ formality of capturing species in solution; (f) pD_1, - $\log_{10}$ initial formality of current-doubling agent

at solution concentration of 0.01 M. Column III lists the values for the hole capture cross section relative to either Sn(II) or CH_3OH with the exception of Mn(II/III) for which the doubling agent was As(III). As was outlined in a recent publication,[4] the hole capture cross section for a non-current-doubling substance relative to a doubling substance, σ/σ_D, is given by

$$(J_p/J_e) - 1 = (\sigma/\sigma_D)([S]/[D]) \qquad (2)$$

where J_p is the hole current that is available for reaction with either the current-doubling substance, D, or the other capturing substance, S; J_e is the electron injection current which is the difference between the cell current and the hole current; and the brackets represent concentration. Columns V and VI list the experimental conditions under which the electron capture cross sections and hole capture cross sections were determined.

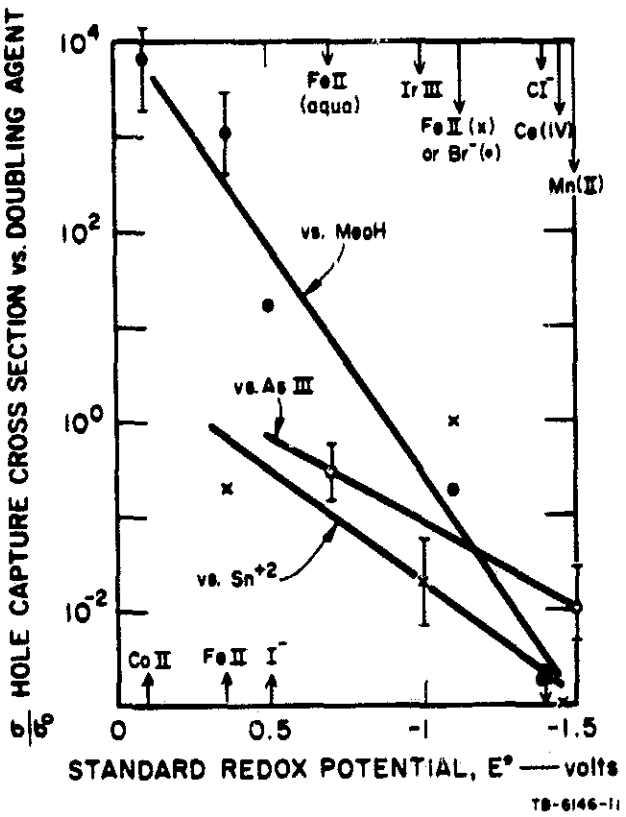

FIGURE 1 HOLE CAPTURE CROSS SECTION OF ONE-EQUIVALENT REDUCING AGENTS

REFERENCES

1. Interim Report No. 1, September 1, 1967 (this contract).

2. T. Freund and S. R. Morrison, Surface Science, 9, 119 (1968).

3. S. R. Morrison and T. Freund, J. Chem. Phys., 47, 1543 (1967).

4. W. Gomes, T. Freund, and S. R. Morrison, J. Electrochem. Soc., 115, 815 (1968).

5. W. Latimer, Oxidation Potentials, 2nd ed., Prentice Hall, 1952.

6. P. Delahay, Electrode Kinetics, Interscience, 1965, p. 173.

SECTION C

IRON CYANIDE AS A SURFACE STATE TO PREVENT ZnO PHOTOLYSIS IN VACUUM*‡

S. Roy Morrison
Stanford Research Institute, Menlo Park, California 94025

ABSTRACT

When ZnO is intermittently irradiated with ultraviolet in vacuum, its dark conductance increases irreversibly, presumably due in part to oxygen photodesorption and in part to photodecomposition of the ZnO. From the theory of one-equivalent surface states and from earlier measurements of the relevant parameters associated with the surface states, it was concluded that an iron cyanide additive should provide characteristics suitable for surface stabilization. In particular, it should act as a recombination center for the photoproduced carriers. Single crystal studies of dark conductance after various time intervals of illumination in vacuum are reported, showing that an iron cyanide surface additive does indeed control the photodecomposition--less than a monolayer decreases the rate by several orders of magnitude. The action of iron cyanide as a recombination center is compared with theory, showing by semiquantitative analysis that carrier generation and recombination should be described by a modified Elovich equation rather than by the more usual formulations applicable to less dense recombination centers. The rate of ZnO decomposition is calculated using a simple model and it is shown that the rate should vary inversely with the square of the additive concentration concentration, as observed for long exposure times.

---

* This research was supported by the Jet Propulsion Laboratory, California Institute of Technology, sponsored by National Aeronautics and Space Administration under Contract NAS 7-100.

‡ To be published in J. Vacuum Science and Tech.

Introduction

In an earlier contribution[1] we discussed the use of foreign surface states to control and stabilize the surface properties of semiconductors. It was concluded that such stabilization and control would be possible when a one-equivalent species with a surface state having a favorable energy level were added in both the oxidation states. In the present work we study the problem of ZnO photolysis in vacuum as an application of these concepts.

When ultraviolet irradiation is incident on zinc oxide in vacuum, several of its properties irreversibly change. Its conductivity increases, as has been observed by many workers.[2,3,4,5] Its optical absorption characteristics change,[6] an effect not only of fundamental but of practical importance in the technology of paints or thermal control coatings. The gas pressure surrounding the zinc oxide increases,[7,8,9] interpreted by the referenced authors in terms of oxygen evolution. The electron spin resonance characteristics change.[10,11]

Possibly the most definite study of the changes with uv/vacuum photolysis has been made by Collins and Thomas.[4] They examined the surface conductance of single crystals, and showed that if after a long oxygen anneal the crystal is exposed to intermittent uv in vacuum, the dark conductance increases rapidly. One conduction electron per photon is obtained during the initial seconds of exposure with undoped ZnO, but the quantum yield rapidly decreases with increased integrated exposure. The overall conductance increase is high with a long exposure, far beyond the amount expected from desorption of chemisorbed oxygen. Thus they concluded that photolysis of the ZnO occurs; the lattice oxygen captures holes, the neutralized oxygen comes off in the gas phase, and the

corresponding zinc is dissolved in the crystal as a donor. This simple model of photolysis can explain directly most of the observations above.

The purpose of the present work was to prevent the vacuum photolysis of ZnO. The method was to add recombination centers to the ZnO that would recombine the photoproduced hole-electron pairs before they could cause such chemical changes. The energy would then be dissipated as heat rather than by chemical transformation of the ZnO or other phase present.

Several phases of the investigation have been reported earlier. These included studies with the objective of identifying appropriate one-equivalent materials with an acceptable surface state energy level and electron and hole capture cross section. A study of electron capture of various foreign species[12] indicated first that the energy level of a species may be related to its chemical properties by a simple model. Second, it indicated that the highest electron capture cross section was obtained with one-equivalent species having an energy level a few tenths of an electron volt below the conduction band. A study of hole capture[13,14] was inconclusive, but there were indications that species with an energy level near the conduction band would have a high hole capture cross section. The energy level of ferrocyanide and ferricyanide ion was estimated by two approaches[12,15] to be about 0.1 or 0.2 eV below the conduction band. From these results, the redox couple ferrocyanide, Fe(II), and ferricyanide, Fe(III), were selected as promising materials for stabilizing the ZnO surface and acting (with both oxidation states present) as a controlled recombination center.

In this paper we will present results of measurements similar to those of Collins and Thomas[4] in that single crystal conductance is monitored to follow the photolysis. However, data will be presented with varying iron cyanide concentrations on the surface, to show how the additive protects the crystal against photolysis. With these results, a

more detailed model of vacuum photolysis is possible, and a semiquantitative analysis of the action of iron cyanide as a recombination center can be made.

Experimental

Lithium-doped ZnO was obtained from 3M Company in wafers 1-mm thick and about 6-mm diam. About 0.2 mm was lapped from each side, then the crystals were etched in concentrated H_3PO_4 for 5 min followed by 0.01 M HNO_3 for 10 sec. Four Aquadag spots were painted on for later contact areas. On each side of the crystal a controlled amount of the two oxidation states of iron cyanide (as potassium salts) was deposited. The edges of the crystal were painted with a saturated solution of the mixed iron cyanides. This was to ensure that photolysis only occurred on the faces of interest, and thus avoid edge effects. Clips for a four-point resistance measurement were attached where Aquadag had been deposited, and the sample was mounted in the vacuum system. The crystal plane facing the pyrex window was tentatively identified as the (0001) plane by its etching pattern,[16,17] but the etching of Li-doped crystals has not been studied, and may be different from the undoped crystals. No attempt was made to keep scattered light from reaching the other crystal face, so the contribution of the back face to the measured conductance change is not known.

The additive as an aqueous solution was deposited by an atomizer spray. The sample was heated to a temperature of about 100°C to evaporate the water as the droplets were deposited. Calibrations of the atomizer spray chamber several months apart resulted in a difference of a factor of two in ion deposition rate, which was considered of adequate precision. We will report below the surface concentration of ions as calculated from the average of our two calibrations.

Our standard light intensity striking the sample which we will denote as I_0, was determined in terms of holes generated in an undoped crystal. The rate of hole generation was measured from the photo current produced in an electrolytic cell[18] with the submerged crystal as the anode. At the standard intensity I_0 the current corresponded to 2×10^{13} cm^{-2} sec^{-1} holes reaching the surface of the undoped sample, which may be a reasonable estimate of the hole current on the Li-doped sample. As will be shown in a later comparison, the compensating errors (the shorter hole diffusion length and the greater optical absorption in the blue of the Li-doped sample) appear to be unimportant, for the degradation rate of our additive-free sample is found to be in substantial agreement with earlier work assuming $I_0 = 2 \times 10^{13}$ holes/cm^2 sec.

A VacSorb pump and a VacIon pump were used, with the control on the VacIon pump providing the only low pressure vacuum gauge. After mounting the sample the system was vacuum baked at 150°C, and following this a pressure at the pump in the 10^{-9} Torr range was reached.

The results to be presented were all obtained on one sample. Other samples, used for the exploratory measurements, showed similar qualitative behavior.

Results

For each run the sample was "annealed" in oxygen at about 0.5 Torr for at least 16 h. The system was then evacuated and the conductance of the sample was continuously recorded. The sample was alternately subjected to "light on" periods (of increasing duration) and "light off" periods (of the order of 10-20 minutes). Up to 100 minutes of integrated illumination time, the intensity I_0 was used; for greater exposures, in order to attain higher fluxes, the illumination intensity was increased to 40 I_0.

In later discussions we use the term "integrated illumination time" to mean $\int_0^t (I/I_0)dt$.

Typical curves showing the transient response, rise, and decay of photoconductance G are shown in Fig. 1 for a sample with 5×10^{14} cm^{-2} ions deposited of Fe(II) and of Fe(III).* As normally found[2,19] for ZnO photoconductance, neither the rise nor fall in conductance follows a simple law, although the curves can be fitted to an Elovich law.

Figure 2 shows the change in "steady state" dark conductance as a function of integrated illumination time. The value of ΔG is $G - G_0$ where G_0 is the original dark conductance before any exposure to illumination and G is the value of the dark conductance ten min after removing the light. The value of G_0 is not noted in Fig. 2, but is usually about the same magnitude as ΔG at 0.02 min. It is apparent that the values of ΔG and of $d\Delta G/dt$ are much lower with increasing surface additive.

The curve for ΔG for the first 10 to 100 min depends on the oxygen annealing. This is illustrated by a comparison of the results for the case with 5×10^{14} cm^{-2} additive. The results of Fig. 1 are the first run, with no previous history of illumination in vacuum. These data are not used in Fig. 2. The open squares in Fig. 2 are the next run, where the sample was annealed for 16 h in 0.3 Torr oxygen. The other curve for this concentration represents a run after 64 h of annealing in oxygen, and it is observed that the initial conductance values are much lower, close to the values in Fig. 1. However, the results for all three runs coincide for $t > 10^2$ min. With no Fe present (blank), the results are insensitive to the annealing pretreatment used. The remaining data of Fig. 2 were obtained after 16 h annealing prior to each run.

---

* With equal parts of Fe(II) and Fe(III), we will label the curves according to the amount of each, not the sum of the two, and will denote this concentration as [Fe].

Figure 3 shows the effect of varying the additive composition, with the total iron cyanide concentration maintained at 10^{16} cm^{-2}. The lowest degradation rate is observed with the mixture. The curves with pure Fe(II) or Fe(III) additive are the first runs, with no previous history of illumination in vacuum.

Figure 4 shows transient photoconductive rise and decay curves with varying light intensity, the measurements made after a sample ([Fe] = 5×10^{14} cm^{-2}) was substantially degraded (after 4×10^{3} min integrated illumination time). As typical with decay curves following an Elovich behavior, the decay does not come to a well defined steady state. Thus the t = 0 value when the light is turned on for the next photoconductive rise curve is not the same for each of the curves but depends on the patience of the experimenter.

From Fig. 4, if we use 0.3×10^{-4} mhos as the dark conductance, we can estimate the steady state photoconductance as a function of light intensity. Such an estimate is shown in Fig. 5 for three different additive concentrations. It is observed that the photosensitivity varies from almost a linear relationship ([Fe] = 10^{16} cm^{-2}) to almost independent of light intensity ([Fe] = 5×10^{14} cm^{-2}).

In two cases at the completion of a run, dry oxygen was leaked in until the pressure at the pump registered 10^{-7} Torr. No change in conductance over a half-hour period was observed. From this we suggest that at "10^{-9} Torr" the residual oxygen pressure probably has little serious effect on the results obtained during the course of a run. In agreement with other workers[2] we found higher pressure oxygen (0.5 Torr, for example) caused an immediate and rapid conductance decrease.

Discussion

The first objective of this research was to show that the presence of a recombination center would prevent the photolysis of ZnO which leads to conductance changes. Clearly from Fig. 2 this objective has been met. It is also evident in Fig. 4 that a mixture of the two oxidation states is necessary for a high recombination velocity. However, more quantitative interpretation can be suggested from these results, both regarding the mechanism of photolysis and the action of foreign surface states as recombination centers.

Clearly the system under study is complex. During illumination a) the donor density is changing (by photolysis), b) the surface barrier may be varying because we are recombining holes and electrons on the same surface states which presumably control the surface barrier, c) the ratio of Fe(II) to Fe(III) may be varying, and finally, d) there is the possibility of nonlinear recombination by lithium acceptors.

We will separate these effects on the basis of the following reasoning. For the early stages of photolysis we will not attempt to interpret the transient rise and fall of photoconductance (Fig. 1), but will examine these results solely in terms of photolysis, the irreversible dark conductance degradation (Figs. 2 and 3). As the model for degradation, we will assume that during illumination lattice oxygen is neutralized and the corresponding zinc dissolves into the lattice and diffuses away from the surface. After long exposure times, when the sample has a relatively steady state concentration of zinc donors, we will examine the transients, the photoconductive rise and fall. Thus the results of Figs. 4 and 5 will be used to interpret the action of iron cyanide as a recombination center.

We will assume the action of the lithium does not vary as we vary the parameters of interest here, and will neglect its probable role as a compensating impurity (compensating the zinc donors) and as a trapping and recombination center.

There are several surface reactions required to describe the hole and electron capture at the surface leading to recombination or photolysis. There is evidence from other work (to be published) that, after a room temperature pretreatment in oxygen, there is little ferrocyanide as such; a reaction

$$Fe(II) + O_2 \rightleftharpoons O_2^- + Fe(III) \qquad (1)$$

[adsorption of some form of oxygen (O_2^-) with the corresponding oxidation of the ferrocyanide] is shifted almost completely to the right. At the initiation of illumination, we thus assume three possibilities for hole capture, and one dominant reversible reaction involving electrons:

$$p + O_2^- \rightarrow O_2\uparrow \qquad (2a)$$

$$2p + O_L^{=} \rightarrow \tfrac{1}{2}\, O_2\uparrow \qquad (2b)$$

$$p + Fe(II) \rightarrow Fe(III) \qquad (2c)$$

$$Fe(II) \rightleftharpoons Fe(III) + e \qquad (2d)$$

where $O_L^{=}$ represents a lattice oxide ion. In vacuum Eqs. (2a) and (2b) represent oxygen photodesorption and ZnO photodecomposition, both irreversible chemical changes. If Eq. (2a) occurs with a high capture cross section, the O_2^- will be rapidly consumed. We will assume that reaction (2a) (oxygen desorption) has a much higher probability than (2b) (decomposition).

Surface Recombination

After an integrated illumination time of 4×10^3 min, when the conductance degradation is no longer rapidly changing, Eqs. (2c) and (2d) are assumed to dominate. Converting rate laws for these reactions to the usual solid state symbolism, we have for U_n, the net electron capture rate, and for U_p, the net hole capture rate:

$$U_n = K_n \{ n_b^* e^{-eV_s/kT} [Fe(III)] - n_i [Fe(II)] \} \quad (3)$$

$$U_p = K_p p_b^* e^{eV_s/kT} [Fe(II)] \quad (4)$$

as it is assumed here and later that on ZnO thermal hole generation does not occur because of the large energy gap. Here V_s is the surface barrier defined as positive with the bands bent up, the square brackets indicate concentration, and the other symbols are those commonly used[20] (the K's are rate constants, p_b^* and n_b^* are the bulk hole and electron concentrations, and n_i is a factor depending on the surface state energy level and temperature, but assumed constant in this system).

At steady state, $U_p = U_n$. Clearly as we change the illumination intensity, we change p_b^*. Steady state can be reestablished either by a change in [Fe(III)], where $\delta[Fe(III)] = -\delta[Fe(II)]$, or by a change in V_s. (We will assume n_b^* is reasonably close to [Zn], the concentration of added zinc, and thus constant.)

It can be shown by theoretical arguments that with $[Fe] \geq 5 \times 10^{14}$ cm^{-2}, any significant change in level population would provide a huge change in V_s whether the surface layer were depletion or accumulation. Thus one expects the dominant variable in Eqs. (3) and (4) to be V_s. We can also

show this directly from the experimental data. The photoconductance is found from Fig. 5 to be at most 3×10^{-4} mhos. From Eq. (5)

$$\Delta G = \Delta n_s e \mu W/L \qquad (5)$$

[where n_s is the number of electrons/cm^2 contributing to the conductance, W/L is the width to length ratio of the crystal (~3 for our sample), μ is the electron mobility, assumed 100 cm^2/V sec], we find the corresponding $\Delta n_s \sim 6 \times 10^{12}$. This corresponds to a charge transfer negligible compared to the additive concentrations. Thus from either a theoretical or experimental basis we conclude [Fe(II)] and [Fe(III)] should be considered as constants in Eqs. (3) and (4).

Now the solution of Eqs. (3) and (4) becomes straightforward, with a few simplifying assumptions. We assume under illumination the hole current to the surface is proportional to the light intensity I and independent of other parameters:

$$U_p = \alpha I = K_p p_s [Fe(II)] \qquad (6)$$

where p_s is the hole density in cm^{-2} at the surface and α is a constant of proportionality. We assume a linear relation between the extra charge in the ZnO and the surface potential

$$e\Delta n_s = C\Delta V_s \qquad (7)$$

where C is the effective capacity and where Δp_s is assumed negligible. With [Fe(II)] $\cong$ [Fe(III)], and assuming the surface state at about 0.1 eV below the conduction band,[12,15] we can easily show that an

accumulation layer should be present for $[Zn] \lesssim 10^{17}$ cm^{-3}. Thus we anticipate that C will be the order of 1 μF/cm^2.[20]

Solution of these equations leads to a steady state photoconductance of

$$\Delta G_{photo} = (CkT\mu W/L) \ln \{1 + (\alpha I/K_n[Fe][n_1])\} \quad (8)$$

which can be compared to the results of Fig. 5. When the value of [Fe] is high, Eq. (8) shows ΔG should become linear in light intensity. This is approached by the results for $[Fe] = 10^{16}$ cm^{-2}. When the value of [Fe] is low, as with the curve for $[Fe] = 5 \times 10^{14}$ cm^{-2} in Fig. 5, ΔG should be proportional to the log of the light intensity with C the only unknown in the expression for the slope. We find from the observed slope approximately C = 2 μF/cm^2, a reasonable value.

Deviations from steady state values lead to an equation of the form

$$d\Delta n_s/dt = B\{1 - \exp \beta\Delta n_s\} \quad (9)$$

where B and β are constants, with its solution,

$$1 - e^{-\beta\Delta n_s} = Ae^{-\beta Bt} \quad (10)$$

where A is the integration constant. This is a modified Elovich equation, highly nonlinear, and easily reconciled to most experimental data. It has been discussed in earlier work.[21] We will not go through the exercise of showing that nonlinear results such as those of Fig. 4 can be fitted to it.

From the photoconductive response studies it appears that the action of the additive as a recombination center follows a conceptually simple, but mathematically nonlinear model.

Photolysis

In this section we wish to calculate the rate of photodecomposition (Eq. 2b), and compare the predictions to Figs. 2 and 3. Unfortunately when we consider the initial stages of illumination, we cannot neglect photodesorption of oxygen, as we did above.

First, let us consider the case with pure ferricyanide and that with pure ferrocyanide on the surface. In the case where Fe(III) is the sole additive, neither (1), (2a), nor (2c) can occur to any appreciable extent. Thus the only hole capture process remaining is photolysis, (2b). Experimentally we note that, with only Fe(III) on the surface at concentration 10^{16} cm^{-2}, the degradation is 100 times more rapid than when 5×10^{15} cm^{-2} each of Fe(II) and Fe(III) is added. As expected, the presence of Fe(II) to compete in the hole capture process is required.

The case (Fig. 3) where Fe(II) is the sole additive represents the next stage of complexity. Clearly with only a donor additive present, in high concentration and at an energy level just 0.1 eV below the conduction band, the surface should be highly degenerate, with a high surface conductance. This is not observed experimentally; the surface conductance prior to illumination is approximately 10^{-9} mhos. This low conductance is of course reconciled by oxidation of the surface state according to Eq. (1). However, if we now assume that (2a) is the hole capture reaction of the highest cross section, then the first chemical step will be the desorption of the O_2^-, and the degenerate surface and the high surface conductance should be reacquired. This effect will appear as an apparent conductance degradation, but there is no photolysis involved. Such photodesorption should result in ΔG proportional to t, nearly the relationship experimentally observed and shown in the curve labeled Fe(II) of Fig. 3.

The most important case, of course, is that of the mixture, where the photolysis rate is low due to the Fe(II), and the surface electron density is maintained low by the presence of the Fe(III). In the initial stages of illumination, according to the above theory, the dominant hole capture process will be photodesorption, so little zinc will be produced (2c). However few electrons will be produced due to the (2d) equilibrium. We suggest, then, that during the initial part of the curves of Fig. 2, photolysis is unnaturally slow because the capture cross section for photodesorption is so high. The transition region of Fig. 2 represents the stage of complete photodesorption of oxygen. This transition occurs later if [Fe] is higher, for from Eq. 1, $[O_2^-]$ will also be higher.

We will be interested only in the analysis of the later stages of photolysis when the O_2^- has been assumed so we can neglect photodesorption. Then we can examine the photolysis reaction (Eq. 2b). This reaction can be separated into a series of irreversible steps, for example as follows:

$$p + O_L^= \xrightarrow{k_1} O_L^- \qquad (11)$$

$$p + O_L^- \xrightarrow{k_2} \tfrac{1}{2} O_2 \qquad (12)$$

$$e + O_L^- \xrightarrow{k_3} O_L^= \quad . \qquad (13)$$

The basis for including a recombination step (Eq. 13) in this series is the observation that the "blank" curve tends to saturate as the concentration of electrons builds up. A recombination step of this form seems

most likely without requiring the introduction of other surface states. Steady state analysis of this set of equations yields

$$d[O_2]/dt = \tfrac{1}{2}k_1 k_2 p_s^2/(k_3[Zn] + k_2 p_s) \qquad (14)$$

with p_s the surface hole density, and where we have substituted [Zn] for the concentration of electrons. Now, if most holes are captured by ferrocyanide, p_s is determined solely by (6), and is inversely proportional to [Fe(II)]. Then the rate of degradation must be described by Eq. (5) and

$$d\Delta n_s/dt = 2d[O_2]/dt = \{k_2 k_1 (\alpha I)^2/K_p^2[Fe]^2\}(k_3[Zn] + k_2 p_s)^{-1} \quad . \qquad (15)$$

If the last denominator term of (15) is negligible, clearly the degradation rate is inversely proportional to $[Fe]^2$, as observed experimentally for $t > 10^3$ min. The degradation ΔG is not proportional to time from Eq. (15) for [Zn] will increase with time.

Equation (15) describes the rate of generation of interstitial zinc at the surface. The rate of removal by diffusion (which must equal the generation rate) is derived from the diffusion law:

$$\partial[Zn]/\partial t = D\partial^2[Zn]/\partial x^2 \qquad (16)$$

Simultaneous solution of these nonlinear photochemical (Eq. 15) and diffusion (Eq. 16) laws will presumably predict a time dependence for ΔG between the linear rate expected if the photochemical steps were completely rate-limiting (Eq. 15), and the $t^{\frac{1}{2}}$ rate expected if diffusion were rate-limiting ([Zn] at x = 0 determined completely by the chemistry). Experimentally, however, in Fig. 2 the values of ΔG for $t > 10^2$ min, where the measurements are meaningful, seem less sensitive to time ($t^{\frac{1}{2}}$ to $t^{\frac{1}{3}}$ law).

The two most likely causes for the apparent discrepancy are: a) the zinc is at a concentration far beyond its solubility limit and is precipitating in the bulk material on dislocations, or b) the effective concentration of neutral zinc in the dark (viz., during the measurement), is much lower than the concentration under illumination (when the theory applies). Such a difference should arise because of hole trapping by the lithium acceptors during illumination.

Conclusions

Some degree of control of the surface properties of a typical semiconductor, ZnO, has been accomplished using a one-equivalent surface state, when added in both oxidation states, as suggested by theory. Thus the theoretical objectives of this research have been met. From a practical standpoint, it would be unfortunate if such large quantities ($\sim 5 \times 10^{14}$ cm^{-2}) of surface additive were needed to significantly affect vacuum photolysis. In practice, however, the additive appears to be much more effective on undoped powders suitable for pigments, as will be discussed in later presentations. From both optical absorption (to be published) and ESR studies,[22] preliminary results show negligible degradation with a surface concentration substantially less than 5×10^{13} cm^{-2}. The difference may derive from the crystal imperfections; i.e., the high dislocation density of our lithium doped crystals may cause a higher quantum yield for photolysis.

ILLUSTRATIONS

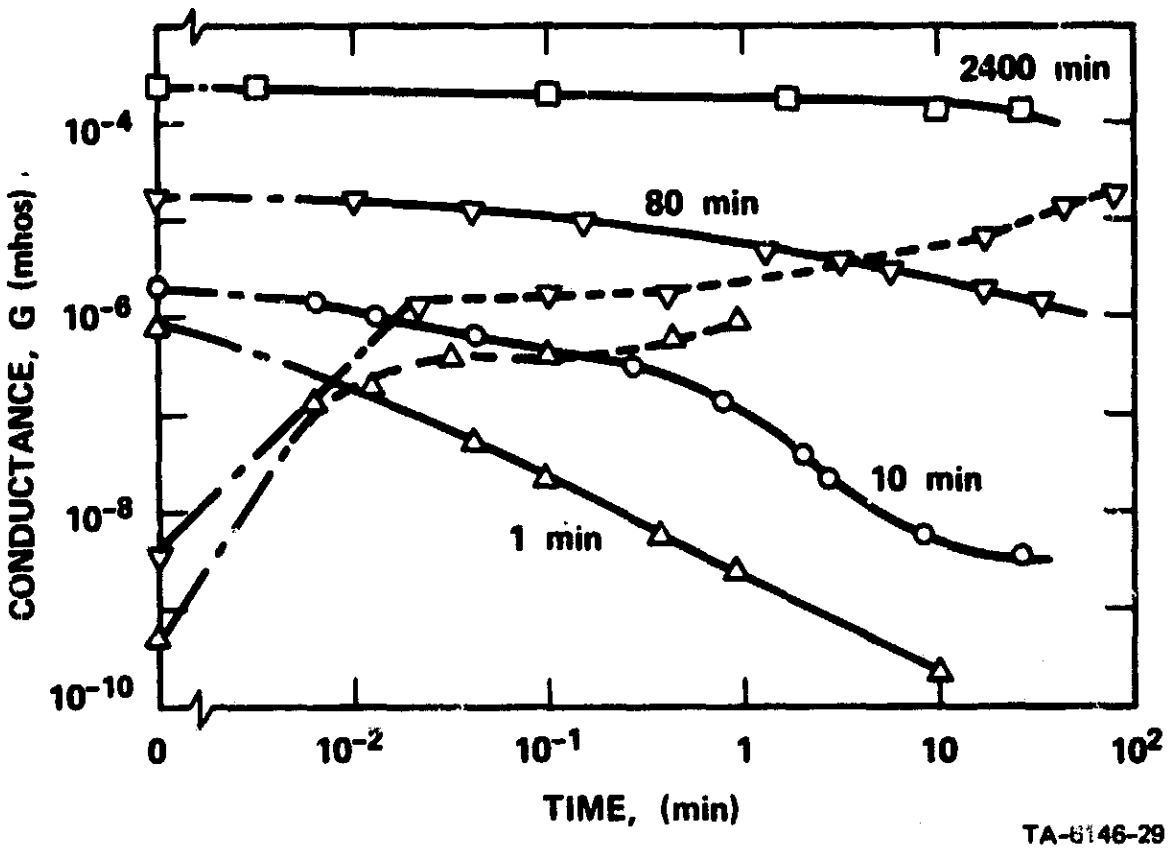

FIGURE 1 TRANSIENT RISE AND DECAY OF CONDUCTANCE. The additive concentration [Fe(II)] = [Fe(III)] = [Fe] = 5×10^{14} cm^{-2}. The parameter indicated on decay curves is the integrated time of illumination prior to readings.

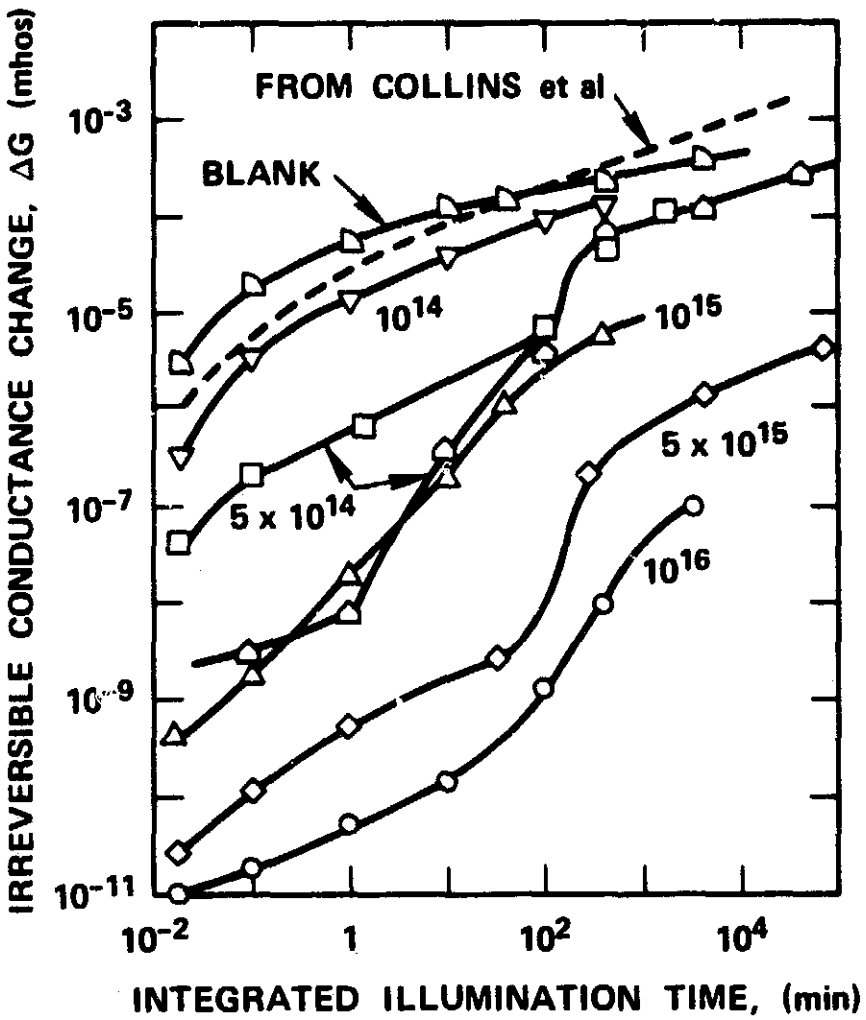

FIGURE 2 DARK CONDUCTANCE INCREASE VERSUS INTEGRATED ILLUMINATION TIME. The numeral indicates the additive concentration in cm^{-2}. The results of Collins and Thomas on additive-free Li-doped ZnO are shown for comparison.

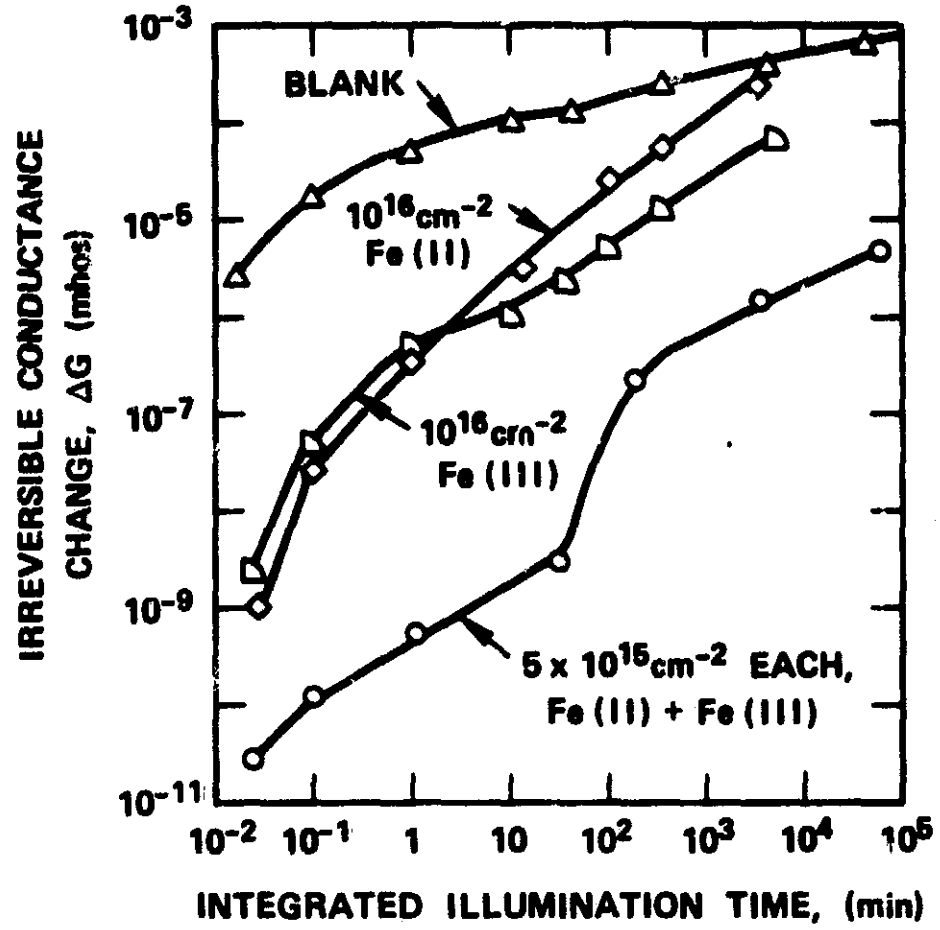

FIGURE 3 DARK CONDUCTANCE INCREASE VERSUS INTEGRATED ILLUMINATION TIME

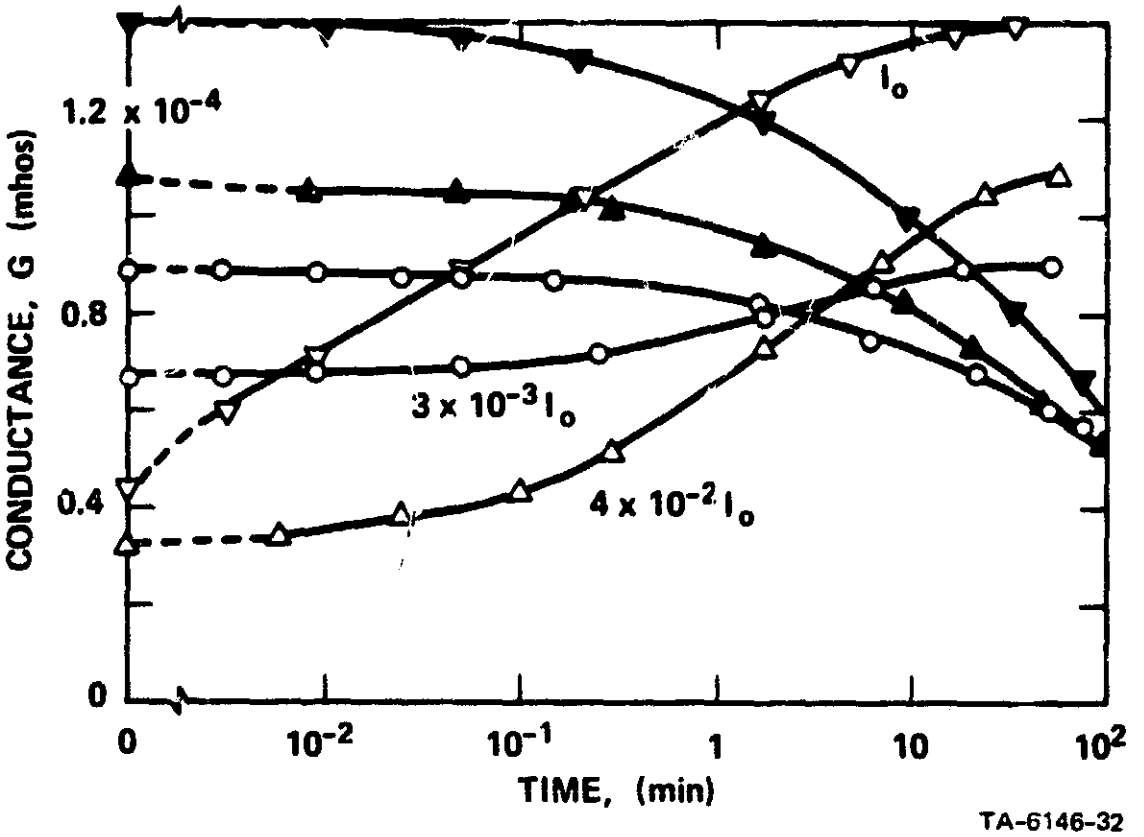

FIGURE 4 TRANSIENT PHOTOCONDUCTIVE RISE AND DECAY WITH VARYING LIGHT INTENSITY. The measurements are all subsequent to 4×10^3 min integrated illumination time, so the steady state dark conductance is varying very slowly. Additive concentration [Fe] = 5×10^{14} cm^{-2}.

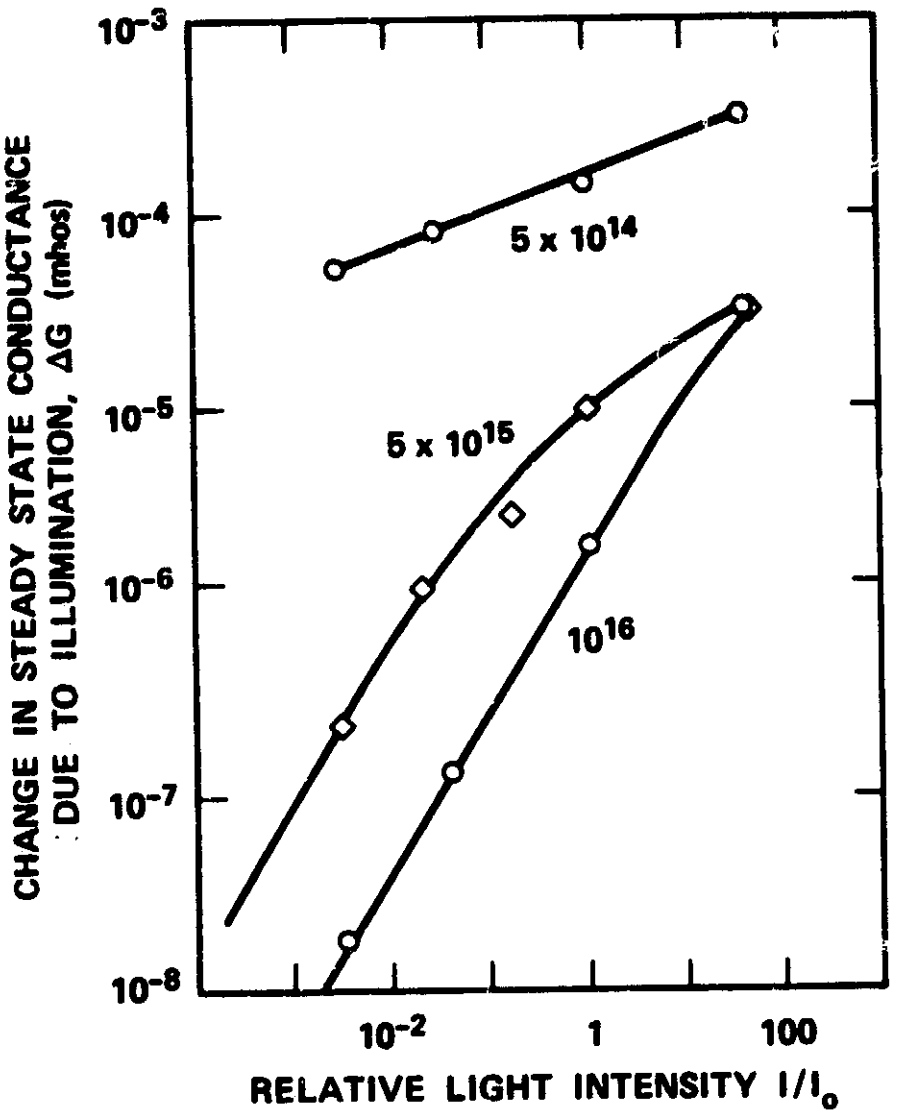

FIGURE 5 STEADY STATE PHOTOCONDUCTANCE VERSUS ILLUMINATION INTENSITY. The additive concentration [Fe] is given in cm^{-2}. The measurements are all subsequent to 4×10^3 min integrated illumination time, so the steady state dark conductance is varying very slowly.

REFERENCES

1. S. R. Morrison, Surface Sci. 10, 459 (1963).

2. P. H. Miller, Jr., Photoconductivity Conference, Atlantic City, N.J., Ed. R. G. Breckenridge (J. Wiley and Sons, Inc., New York, 1954).

3. E. Mollwo, Photoconductivity Conference, Atlantic City, N.J., Ed. R. G. Breckenridge (J. Wiley and Sons, Inc., New York, 1954).

4. R. J. Collins and D. G. Thomas, Phys. Rev. 112, 388 (1958).

5. R. B. Lal and G. Arnett, Nature 208, 1305 (1965).

6. J. S. Blakemore, IEEE Trans. on Aerospace and Electronic Systems AES-2, 332 (1966).

7. Y. Fujita and T. Kwan, Bull, Chem. Soc. Japan 31, 379 (1958).

8. D. B. Medved, J. Chem. Phys. 28, 870 (1958).

9. L. L. Basov and Yu P. Solonitsyn, Kinet. Katal. 6, 752 (1965).

10. C. H. Geisler and G. L. Simmons, Phys. Letters 11, 111 (1964).

11. T. Kwan, K. M. Sancier, Y. Fujita, M. Setaka, S. Fukuyawa, and Y. Kirino, J. Res. Inst. for Catal., Hokkaido Univ. 16, 53 (1968).

12. S. R. Morrison, Surface Sci. 16, 35 (1969).

13. S. R. Morrison and T. Freund, Electrochim. Acta 13, 1343 (1968).

14. W. Gomes, T. Freund, and S. R. Morrison, J. Electrochem. Soc. 115, 818 (1968).

15. S. R. Morrison, Surface Sci. 13, 85 (1968).

16. A. N. Mariano and R. E. Hanneman, J. Appl. Phys. 34, 384 (1963).

17. G. Heiland, P. Kunstmann, and H. Pfister, Z. Physik 176, 485 (1963).

18. S. R. Morrison and T. Freund, J. Chem. Phys. 47, 1543 (1967).

19. H. Van Hove and A. Luyckx, Sol. State Comm. 4, 603 (1966).

20. A. Many, Y. Goldstein, N. B. Grover, "Semiconductor Surfaces," Intersciences, New York (1965).

21. S. R. Morrison, Phys. Rev. 114, 437 (1959).

22. K. Sancier, to be published.

SECTION D

ESR MEASUREMENTS OF VACUUM PHOTOLYSIS OF ZnO POWDERS

Abstract

In the present study ESR is utilized to investigate photodamage of ZnO in powder form and to determine the effects of iron cyanide surface additives and of dislocations. The principal ESR criterion of photodamage is the intensity of the resonance at a g value of about 1.96. This resonance increases in intensity upon ultraviolet irradiation, indicating an increase in the density of unpaired electrons in the ZnO. For the conditions of irradiation, photodamage was not observable when the iron cyanide surface additive was present on ZnO at 10^{-2} monolayers or more, and a minimum in damage appears to occur for a ferri/ferrocyanide ratio of about unity. These results are in qualitative agreement with those on single crystals with iron cyanide surface additives. Preliminary measurements on ZnO damaged by 1-MeV electrons indicate that iron cyanide may also be effective as a protection against particulate damage.

Detailed study reveals two resonances with g values of 1.9564 and 1.9600. Based on the response of the two ESR signals when the ZnO is irradiated and subsequently exposed to oxygen, the signals may correspond to the photodamage defects with optical absorptions in the infrared and visible, respectively. The temperature dependence of the $g \sim 1.96$ line indicates that the paramagnetic electrons are principally in the conduction band of ZnO and that this description is slightly altered at high donor densities.

An ESR investigation of dislocated ZnO (produced by milling) shows that ultraviolet irradiation in vacuum caused the $g \sim 1.96$ line to increase faster than it did for undislocated ZnO.

A preliminary ESR investigation of irradiation damage to lanthanum oxide and zirconium oxide was made using ultraviolet light and 1-MeV electrons; however, the results are inconclusive and further work is needed.

Introduction

The investigation using single crystals of ZnO has shown that a surface additive of iron cyanide provides surface states that are effective in reducing vacuum photolysis of ZnO (Sections A to C). This finding provides valuable information for the design of stable ZnO pigments for thermal control coatings. However, in practice such pigments are used in powder form, and therefore it is desirable to determine the conditions under which the iron cyanide surface additive is effective in reducing vacuum photolysis of ZnO powders.

There are very good reasons for selecting the ESR technique to investigate photodamage in powders. (1) In ZnO there are several paramagnetic centers which, in principle, may be involved in photolysis: donors such as ionized interstitial zinc and ionized oxygen ion vacancies; electrons in the conduction band; holes in the valence band resulting from photoexcitation; various defects such as dislocations and F-centers; and chemisorbed oxygen species such as O_2^-, O^-, and O. (2) The ESR technique has been extensively applied to study ZnO, and several of these studies deal directly with photoeffects.[1-11] (3) ESR is a high frequency technique (10^{10} Hz) and as such is much more suitable for studying semiconductor powders than the dc or low frequency ac techniques that are applicable to single crystals.

In our exploratory studies it was found that the $g \sim 1.96$ line provided a sensitive parameter with which to monitor changes of paramagnetic centers in ZnO due to illumination in vacuum. Thus it became important to understand in detail the origin of the $g \sim 1.96$ line. Although numerous papers have dealt with the nature of the paramagnetic center giving rise to this resonance, the origin of the resonance is still not completely understood. The interpretations fall into two principal categories according to whether the signal is assigned to a paramagnetic electron (1) localized on a donor level[5,7,8,10-13] (where the donor level can arise from defects such as interstitial zinc ions, oxygen ion vacancies, an F-center, or halogen donors), or (2) nonlocalized, in a shallow donor band and/or conduction band.[9,14,15] The situa-

tion is further confused by complexities associated with the g ~ 1.96 line that suggest the existence of more than one paramagnetic center, e.g., more than one type of donor.[5,6,9-13,16] Evidence of complexities is deduced from the effects on ESR spectra by varying pretreatment, doping, adsorption of gases, and temperature of the ZnO. The complexity of the g ~ 1.96 line is illustrated in Table I, which summarizes for various treatments of ZnO the g values, uv sensitivities, and assignments of the resonances reported in various investigations, including that of the present study (items (m) through (o)). At this point two generalizations may be made from the table: (1) two resonances with g values of about 1.957 and 1.960 are observable, and (2) the resonance at the lower g value is photosensitive.

Work performed under the contract consists first of an investigation (using the g ~ 1.96 line as a criterion) of photodamage to ZnO, in particular a study of the effects of the iron cyanide surface additive, and second a study of the nature of the g ~ 1.96 paramagnetic center by measurement of the temperature behavior of the resonance.

Experimental

The details of the ESR equipment are described in Section E. All ESR measurements were made at room temperature.

The zinc oxide samples with surface additives of iron cyanide were prepared in the following way. A 1-g sample of ZnO (N.J. Zinc Co. S.P. 500) was placed in a 15-ml Buchner funnel with a medium frit, and a 5-ml aliquot of an iron cyanide solution was added, mixed with a small glass rod for 1 min, and suction was then applied for 1 min so that all excess solution was removed from the funnel. Such funnels containing ZnO treated with different solutions were placed in an air oven to dry at 400°K for 1 hr, and then the caked ZnO was gently broken up and transferred to bottles. About 0.1 g of these air dried ZnO samples was transferred to quartz tubes (3 mm i.d.) and pretreated in either of two different ways, unless otherwise specified. For ZnO(I) the quartz tube was fused to a vacuum system (oil diffusion pump with traps in liquid nitrogen) in such a way that during evacuation the ZnO could be uv irradiated

or examined by ESR; the pretreatment was a heat treatment at 525°K first in air for 1 hr and then in vacuum (~10^{-4} torr) for 10 min. For ZnO(II) the quartz tube was sealed to a vacuum system, the ZnO was evacuated and heated at 425°K for 0.5 hr, then at 525°K for 0.5 hr, and finally sealed off at a pressure of about 10^{-5} torr. In order to minimize outgassing of the quartz during seal-off, the part of the tube concerned was heated by a furnace to 600°K during the evacuation.

The ZnO samples at a distance of 50 cm were irradiated with unfiltered light from a 200-W mercury-xenon lamp (PEK 210) in a housing equipped with quartz optics and a front surface mirror (system f-number, f/0.55). Irradiation of ZnO(I) was performed in situ but with the ESR cavity removed in order to prevent heating the cavity. Irradiation of ZnO(II) was performed with the sealed tube mounted, along with other samples of a given set, on a quartz rod rotated at about 1 rpm in order to provide uniform irradiation on all sides of the sample.

Solutions containing 0.01 M iron cyanide, which were freshly made up from $K_3Fe(CN)_6$ and $K_4Fe(CN)_6 \cdot 3H_2O$ (Baker's reagent grade), were mixed and diluted to provide solutions with (1) total iron cyanide concentrations in the range of 10^{-2} to 10^{-8}M at a ratio of ferri/ferrocyanide of unity, and (2) ratios of ferri/ferrocyanide in the range of 0.01 to 100 for given total iron cyanide concentrations, e.g., 10^{-6}M.

Lanthanum oxide and zirconium (Research Organic/Inorganic Chemical Co., 99.99+% and 99.5%, respectively) were selaed in individual quartz tubes after heating in situ to 775°K in vacuum for one hr.

Some powder samples in sealed tubes were irradiated with 1-MeV electrons for 1 min with a fluence of 6 x 10^{19} eV/gm. In these experiments the powder was transferred to one end of the tube for electron irradiation and to the other end, which was shielded with lead during the irradiation, for ESR examination.

Results and Discussion

Character of the g ~ 1.96 Line

The appearance of the resonance at g ~ 1.96 and its response to uv irradiation and oxygen adsorption were different for ZnO(I) (continuous pumping) and ZnO(II) (sealed after evacuation). The ESR spectra at g ~ 1.96 for ZnO(I) are shown in Fig. 1. Two lines are evident after the pretreatment, and differences in their behavior are illustrated by their response to uv irradiation and to subsequent exposure to 10 torr oxygen. The g values for these lines were estimated from the cross-over point of the derivative curves to be g_α = 1.9600 and g_β = 1.9564. The intensity of the g_β line was strongly increased by uv irradiation, and after irradiation its intensity decreased with time and with exposure of the ZnO to oxygen. The g_β line vanished when the ZnO was exposed to air at 760 torr, but the effect cannot be reversed by evacuation of the ZnO at room temperature. The g_α line appears to be much less affected by irradiation and subsequent exposure of the ZnO to oxygen.

The decrease of the g_β line with time after irradiation may result in part from electron-hole recombination and in part from the initial lowering of the sample temperature after the irradiation. However, the decrease is most probably caused by readsorption of residual oxygen present on the glass due to desorption from the ZnO during the relatively short evacuation time of the pretreatment.

By contrast, for the case of ZnO(II) only a broad structureless line at g ~ 1.96 was observed in the ESR spectra when the ZnO had been sealed off under conditions that reduced the residual oxygen to low values, i.e., prolonged evacuation and heating of both ZnO and glass. However, evidence of the existence of two resonances in the ESR spectrum of ZnO(II) was indicated by shifts in the g value toward lower values (g_β) upon irradiation and to higher values (g_α) upon subsequent exposure of the sample to oxygen. For example, for ZnO(II) the g value was 1.9570 both after heating in vacuum and after irradiation, and 1.9590 after subsequent exposure to air.

Incidentally, the ESR spectra of ZnO(II) samples sealed in

quartz tubes remained unchanged once the temperature of the samples stabilized at room temperature. This behavior indicates that the adsorption of available oxygen caused the slow decrease in the intensity of the g_β line. With ZnO(II) no change was observed since the oxygen pressure was low.

The uv sensitivity of the line at $g_\beta = 1.9564$ is similar to that at g = 1.9555 reported by Hahn, Nink, and Severin.[7] The present investigation confirms the earlier observation[7] and, in addition, shows that uv irradiation increases both the g_α and g_β lines and that only the g_β line is reduced in intensity by exposure of the ZnO to oxygen.

It is of considerable interest to note that the behavior of the g_α and g_β lines appears to parallel the behavior of optical damage reported in the visible and infrared spectral regions of irradiated ZnO, respectively. In both cases there is evidence for two defects, one recovering upon oxygen exposure, and one "irreversible." Thus it appears that uv irradiation in vacuum gives rise to two principal damage centers that can be detected either optically or by ESR. The latter is probably the more sensitive technique since significant changes are observable after irradiation for 1 hr.

We speculate that these centers are associated with interstitial zinc (g_β) and with excess zinc, which has exceeded the solubility in the ZnO lattice and precipitated at crystal defects such as dislocations (g_α). The results of the temperature dependence of the $g \sim 1.96$ line (Section E) indicate that the paramagnetic electrons are partly in the conduction band (g_β) and partly associated with a donor band at high donor densities (g_α).

Pretreatment

Several considerations enter into the selection of the pretreatment conditions of the ZnO prior to uv irradiation. First, if the pretreatment temperature is too high, there is an interaction between iron cyanide and ZnO. Second, the initial donor density (spin density of the 1.96 line) depends on the pretreatment, and for high sensitivity

we want the initial value to be low. Third, we must remove the recombination center associated with H_2O. The restrictions associated with each of these will be discussed below.

In the first case, when iron cyanide was present on the ZnO, the resonance line disappeared for heating temperatures of 525°K and above, while a substantial increase in the resonance intensity was observed above this temperature when the ZnO had been in a slurry of only water. This relationship is shown in Fig. 2 where the relative spin density is plotted for ZnO(I) after drying from slurries containing water (curve A) or from a 0.01M iron cyanide solution with a ferri/ferro ratio of unity. For convenience the relative spin density is approximated by the product of $I^*_{1.96}\Delta h^2$, where $I^*_{1.96} = I_{1.96}/I_p$, $I_{1.96}$ is the peak-peak intensity, Δh is the line width of the resonance, and I_p is the intensity of the reference signal (0.1% pitch in KCl). The increase of spin density for curve A above 475°K is believed to correspond to the onset of desorption of chemisorbed species, such as oxygen and water, which leads to electron transfer from the surface to the bulk of ZnO. The reason for the decrease of curve B at about 500°K is not definitely known, but it is probably associated with a reaction such as

$$Fe^{+3} + e(.196) \rightarrow Fe^{+2} \qquad (1)$$

which represents the capture by ferricyanide surface states of the conduction electrons of the bulk. This reaction is apparently favored at high iron cyanide concentrations and is of less importance at low concentrations, as can be seen from the VAC-HEAT curves in Figs. 3 and 4 for ZnO(I) and ZnO(II), respectively; note that the ordinate scales differ.

It is of interest to note that as the iron cyanide concentration is increased, the spin density of the resonance drops to low values when the concentration is in a range of about 10^{-4} to 10^{-5}M. This amount of iron cyanide additive on the ZnO surface is about equal to the total number of donors in ZnO. That is, semiquantitative measurements of amount of iron cyanide retained during pretreatment show that a 10^{-5}M iron cyanide solution will provide a surface coverage of 10^{-4} monolayers,

assuming complete dispersal of the additive and a surface area of ZnO of $3m^2/g$. This amount of additive is sufficient to react (according to equation 1) with all the donors in the ZnO, which was found by an absolute spin measurement to have a donor density of $10^{16}cm^{-3}$.

The second consideration in selecting the pretreatment conditions is to optimize the initial donor density. A low initial donor density, such as that obtained in ZnO(I) by heating in air, provides an opportunity to observe uv effects leading to a relatively small increase in spin density of the $g \sim 1.96$ line; whereas a high initial spin density, such as that obtained in ZnO(II) by heating in vacuum without heating in oxygen, results in a high spin density and leads to difficulty in recognizing the relatively small increases caused by uv irradiation.

This point is illustrated in Figs. 3 and 4, which show that the spin densities of the resonance for given treatments, e.g., after vacuum heating or irradiation, are much lower for ZnO(I) than for ZnO(II), but that changes caused by uv irradiation are more evident in the former case.

The third consideration in selecting pretreatment conditions is to assure that the iron cyanide surface states provide the dominant electron-hole recombination centers. In other words, chemisorbed species such as oxygen and water are known to be surface recombination centers for electron-hole pairs, and these must be desorbed in order to minimize their effects relative to that of the iron cyanide. It is assumed that such chemisorbed species on thermal control pigments would eventually be photodesorbed in the high vacuum of outer space, and then the iron cyanide additive would become the effective recombination center. Therefore, in laboratory tests it is necessary to desorb such volatile species. However, in the presence of iron cyanide the desorption temperature is limited by considerations discussed in connection with reaction (1); therefore the desorption temperature should probably not exceed $525^{\circ}K$.

Furthermore, the desorption temperature sequence will influence

the character of the chemisorbed oxygen, and hence the nature of the recombination center, and considerable evidence has been found to support a process of interconversion of chemisorbed oxygen species,[11] any one of which may serve as a recombination center for electron-hole pairs. For example, the O_2^- species is believed to be stable up to temperatures of about 455°K but begins to convert to the O^- species at about 465°K.[20] However, during heating in vacuum, desorption of O_2^- can occur at about 425°K but desorption of O^- requires much higher temperatures. Accordingly, in the pretreatment for ZnO(II), the vacuum heating at 425°K provides for O_2^- desorption, and after most of the oxygen is desorbed and there is little likelihood of conversion to O^-, later heating at 550°K provides for desorption of water and carbon dioxide.

The Effects of Iron Cyanide Surface Additives

It is found by ESR examination, as discussed above, that the changes in properties of ZnO upon pretreatment are different depending upon the presence or absence of iron cyanide additives. Here we show that the changes of properties due to illumination in vacuum are different depending on the presence or absence of iron cyanide. In particular, in the presence of iron cyanide there is a much lower sensitivity to illumination in vacuum. These property changes are monitored by the $g \sim 1.96$ line and will be discussed in terms of (a) the effect of the surface concentration of the additive and (b) the ratio of ferricyanide to ferrocyanide.

The effect of iron cyanide concentration is shown for ZnO(I) and ZnO(II) in Figs. 3 and 4. Three curves are shown, with the spin density $M^*_{1.96}$ measured: (1) after the vacuum-heat pretreatment, (2) as a result of uv irradiation, and (3) after subsequent exposure of the ZnO to oxygen. The iron cyanide is added to the ZnO as described in "Experimental," and for these measurements the ferri/ferro ratio was unity. The effect of irradiation on the spin density (the change between curve 1 and curve 2) is shown more clearly in Fig. 3 [ZnO(I)] where the pretreatment of heating in oxygen has provided a low initial spin density. It is clear that irradiation has little effect on spin density for iron

cyanide concentration $\geq 10^{-3}$M, i.e., a surface coverage of about 10^{-2} monolayers or more. Similar behavior is indicated for the ZnO(II) sample based on data in Fig. 4 obtained at 10^{-6} and 10^{-7}M iron cyanide and further substantiated by the data obtained at 10^{-4}M (large solid point) from results to be presented later in this report.

After exposing the irradiated ZnO to oxygen (curve 3 of Figs. 3 and 4), the spin density decreased. However, it is not clear from the present results to what extent the residual spin density values (curve 3) are determined by the vacuum-heat pretreatments or by the photodamage during irradiation.

Addition of iron cyanide to ZnO also caused an increase in another resonance, that of the broad asymmetric resonance (~1000 Oe) at a g value of about 2.2, which is present in the starting material. Since the ZnO is reported to contain 1 ppm iron*, and ferric ions are reported to give rise to such a resonance,[19] it is tentatively concluded that the increase of the resonance upon addition of iron cyanide is also due to ferric ions. Upon uv irradiation this resonance decreases in peak-peak amplitude by a factor of as much as 0.5, suggesting that ferric ions capture photoproduced electrons and perhaps are converted to ferrous ions or to a ferric ion complex with a broader resonance, which is more difficult to detect. Quantitative measurements of spin density are almost impossible to make because of the broad asymmetric character of this line.

The effect of the ferri/ferro ratio was small and hence difficult to measure experimentally. However, the photodamage may be expected to pass through a minimum for a ferri/ferro ratio in the vicinity of unity. That is, such a recombination center of electron-hole pairs must capture electrons by means of ferric ions at the same rate as holes are captured by ferrous ions, and about equal concentrations of these ions will be required if the respective capture cross sections for electrons and holes are equal.

---

* N. J. Zinc Co., private communication.

The dependence of photodamage on the ferri/ferro ratio was investigated for ZnO(II) exposed to 10^{-6}M iron cyanide. The effect of irradiation time after the vacuum-heat pretreatment is shown in Fig. 5. For the ratios 0.01, 0.1, and 100 the spin density of the resonance increased rapidly within the first hour and then levelled off, whereas for the ratios 1 and 10 very little change in spin density seems to have occurred. The change of spin density after 17 hours' irradiation (Fig. 6) shows a minimum in the vicinity of unity. However, the uncertainties in the data, indicated by the error bars obtained from the variations in the points of Fig. 5, are large. Therefore further work is recommended to determine with greater certainty the effect of ferri/ferro ratio; probably ZnO(I) would be a better substance to study because it has a smaller spin density before irradiation than ZnO(II).

In summary, the iron cyanide surface additive on ZnO in surface coverage of 10^{-2} monolayers or more tends (1) to reduce the spin density of the $g \sim 1.96$ line when the solid is heated in vacuum, and (2) to reduce the tendency of subsequent uv irradiation to increase the spin density of this line. The results in the former case (heating in vacuum) may be associated with capture of conduction electrons of ZnO by ferricyanide at the surface. The results in the latter case (irradiation) show, however, that sufficient ferricyanide must be still present on the surface to provide the ferri/ferro couple required for an electron-hole recombination center and for the observed photodamage protection of the ZnO.

With powders, 10^{-2} monolayers of iron cyanide provide protection, where from the electrical conductivity studies of single crystals of ZnO with iron cyanide additives (Section C) it was determined that 0.1 monolayer was required for observable photodamage protection. The larger surface coverage required for single crystals may be caused either by a tendency of single crystals[1] to have a greater density of dislocations, which may act as hole traps, or of single crystal surfaces to promote growth of larger iron cyanide crystals, which thus reduce the efficiency of surface coverage.

Microwave Skin Effects

The electrical conductivity of ZnO increases with various treatments such as heating in vacuum and uv irradiation, and the presence of iron cyanide seems to enhance the effect. It was essential to determine if the increases in electrical conductivity resulted in microwave skin depth limitations for, if so, the ESR resonance signal intensities would be reduced, and the apparent measured spin density would be too low.

The increase of electrical conductivity is evidenced during ESR measurements by (1) a decrease in cavity Q, which is indicated by the oscilloscope presentation of the cavity mode sweep pattern, (2) by the decrease of the intensity of a reference ESR signal, i.e., I_p, and (3) by a change in the dc bias of the crystal detector (Section E).

In order to test this possibility, samples were prepared where the intergranular conductivity was maintained low by diluting the ZnO. The ZnO was diluted with zirconium dioxide, which is a relatively good insulator and is not easily damaged by uv irradiation. The ESR results obtained from irradiation of ZnO and of ZnO:ZrO_2 mixtures (1:9 weight ratio), without or with iron cyanide applied from 10^{-4} to 10^{-7}M solutions, are tabulated in Table II. For these measurements the samples were pretreated according to the procedure for ZnO(II) except that ZrO_2 was added after the iron cyanide treatment and before the final heating in vacuum. The samples were heated in vacuum either in the "dry" state or after wetting with 1 ml water/g powder ("wet" in Table II) and drying at 400°K. The relative spin densities were measured after a sequence of three steps: heating in vacuum, uv irradiation for one hour, exposure to one atmosphere air. For the ZnO exposed to 10^{-7}M iron cyanide the results for pure "None" and "dry" samples are almost identical and in essential agreement with the data in Fig. 4. Therefore, based on this agreement the absence of a skin effect is demonstrated. The lower values of spin densities for the "wet" sample are probably caused by some loss of iron cyanide (10^{-7}M) when the ZnO-ZrO_2 slurry was dried. Such a loss could occur by partial transfer of the iron cyanide to ZrO_2 crystals.

For the ZnO exposed to 10^{-4}M iron cyanide the spin density was negligible and, since intergranular conductivity must be minimal in these samples, it is concluded that a skin effect is most likely absent. Based on this conclusion an additional point was added to Fig. 4 (the large solid point).

It is concluded that the ESR spin density measurements seem not to have been affected by a microwave skin effect.

Effect of Dislocations

We have developed a model for photodegradation (see Interim Report, Nov. 1968, this project) relating photodamage to dislocations. It was suggested that the dislocations may serve as hole-traps or as sites for precipitation of excess zinc formed as a result of uv photolysis of the metal oxide, and this excess zinc and the strains produced in the crystal by the precipitation may be associated with the excess visible absorption of the photodegraded ZnO.

In order to investigate the effects of dislocations, it seemed natural to extend the ESR measurements to study photodamage of ZnO that was ground mechanically in order to introduce dislocations. Grinding ZnO has been reported to result in an asymmetric ESR triplet signal which disappears upon heating above 373^{0}K;[18] however, effects of uv irradiation were not studied by those authors.

In our study, several grams of ZnO powder were ground with a glass mortar and pestle until the powder was faintly yellow. The ESR spectrum of this powder in the presence of 760 torr air, shown in Fig. 7, exhibits five principal signals which are tabulated as to normalized peak-peak intensities and g values in Table III. Upon evacuation, especially at an elevated temperature, four signals (c, e, f, and g) disappeared which indicates either that desorption of paramagnetic adsorbed species occurred or that traps such as F-centers were emptied. As a result of heating in vacuum the intensity of one resonance (a) at g = 1.9574 increased, a result expected upon desorption of chemisorbed species. Ultraviolet irradiation caused an enhancement of this signal and

also the appearance of a resonance (b) at g = 2.0037. Resonances (b) and (c) are probably identical, and the apparently higher g value of resonance (c) may result merely from the overlap by the intense resonance (e). Subsequent exposure of the ZnO to air resulted in the expected decrease of resonance (a), an increase in resonance (b), and the appearance of a resonance (d) at g = 2.0092. By contrast to the dislocated ZnO, the ESR spectrum of Zno from the "bottle" exhibited only resonance (a) at about one-half the intensity of dislocated ZnO for the "Air, 760 torr" treatment of Table III.

It was of interest to determine whether differences in photodamage are exhibited by normal and dislocated ZnO using the resonance at g ~ 1.96 as a criterion. For this purpose it was convenient to use the mechanically damaged ZnO diluted with ZrO_2 in a 1:9 weight ratio. The dry powders were mixed gently, and then heated at 525°K in vacuum for 1 hr. The results in Table IV list for quantitative comparison the relative spin densities for the normal and dislocated samples, and for specific treatments give the percentage change between the normal and the dislocated sample. Irradiation produced an increase of 24%, which is significant compared to the relatively small changes resulting from the other two treatments.

In summary, we conclude from these results that the ESR technique has revealed several resonance signals, which qualitatively demonstrate that dislocations enhance photodamage. The interpretation of the resonances should, however, be postponed for future study.

1-MeV Irradiation of Oxides

Semiconductors, such as La_2O_3 and ZrO_2, are potentially useful as pigments in thermal protection coatings because their band gaps are larger than that of ZnO; hence, the solids should absorb less solar ultraviolet light. A preliminary ESR investigation was made on these powders to determine whether photodamage could be observed.

Ultraviolet irradiation for one hour of vacuum heated La_2O_3 powder showed essentially no significant changes in ESR spectra at room temperature or at 77°K. However, irradiation of vacuum heated ZrO_2 for

about one hour resulted in a very weak ESR line at about g = 2.00, which increased slightly after continued radiation.

In order to increase photodamage, 1-MeV electrons were used to irradiate the powders; however, no significant changes in ESR were observed for the irradiation conditions employed.

In addition, two samples of ZnO(II) exposed to iron cyanide (ferri/ferro = 1) were irradiated with the 1-MeV electrons. As a result of this irradiation the g = 1.9580 line appeared in the sample treated with 10^{-7}M iron cyanide but did not appear for the sample treated with 10^{-2}M iron cyanide. Thus, the ESR criterion indicates that protection of the iron cyanide additive is qualitatively the same for irradiation by uv and by high energy electrons. This preliminary study is very intriguing and such studies should be pursued further.

REFERENCES

1. R. L. Kroes, A. P. Kulshreshtha, T. Mookherji and J. D. Hayes, Studies of U.V. Irradiation Effects in ZnO-type Thermal Control Coating Pigments," AIAA 4th Thermophysics Conf., San Francisco, June 16-18, 1969, Paper No. 69-639.

2. J. Schneider and O. Schirmer, "ESR in Photoexcited Li dcped ZnO," Z. Naturforschung 18A, 20 (1963).

3. E. V. Baranov, V. E. Kkolmogorov, and A. T. Terenin, "Photoinduced ESR Signals in ZnO," Doklady Phys. Chem. 146, 125 (1962).

4. F. Van Craeynest, W. Maenhout-Van der Vorst, and W. Dekeyser, "Interpretation of the Yellow Color of Heat Treated ZnO Powder," Phys. Status Solidi 8, 841 (1965).

5. P. H. Kasai, "ESR Studies of Donors and Acceptors in ZnO," Phys. Rev. 130, 989 (1963).

6. G. H. Geisler and G. L. Simmons, "High Temperature Induced ESR Signals in ZnO," Phys. Letters 11, 111 (1964).

7. D. Hahn, R. Nink, and D. Severin, "ESR Signal g = 1.957 in ZnO," Phys. Kondens. Materie 5, 371 (1966).

8. R. B. Lal and G. M. Arnett, "ESR of Photosensitive Donors in ZnO," J. Phys. Soc. Japan 21, 2743 (1966).

9. R. J. Kokes, "Influence of Chemisorption of Oxygen on the ESR of ZnO," J. Phys. Chem. 66, 99 (1962).

10. J. Schneider and A. Räuber, "ESR of Donors in ZnO," Z. Naturforschung 16A, 713 (1961).

11. T. Kwan, K. M. Sancier, Y. Fujita, M. Setaka, S. Fukuzawa, and Y. Kirino, "Photoadsorption and Photodesorption of Oxygen and Inorganic Semiconductors as Investigated by ESR," J. Res. Inst. Catalysis, Hokkaido Univ., 16, 53 (1968).

12. M. Codell, H. Gisser, J. Weisberg, and R. D. Iyengar, "ESR Study of Hydroperoxide on ZnO," J. Phys. Chem. 72, 2460 (1968).

13. H. Ueda, J. Can. Chem. 46, 891 (1968).

14. K. A. Müller and J. Schneider, "Conduction ESR in Group II-VI Semiconductors and Phosphors," Phys. Letters 4, 288 (1963).

15. M. Setaka, K. M. Sancier, T. Kwan, "ESR Investigation of Electrical Conductivity Parameters of ZnO During Surface Reactions," J. Catalysis (in press).

16. R. J. Kokes, "Study of Oxygen Species on ZnO by ESR," Proc. Int'l. Congr. Catalysis, 3rd Amsterdam, p. 482 (1965).

17. R. D. Iyengar, V. V. Subba Rao, and A. C. Zettlemoyer, "ESR Studies of the Interaction of O_2, NO_2, NO and Cl_2 with ZnO," Surface Science 13, 251 (1969).

18. V. B. Golubev and V. B. Evdokimov, Zh. Fiz. Khim. 38, 477 (1964).

19. K. Sancier and H. Inami, J. Catalysis 11, 135 (1968).

20. H. Chon and J. Pajares, J. Catalysis 14, 257 (1969).

Table I

SUMMARY OF INDICATIONS OF TWO-FOLD CHARACTER OF g ~ 1.96 LINE OF ZnO

Pretreatment	g Values	UV Sensitive*	Assignment	Ref
(a) 1175°K - air	$g_{\|\|}$ = 1.956 $g_{\perp}$ = 1.957	+	} oxygen ion vacancy	5
(b) -	$g_{\|\|}$ = 1.956 $g_{\perp}$ = 1.955	+	} mobile electrons either in conduction band and/or shallow donor bands	14
(c) 1175°K + Cl^-	1.960		substitutional halogen donor	5
(d) 1250°K - air	1.957	+-	surface and bulk donors	6
(e) None	1.957+	+	bulk donor	6
(f) 1200°K - air, then 1125°K - air	1.9555 1.9580	+ -	interstitial oxygen ions oxygen defects	7
(g) 775°K - vac	1.9567		interstitial Zn_i^+	12
(h) 775°K - vac, then O_2 or TBHP	1.9660 1.9620		interstitial Zn_i^+ oxygen ion vacancy	12 12
(i) 775°K - O_2, vac	1.9607		oxygen ion vacancy	12
(j) 775°K - vac, then O_2, NO, etc.	1.957 1.961		cf (f)	17
(k) 1425°K - vac - Zn	1.957	+	electrons bound at donor sites	10
(l) None - air	1.9539	+	F-center	8
(m) 575°K - vac + O_2	1.9564(β) 1.9600(α)	+ -	precipitated Zn_p^+ interstitial Zn_i^+	This paper
(n) 575°K - vac, 95°K 550°K	1.9578(β) 1.9600(α)			Section E
(o) ZnO:In - vac 525°K	1.9490			Section E

* Increase in ESR intensity indicated by +, no effect by - .

Table II

TEST OF MICROWAVE SKIN EFFECT:
EFFECT OF MIXING ZrO_2 WITH ZnO ON THE UV DAMAGE
MEASURED BY THE RELATIVE SPIN DENSITY OF THE g ~ 1.96 LINE

ZnO[a]	Diluent[b]	Relative Spin Density,[c] $M^*_{1.96}$		
		Heat - Vac	UV 1 hr	Air
ZnO · 10^{-7} Fe	None	48	64	10
	ZrO_2, dry	43	64	13
	ZrO_2, wet	24	45	8
ZnO · 10^{-4}M Fe	None	Nil	Nil	2
	ZrO_2, dry	Nil	Nil	Nil
	ZrO_2, wet	Nil	Nil	5

(a) Pretreatment as for ZnO(II).

(b) Ratio of ZnO/ZrO_2 is 1/9 by weight; for "dry" sample components just mixed, and for "wet" sample 1 g dry mix was wetted with 1 ml water and dried in air at 400°K.

(c) Experimental values of $M^*_{1.96}$ of ZnO with ZrO_2 have been increased by factor 10 to normalize to pure ZnO.

Table III

RELATIVE PEAK-PEAK INTENSITIES

OF ESR LINES OF DISLOCATED ZnO[a]

Treatment	g value[b]						
	a	b	c	d	e	f	g
	1.9574	2.0037	2.0044	2.0093	2.0136	2.0187	2.0368
• Air - 760 torr	55	Nil	20	Nil	200	30	55
• Vac - 300°K	45	Nil	10	Nil	150	10	Nil
• Vac - 450°K	180	Nil	Nil	Nil	Nil	Nil	Nil
• UV - 1.5 hr	820	60	Nil	Nil	Nil	Nil	Nil
• Air - 760 torr	350	90	Nil	35	Nil	Nil	Nil

(a) ZnO ground with glass mortar and pestle until a faint yellow.

(b) The letters designating the resonances have no relationship to the letters designating pretreatment in Table I.

Table IV

EFFECT OF UV ON RELATIVE SPIN DENSITY OF g = 1.957 LINE OF NORMAL AND DISLOCATED ZnO MIXED WITH ZrO_2 (1:9)[a]

Treatment	Relative Spin Density, $M^{*}_{1.96}$		
	Normal	Dislocated	% Change
Vac - 525°K	14.4	14.2	-1
UV - 1 hr	14.9	18.5	24
Air - 760 torr	1.9	1.8	-5

(a) Zno ground with glass mortar and pestle prior to mixing with ZrO_2.

FIGURE CAPTIONS

Figure 1 ESR spectra in the vicinity of $g \sim 1.96$ line for ZnO(I) before and after ultraviolet irradiation. Curve at 60 min obtained after ZnO was exposed to 10 torr O_2. $g_\alpha = 1.9600$ and $g_\beta = 1.9564$.

Figure 2 Effect of vacuum heating on the relative spin intensity, $I^*\Delta h^2$, of ZnO prepared from (A) water slurry and (B) slurry containing 0.01M iron cyanide with ferri/ferro ratio = 1.

Figure 3 Effect of iron cyanide concentration at ferri/ferro ratio = 1 for ZnO(I): (1) heated at 525°K in air one hour and then in vacuum 10 min, (2) ultraviolet irradiated one hr, and (3) exposed to air and evacuated.

Figure 4 Effect of iron cyanide concentration at ferri/ferro ratio = 1 for ZnO(II):

(1) vacuum heated at 425°K 30 min, then at 525°K 30 min,

(2) ultraviolet irradiated 1 hr, and

(3) exposed to air and evacuated.

Figure 5 Effect of ultraviolet irradiation time on relative spin density, $M^*_{1.96}$, of ZnO(II) treated with 10^{-6}M iron cyanide with different ratios of ferri/ferro cyanide.

Figure 6 The effect of ferri/ferro ratio for ZnO(II) treated with 10^{-6}M iron cyanide on the change of relative spin density, $\Delta M^*_{1.96}$, caused by ultraviolet irradiation for 17 hours.

Figure 7 ESR spectrum of mechanically ground ZnO in air at 760 torr.

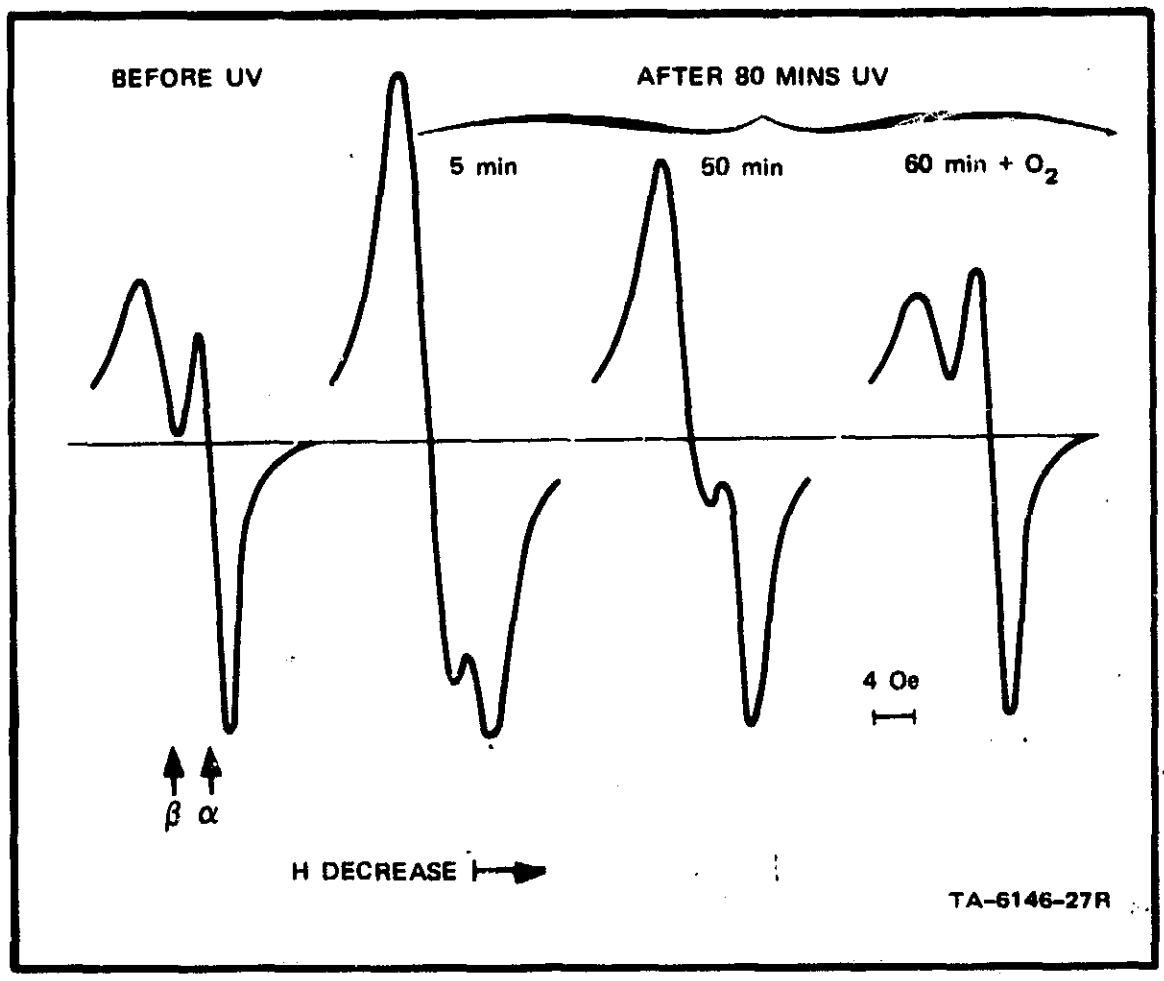

FIGURE 1 ESR SPECTRA IN THE VICINITY OF g ~ 1.96 LINE FOR ZnO(I) BEFORE AND AFTER ULTRAVIOLET IRRADIATION. Curve at 60 min obtained after ZnO was exposed to 10 torr O_2. g_α = 1.9600 and g_β = 1.9564.

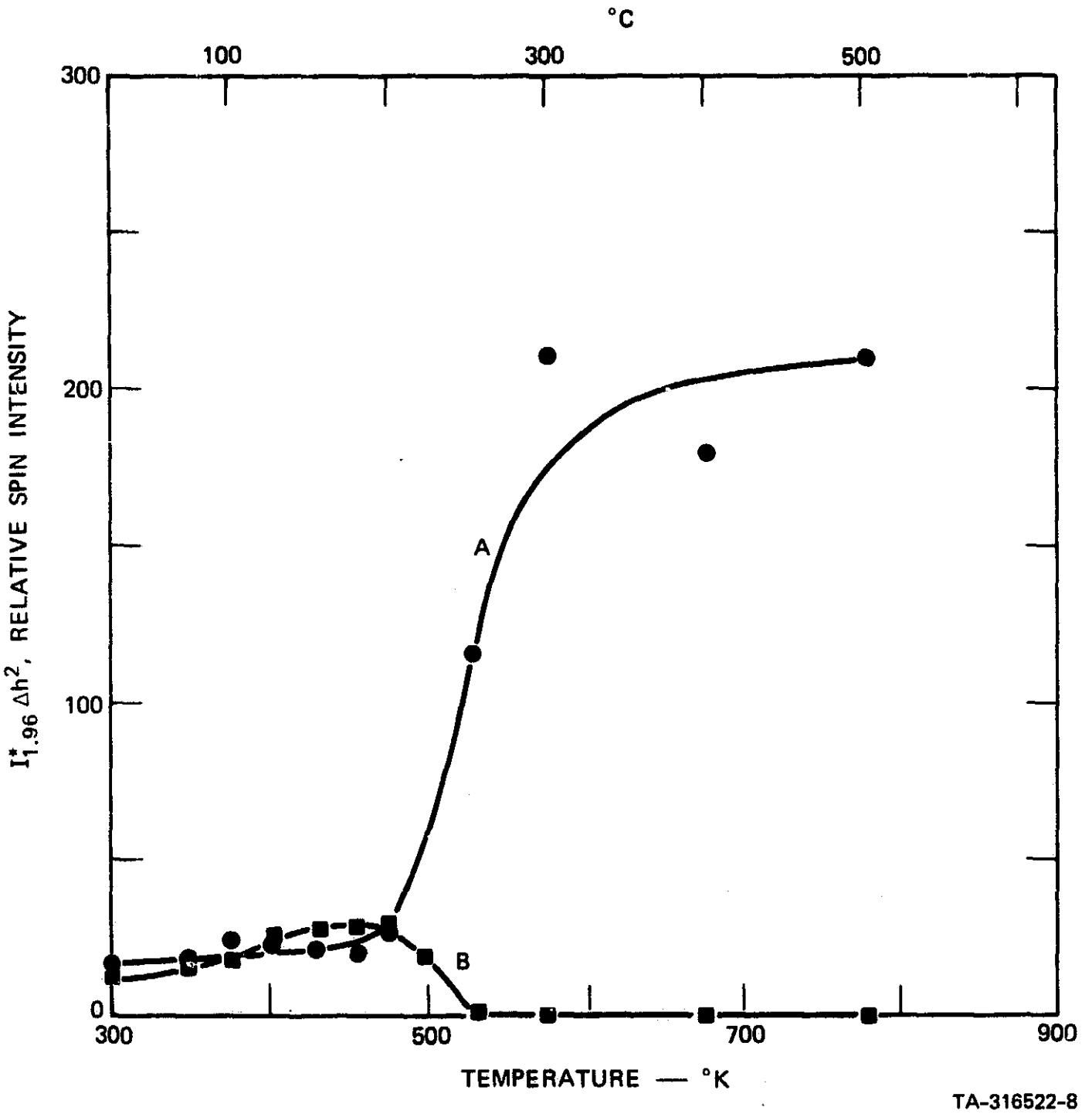

FIGURE 2 EFFECT OF VACUUM HEATING ON THE RELATIVE SPIN INTENSITY, $I^*\Delta h^2$, OF ZnO PREPARED FROM (A) WATER SLURRY AND (B) SLURRY CONTAINING 0.01M IRON CYANIDE WITH FERRI/FERRO RATIO = 1

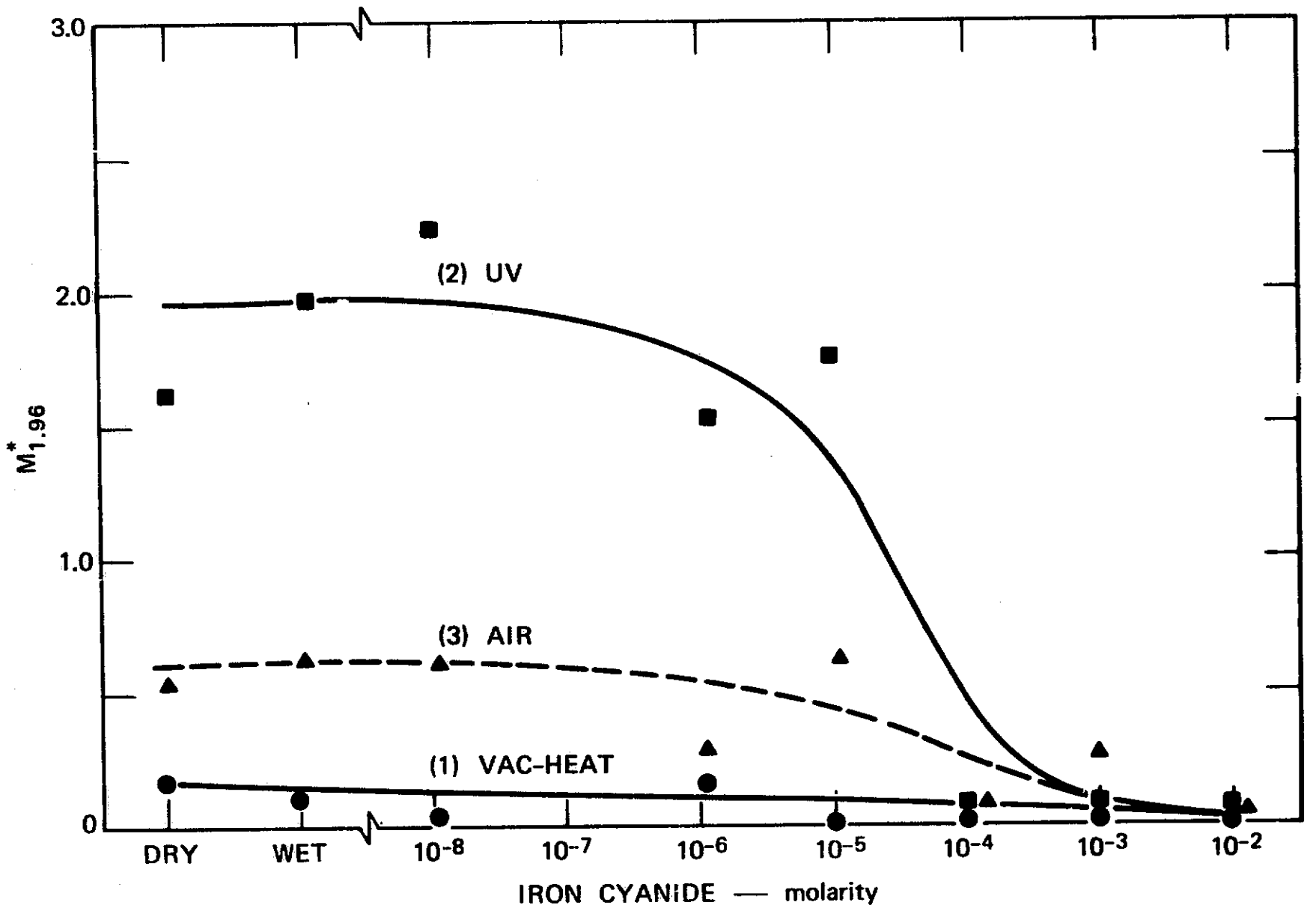

FIGURE 3 EFFECT OF IRON CYANIDE CONCENTRATION AT FERRI/FERRO RATIO = 1 FOR ZnO(I): (1) HEATED AT 525°K IN AIR ONE HOUR AND THEN IN VACUUM 10 MIN, (2) ULTRA-VIOLET IRRADIATED ONE HOUR, AND (3) EXPOSED TO AIR AND EVACUATED

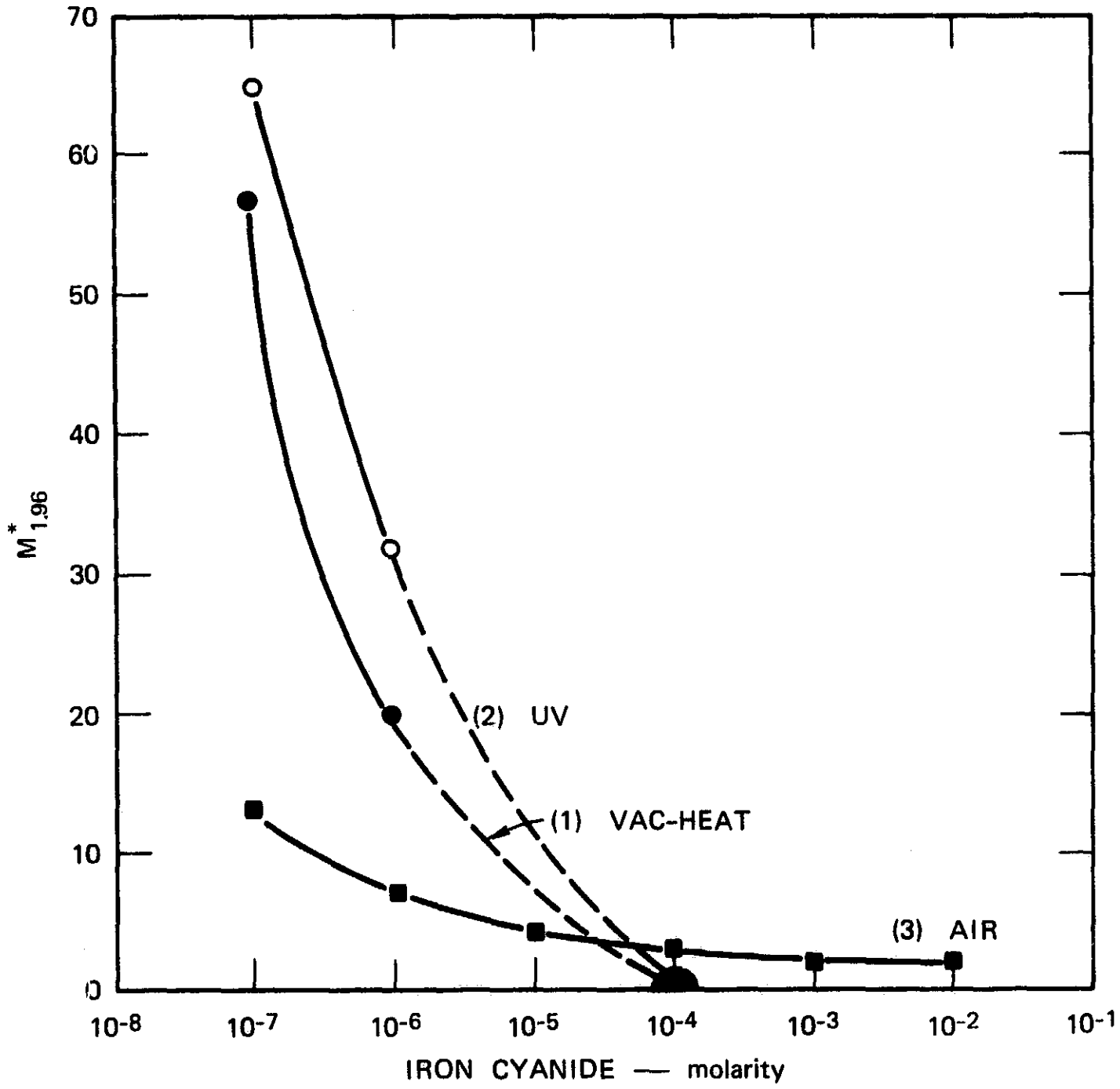

FIGURE 4 EFFECT OF IRON CYANIDE CONCENTRATION AT FERRI/FERRO RATIO = 1 FOR ZnO (II):

(1) Vacuum heated at 425°K 30 min, then at 525°K 30 min,
(2) Ultraviolet irradiated 1 hour, and
(3) Exposed to air and evacuated.

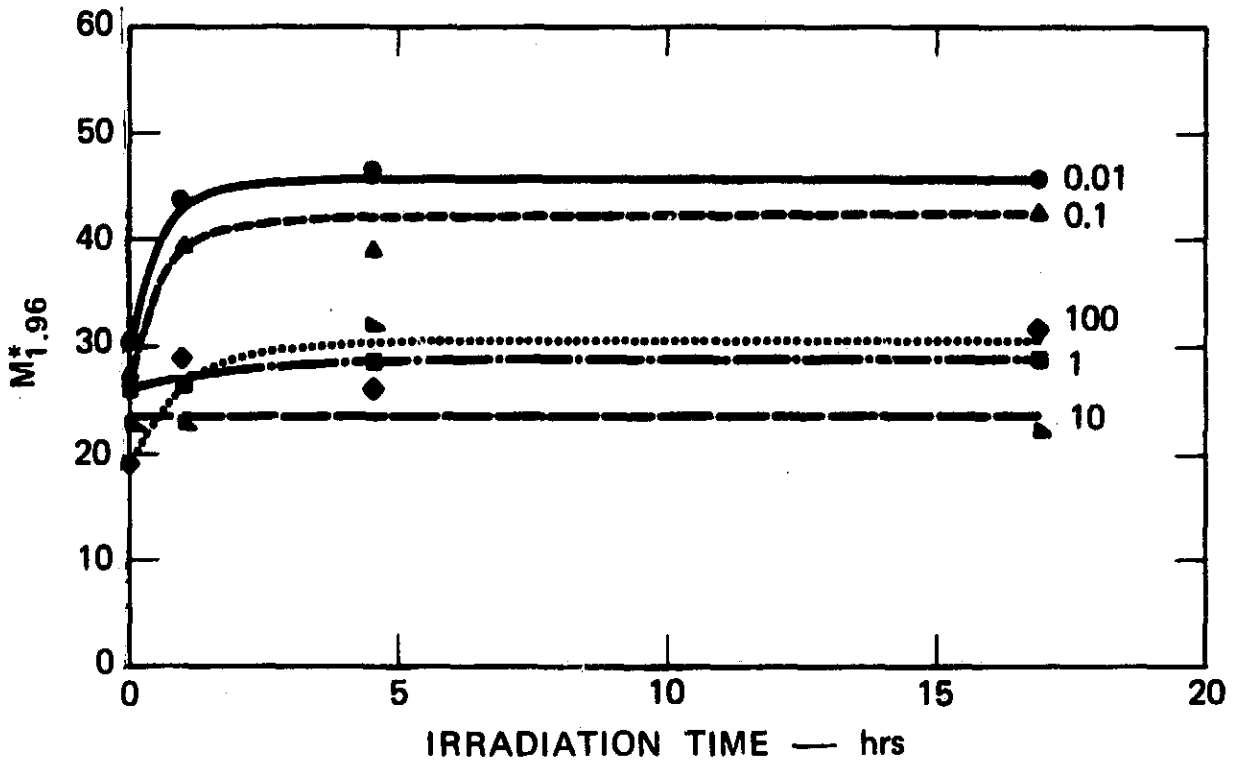

FIGURE 5 EFFECT OF ULTRAVIOLET IRRADIATION TIME ON RELATIVE SPIN DENSITY, $M^*_{1.96}$, OF ZnO(II) TREATED WITH 10^{-6}M IRON CYANIDE WITH DIFFERENT RATIOS OF FERRI/FERRO CYANIDE

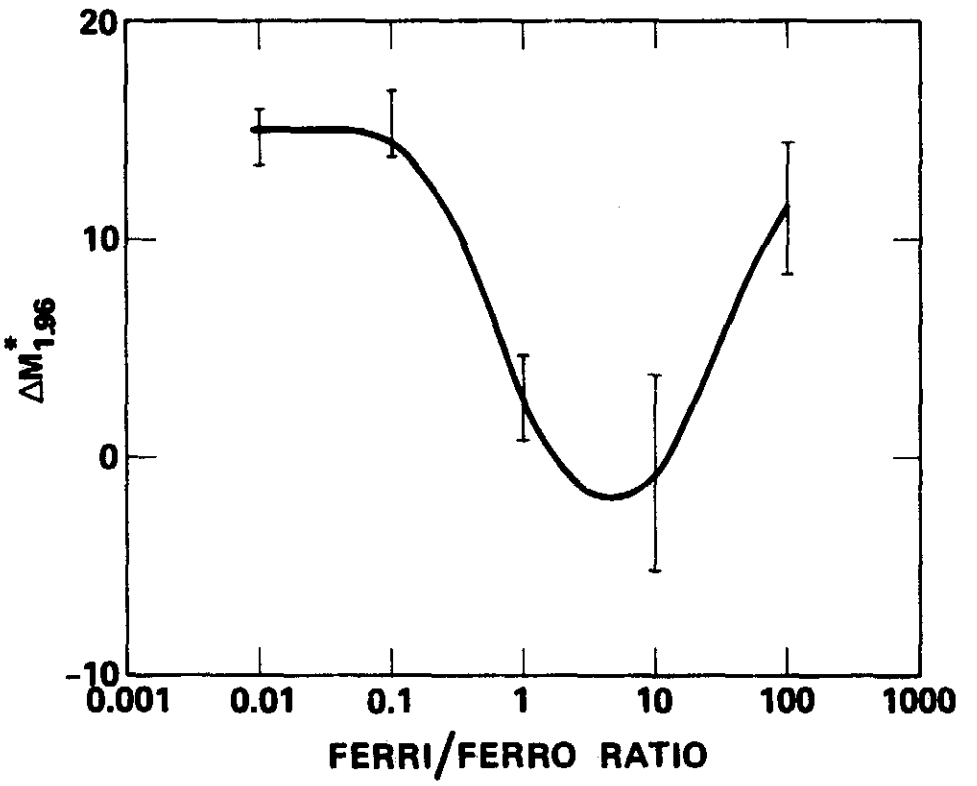

FIGURE 6 THE EFFECT OF FERRI/FERRO RATIO FOR ZnO(II) TREATED WITH 10^{-6}M IRON CYANIDE ON THE CHANGE OF RELATIVE SPIN DENSITY, $\Delta M^*_{1.96}$, CAUSED BY ULTRAVIOLET IRRADIATION FOR 17 HOURS

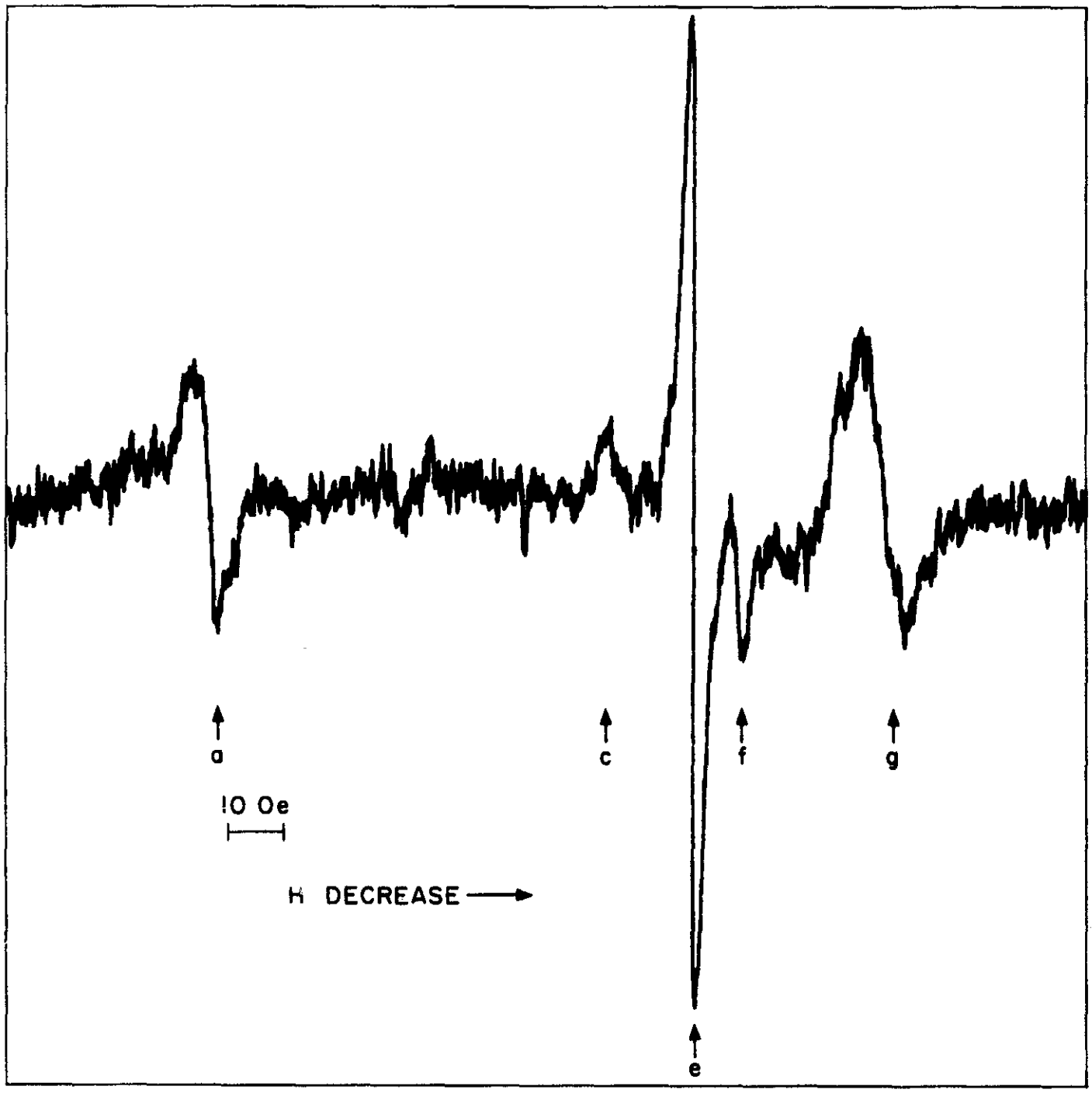

FIGURE 7 ESR SPECTRUM OF MECHANICALLY GROUND ZnO IN AIR AT 760 TORR

SECTION E

IONIZATION ENERGY OF DONORS IN ZnO POWDER DETERMINED BY EXTENDED ESR MEASUREMENTS*

K. M. Sancier

Solid State Catalysis Laboratory
Stanford Research Institute
Menlo Park, California 94025

Abstract

Ionization energies of donors in powder samples of ZnO, both undoped and In-doped, and of mixtures of ZnO and ZrO_2 were determined by two methods: (1) using the temperature dependence of ESR measurements of the $g \sim 1.96$ line and (2) using two electrical conductivity parameters, $1/I_p$, the reciprocal ESR intensity of a reference sample, and I_{cc}, the dc bias current of the microwave crystal detector. A theoretical treatment was developed to account for the temperature dependence of magnetic susceptibility and for the population of the donor level and the conduction band according to the semiconductor band model, and electron mobility. The donor ionization energies calculated with the electrical conductivity parameters are between 0.033 and 0.049 eV, in the range of reported values. The donor ionization energy obtained from the $g \sim 1.96$ line is about 0.011 eV for ZnO and ZnO + ZrO_2 and essentially zero for ZnO:In. It is concluded that the $g \sim 1.96$ line of ZnO can be assigned principally to electrons in the conduction band, but the lower temperature dependence of this resonance is tentatively attributed to the presence of high local densities of a modified zinc donor.

* This research was supported by the Jet Propulsion Laboratory, California Institute of Technology, sponsored by National Aeronautics and Space Administration under Contract NAS 7-100.

Introduction

Despite the considerable volume of published research on zinc oxide, its physical properties are still not adequately understood. Further studies have been spurred by applications of ZnO to electrophotography and more recently by the need for an ultraviolet-stable white pigment as a thermal control coating for satellites in outer space. Both these technologies are based on the solid-state properties of ZnO in the powder form. As ESR is particularly suited for determining the properties of samples in the form of powders, we have developed the ESR technique to provide information about the properties of ZnO donors in powdered samples. This paper concerns an investigation of the temperature dependence of the ESR line at $g \sim 1.96$, which appears to be associated with the mechanism of ultraviolet damage, and of two electrical conductivity parameters measurable by extended ESR measurements.

The character of the paramagnetic center in ZnO giving rise to the ESR signal at $g \sim 1.96$ is still open to question, although numerous papers have dealt with the subject.[1-11] Interpretations of the paramagnetic center fall into two categories according to whether the signal is assigned to an electron (1) on a donor level[1,4,8,10] or (2) in a shallow donor and/or in the conduction band.[2,3,11] The situation can be described by the reversible reaction

$$Zn_i \rightleftarrows Zn_i^+ + e \ . \qquad (1)$$

According to this relation, the donor, which we assume to be interstitial zinc, Zn_i, is ionized to form an ionized donor Zn_i^+ and an electron in the conduction band e. Both Zn_i^+ and e are expected to be paramagnetic. At room temperature the forward reaction is almost complete, since from Hall effect measurements the energy level for this ionization is about 0.05 eV below the bottom of the conduction band.[12] Much higher temperatures are required[12] for ionization of an electron from Zn_i^+. At higher donor densities, a donor band may form which may become degenerate with respect to the conduction band.[3]

The evidence favors the assignment of the paramagnetic center to

an electron in the conduction band. The strongest evidence for this assignment derives from the fact that the g ~ 1.96 line intensity is rapidly reduced to low values when an electron acceptor such as oxygen is sorbed on ZnO.[11,13,14] Under these conditions chemisorption of the oxygen removes only electrons from the conduction band, whereas the more slowly diffusing Zn_i^+ remains in the bulk. According to this view the paramagnetic Zn_i^+ centers do not give rise to an observable ESR signal. After chemisorption has ceased, the residual g ~ 1.96 line intensity is attributed to the central volume of a ZnO crystallite not included in the space charge region. Further support for assigning the paramagnetic center to conduction electrons is based on the absence of hyperfine splitting when ZnO is doped with donors such as gallium and aluminum, which possess nuclear moments.[2]

When the resonance has been attributed to an electron localized on a donor level, the latter has been assigned not only to interstitial zinc ions, Zn_i^+, but also to oxygen ion vacancies,[1,9,10] to an F center where the electron is trapped at an oxygen vacancy,[7] and to halogen donors.[4] The suggestion of the existence of more than one type of donor site is supported by the complexity of the g ~ 1.96 line, which depends upon pretreatment, doping, subsequent adsorption of gases, ultraviolet irradiation, microwave power level, and temperature.[2,4-6,8-10]

Studies of the temperature dependence of the ESR signal at g ~ 1.96 should provide useful information about the nature of the paramagnetic center. However, past temperature studies on the g ~ 1.96 line have not adequately accounted for all necessary factors. For example, the temperature data of Schneider and Rauber[1] on a ZnO single crystal were corrected by Müller and Schneider[3] by applying approximations for the temperature dependence of magnetic susceptibility, microwave skin depth, and ESR line width. The corrected results showed no temperature dependence of spin intensity, and it was proposed that the electron was simultaneously in the conduction band and a shallow donor band. In two separate studies with powdered ZnO, it was reported that lowering the temperature from 300° to 77°K increased the signal intensity by a factor of about 4, but account was not taken of the temperature dependence of

the magnetic susceptibility[2] nor of ESR line width or ESR sensitivity changes.[2,15]

The present paper attempts to reexamine the temperature dependence of the ESR signal at $g \sim 1.96$ and to present other relevant data on the electrical conductivity of ZnO powder samples as obtained from the extended ESR technique.[11]

Theory

The ESR measurements provide three parameters, each of which is related to the conduction electron density, n_c, in the ZnO powder samples. In this section we develop expressions by which the three parameters can be used for estimating n_c as a function of temperature, and later in the experimental section the data are tested according to the theory.

In the extended ESR technique, three parameters were developed for describing the change of the density of charge carriers, i.e., electrons in powdered ZnO, as a result of surface reactions such as oxygen chemisorption occurring at a constant temperature. These parameters are (1) $M^*_{1.96}$, the first moment of the $g \sim 1.96$ line, which is normalized for changes in cavity Q and which can be calibrated in absolute spins; (2) I_{cc}, the dc bias current of the microwave crystal detector; and (3) $(1/I_p)$, the reciprocal peak-peak intensity of a reference ESR signal. In the present work, I_p is the signal intensity of a pitch (carbon) sample in the dual cavity accessory, and its value is used to normalize the measured first moment $M_{1.96}$, i.e., $M^*_{1.96} = M_{1.96}/I_p$.

For present purposes, we wish to develop the temperature dependences of these parameters while assuming that chemisorption effects do not occur.

Temperature Dependence of $M^*_{1.96}$

In the case of the first moment, $M^*_{1.96}$ is proportional to the complex magnetic susceptibility, which in turn can be approximated by a Curie law dependence,

$$M^*_{1.96} = Cn_c/T \ , \qquad (2)$$

where C is a constant, n_c is the number of paramagnetic electrons assumed to be in the conduction band of ZnO, and T is the absolute temperature.

For a semiconductor with a donor whose ionization energy with respect to the bottom of the conduction band is E_D, the quantitative relationship of the temperature dependence of n_c, the electron density in the conduction band, and n_D, the density of unionized donors, is given by[13]

$$n_c^2/n_D = N_c \left[(m^{(n)}/m)^{3/2} D^{-1}\right] \exp(-E_D/kT) , \quad (3)$$

where the term in brackets contains constants (electronic mass m, density-of-states effective mass $m^{(n)}$, and spin degeneracy of donor states D) and for ZnO is 0.18,[12] and N_c is the effective density of states of the conduction band and is temperature dependent according to

$$N_c = 2 (2 \pi m k T/h^2)^{3/2} . \quad (4)$$

Combination of equations 3 and 4 with evaluation of some of the constants gives

$$n_c^2/n_D T^{3/2} = 8.7 \times 10^{14} \exp(-E_D/kT) . \quad (5)$$

In order to test this relationship, the term on the left side of the equation can be evaluated by assuming that n_D can be calculated from the expression

$$N_D = n_c + n_D \quad (6)$$

and that N_D, the donor density, is equal to n_c at sufficiently high temperatures where all donors are ionized, i.e., where $n_D = 0$.

Temperature Dependence of ΔI_{cc} and $\Delta(1/I_p)$

The parameters ΔI_{cc} and $\Delta(1/I_p)$ depend upon the electrical conductivity, σ, of the ZnO according to

$$\sigma = \epsilon \mu n_c \quad (7)$$

where ϵ is the electronic charge and μ is the mobility of the electron. It should be noted that the evaluation of n_c by means of $M^*_{1.96}$ is independent of the electron mobility. The temperature dependence of μ and n_c can be approximated by the equations

$$\mu = AT^{-3/2} , \tag{8}$$

$$n_c = B \exp\ (-E_D/kT) , \tag{9}$$

where A and B are constants.

Differentiating equations 7 to 9 with respect to temperature and combining leads to the approximation

$$\ln \left[T^{5/2}\ \frac{\Delta\sigma}{\Delta T}\right] = -\ \frac{E_D}{kT} + \ln\left\{K\left[\frac{E_D}{kT} - \frac{3}{2}\right]\right\} , \tag{10}$$

where the incremental function was substituted for the differential and $K = AB\epsilon$. The value of E_D can be evaluated graphically by plotting logarithm $[T^{5/2}\ \Delta\sigma/\Delta T]$ against reciprocal temperature and assuming that the last term on the right of equation 6 will be slowly varying except at very low temperatures. The appropriate values of $\Delta\sigma/\Delta T$, i.e., $\Delta\sigma_{cc}/\Delta T$, and $\Delta\sigma_p/\Delta T$, are obtained graphically from the temperature dependences of I_{cc} and $1/I_p$, respectively.

Experimental Details

Powdered ZnO was introduced as a 1.5-cm column into a quartz tube 3 mm i.d. and evacuated at about 10^{-5} torr. It was heated at 425°K for 30 minutes, then heated at a higher temperature (cf below) for 30 minutes, and finally the tube was sealed off in vacuum. Three different samples were employed: ZnO (New Jersey Zinc Co., S.P. 500) heated to 575°K; ZnO:In, doped with 6.8×10^{17} cm^{-3} indium (New Jersey Zinc Co.), heated to 575°K; and a 1:9 mixture by weight of ZnO (S.P. 500) and ZrO_2 (Research Organic/Inorganic Chemicals, 99.5%) heated to 525°K.

The ESR measurements were made with a Varian V-4502 X-band spectrometer equipped with a 12-inch magnet, a Fieldial, and a dual cavity (TE_{104}) operated from the microwave bridge in the low-power mode. The ZnO sample was inserted in the one cavity employing 10^5 Hz modulation at

2.50 Oe and containing a temperature-controlled dewar (Varian). Either a sample of 0.1% pitch in KCl (Varian) for measuring cavity sensitivity (I_p) or a MgO:Mn sample for measuring g values was inserted in the other cavity employing 400 Hz modulation. The procedure for normalizing the first moments and obtaining absolute spin intensities has been described earlier.[13]

Results and Discussion

The results and treatment of data for the ZnO sample heated in vacuum to 575°K will be presented in detail, while for the other two samples only the calculated results will be presented.

The temperature dependences of the three parameters for ZnO are shown in Fig. 1, where data were taken starting at the lowest temperature for each curve. The parameter $1/I_p$ is the reciprocal peak-peak intensity of the 0.1% pitch sample, in the accessory cavity, which remained essentially at room temperature. The parameter I_{cc} is the summation of the incremental changes of the crystal current as measured from the lowest temperature; these data were obtained in a separate experiment. After the highest temperature measurement, the values at room temperature were remeasured and were found to be reproduced to within ±1%.

Some qualitative observations should be made at this point. First, the three curves have similar shapes, each with a positive slope and with a linear region at low temperatures, and a tendency to approach a limiting value at high temperatures. Such behavior is consistent with an increase in the electron density in the conduction band of an n-type semiconductor and an ultimate limit resulting from complete ionization of donors. Second, on the basis of the earlier discussion in which the paramagnetic centers were assigned to electrons in the conduction band, the $M^{*}_{1.96}T$ parameter should be related to the conduction electron density.

Similar effects were found with the ZnO - ZrO_2 sample that was examined to determine whether a microwave skin effect occurred with ZnO.

The ZrO_2 was selected because it is a good insulator and can be easily outgassed. The zinc oxide sample doped with indium, ZnO:In, was examined to determine the ionization energy of a doped sample; however, the $M^*_{1.96}T$ parameter showed essentially no temperature dependence.

The data in Fig. 1 will now be treated quantitatively according to the theory described above. The data derived from the $g \sim 1.96$ line are plotted in two ways in Fig. 2. For one curve, only a Curie law compensation is used (equation 2) and the logarithm of $M^*_{1.96}T$ is plotted against reciprocal temperature. For the second curve, the population of donor and conduction band states is explicitly introduced according to equation 5 and the logarithm of $(n_c^2/n_D T^{3/2})$ is plotted against reciprocal temperature. For this curve the donor density, N_D, was taken to be $2 \times 10^{16} cm^{-3}$ based on an absolute spin density determination at room temperature. In order to calculate n_c and N_D at various temperatures, using equation 6, it was assumed at the highest temperature of the experiment that $n_c = N_D$ and that $n_D = 0$. Because of this assumption, the calculated points at the highest temperatures are subject to the greatest error, and this consideration may account for the divergence of the results at the two highest temperatures in Fig. 2.

The donor ionization energies calculated from the linear part of the curves in Fig. 2 are about equal, 0.011 eV with only the Curie law correction and 0.016 eV with additional band model corrections. The latter value is closer to the accepted value of the donor ionization energy, and the close agreement obtained with only the Curie law correction probably results from compensating temperature-dependent effects. The donor density used in the band model expression does not affect the slope of the line in Fig. 2, i.e., does not affect E_D, but it does very much affect the intercept, the theoretical value of which is 8.7×10^{14} cm^{-3} according to equation 5. The experimental intercept of about $2 \times 10^{14} cm^{-3}$ is in satisfactory agreement with the theoretical value and gives confidence in the choice of donor density and the application of the theory.

The data on the electrical conductivity parameters, I_{cc} and

$1/I_p$, treated according to the theory of equation 5, are shown in Fig. 3 by a plot of log $(T^{5/2}\ \Delta\sigma/\Delta T)$ against reciprocal temperature. For convenience the curves have been marked σ_{cc} and σ_p to correspond to the data from the conductivity parameters I_{cc} and $1/I_p$, respectively. The required values of $\Delta\sigma/\Delta T$ were obtained by graphical analysis of the curves in Fig. 1 at the appropriate temperatures. Incidentally, the fact that $\Delta\sigma/\Delta T$ is constant at low temperatures, i.e., in Fig. 1 for the I_{cc} and $1/I_p$ curves up to about 330°K, suggests that in this temperature range compensation occurs between the effects of the electron mobility and of the electron density in the conduction band. The slopes of the linear sections of the two curves in Fig. 3 lead to approximately the same donor ionization energies, E_D = 0.038 to 0.041 eV, which are in the range of about 0.03 to 0.07 eV reported for a variety of ZnO single crystals (Fig. 2, reference 12). The variations within this range and the departure from the accepted value of E_D = 0.051 eV for doped ZnO crystals has been ascribed to variabilities of the donors in undoped ZnO and to stoichiometric excess zinc of some other form that is also a donor.[12] Some caution may also be necessary in extending the results of single crystals to powders.

The ionization energies calculated from the curves in Figs. 2 and 3 are summarized in Table 1, along with the ionization energies obtained from some of the parameters for the two other samples. The agreement between the ZnO and $ZnO\text{-}ZrO_2$ results in Table 1 indicates that skin depth effects are not significant in the ZnO experiment.

For the zinc oxide sample doped with indium, ZnO:In, the values of the donor ionization energies, 0.042 and 0.033 eV (Table 1), obtained from the two conductivity parameters $1/I_p$ and I_{cc}, respectively, are in satisfactory agreement and also are in substantial agreement with the energy value 0.031 eV reported for single crystals of a similar doped level.[16] However, it is difficult to reconcile this expected behavior with the absence of a temperature dependence of the $M^*_{1.96}T$ parameter (Table 1), especially if the three parameters depend only on conduction electrons.

It may be significant that for all three samples lower donor ionization energies were obtained from the $M^{*}_{1.96}T$ parameter than from the two electrical conductivity parameters. It is therefore tempting to speculate that there is a common cause for the lower ionization energies obtained from the data on the $g \sim 1.96$ line. The temperature behavior of the g values and line widths may provide a hint of the cause. In the case of ZnO, the g value increased from 1.9578 to 1.9600 and the line width decreased from 5.6 to 4.5 Oe as the temperature was increased from 95° to 550°K. Fro the ZnO:In sample the g value was a minimum of 1.9490 at 300°K and increased gradually to about 1.9500 at both 100° and 475°K, and the line width increased linearly from 3.0 to 7.0 Oe as the temperature was increased from 100° to 500°K.

These variations in g value and line width can be interpreted by postulating two types of donors. In the case of ZnO there is ample evidence that the $g \sim 1.96$ line is composed of two lines, and our results[17] with oxygen sorption show that the two components have g values of 1.9564 and 1.9600, almost identical to those observed in this study at low and high temperatures, respectively. In this study the line width was too broad to observe the separate components. We have tentatively assigned these two resonances to excess zinc precipitated at defects such as dislocations and to interstitial zinc, respectively.[17] The concept of excess precipitated zinc is supported by the present observation that the donor density in the ZnO determined by an absolute spin measurement is larger by a factor of about 10^2 than the solubility of zinc in ZnO at 575°K reported[12] to be about $2 \times 10^{14} cm^{-3}$. Therefore, it appears that all donors contribute to the $g \sim 1.96$ lines. High donor densities will cause formation of a donor band, which at a donor density of $6 \times 10^{18} cm^{-3}$ will touch the bottom of the conduction band[12] and will result in smaller ionization energies. Accordingly, it is tentatively postulated that high local concentrations of excess zinc result in local donor bands which tend to reduce the temperature dependence of the $g \sim 1.96$ line.

Also in the case of ZnO:In, there is ESR evidence, although not conclusive, of two types of donors which may result in a complex tempera-

ture dependence of the resonance. For example, two types of donors would be consistent with the combined observations that as temperature is increased the g value passes through a minimum and the line width increases substantially as if a single resonant center predominated at low temperature and two centers existed at high temperatures. Note that for ZnO an opposite temperature dependence of line width was observed. Furthermore, the resonance center in ZnO:In is evidently not equivalent to that in ZnO, based on the difference in their g values, 1.949 and 1.96, respectively.

In conclusion, extended ESR measurements have been applied to measure donor ionization energy of zinc oxide samples in the powder form, and the results support the assumptions developed in theoretical models. The results thus provide at least qualitative support for assigning the $g \sim 1.96$ line predominantly to electrons in the conduction band, except when high donor densities cause near-degeneracy of conduction and donor bands. This interpretation at high donor densities is consistent with the suggestion that more than one type of zinc donor is present. The electrical conductivity parameters, however, apparently are not affected by the degeneracy effect.

Acknowledgment

The author gratefully acknowledges the stimulating discussions on semiconductor properties with Dr. S. R. Morrison.

REFERENCES

1. J. Schneider and A. Rauber, Z. Naturforschung 16A, 713 (1961).

2. R. J. Kokes, J. Phys. Chem. 66, 99 (1962).

3. K. A. Müller and J. Schneider, Phys. Letters 4, 288 (1963).

4. P. H. Kasai, Phys. Rev. 130, 989 (1963).

5. C. H. Geisler and G. L. Simmons, Phys. Letters 11, 111 (1964).

6. R. J. Kokes, 3rd Int'l. Congress on Catalysis, Amsterdam, 1964 (North Holland Publishing Co., Amsterdam), p. 13.

7. R. B. Lal and G. M. Arnett, J. Phys. Soc. Japan 21, 2743 (1966).

8. M. Codell, H. Gisser, J. Weisberg, and R. D. Iyengar, J. Phys. Chem. 72, 2460 (1968).

9. D. Hahn, R. Nink, and D. Severin, Phys. Kondens. Materie 5, 371 (1966).

10. H. Ueda, J. Can. Chem. 46, 891 (1968).

11. M. Setaka, K. M. Sancier, and T. Kwan, J. Catalysis, accepted for publication.

12. A. R. Hutson, Phys. Rev. 108, 222 (1957).

13. K. M. Sancier, J. Catalysis 5, 314 (1966).

14. K. M. Sancier, J. Catalysis 9, 331 (1967).

15. R. L. Kroes, A. P. Kulshreshtha, T. Mookherji, and J. D. Hayes, American Institutes of Aeronautics and Astronautics, San Francisco June (1969), Paper No. 69-639.

16. D. G. Thomas, J. Phys. Chem. Solids 9, 31 (1958).

17. Unpublished results; cf Section D.

Table 1

SUMMARY OF DONOR IONIZATION ENERGIES, E_D(eV) [a]

Sample	$M^*_{1.96}T$	$\frac{n_c^2}{n_D T^{3/2}}$	$T^{5/2}\frac{\Delta\sigma_p}{\Delta T}$	$T^{5/2}\frac{\Delta\sigma_{cc}}{\Delta T}$
ZnO	0.011	0.016	0.041	0.038
ZnO-ZrO_2	0.012	-	0.049	-
ZnO:In	Nil	-	0.042	0.033

(a) For ZnO calculated from the curves in Figs. 2 and 3.

FIGURE CAPTIONS

Figure 1 Temperature dependence of the ESR parameter $M^{*}_{1.96}T$ and and the electrical conductivity parameters $1/I_p$ and I_{cc} for ZnO. The I_{cc} data were obtained in a separate experiment.

Figure 2 Plot of the functions log $(n_c^2/n_D T^{3/2})$ and log $M^{*}_{1.96}T$ against reciprocal temperature for ZnO.

Figure 3 Plot of the function log $(T^{5/2}\Delta\sigma/\Delta T)$ against reciprocal temperature for ZnO. The notations σ_p and σ_{cc} refer to the electrical conductivity parameters $1/I_p$ and I_{cc}, respectively.

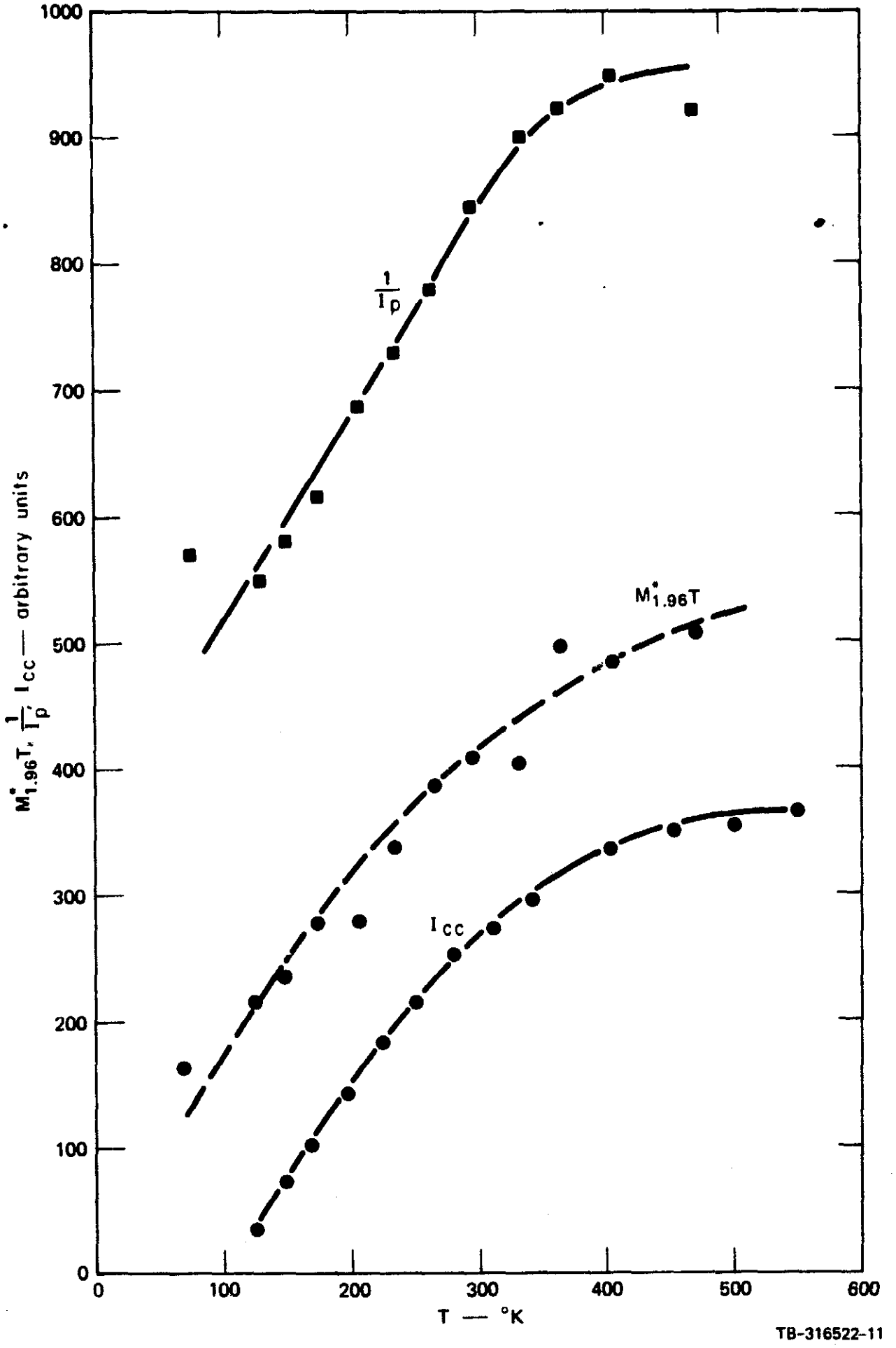

FIGURE 1 TEMPERATURE DEPENDENCE OF THE ESR PARAMETER $M^*_{1.96}T$ AND THE ELECTRICAL CONDUCTIVITY PARAMETERS $1/I_p$ AND I_{cc} FOR ZnO. The I_{cc} DATA WERE OBTAINED IN A SEPARATE EXPERIMENT.

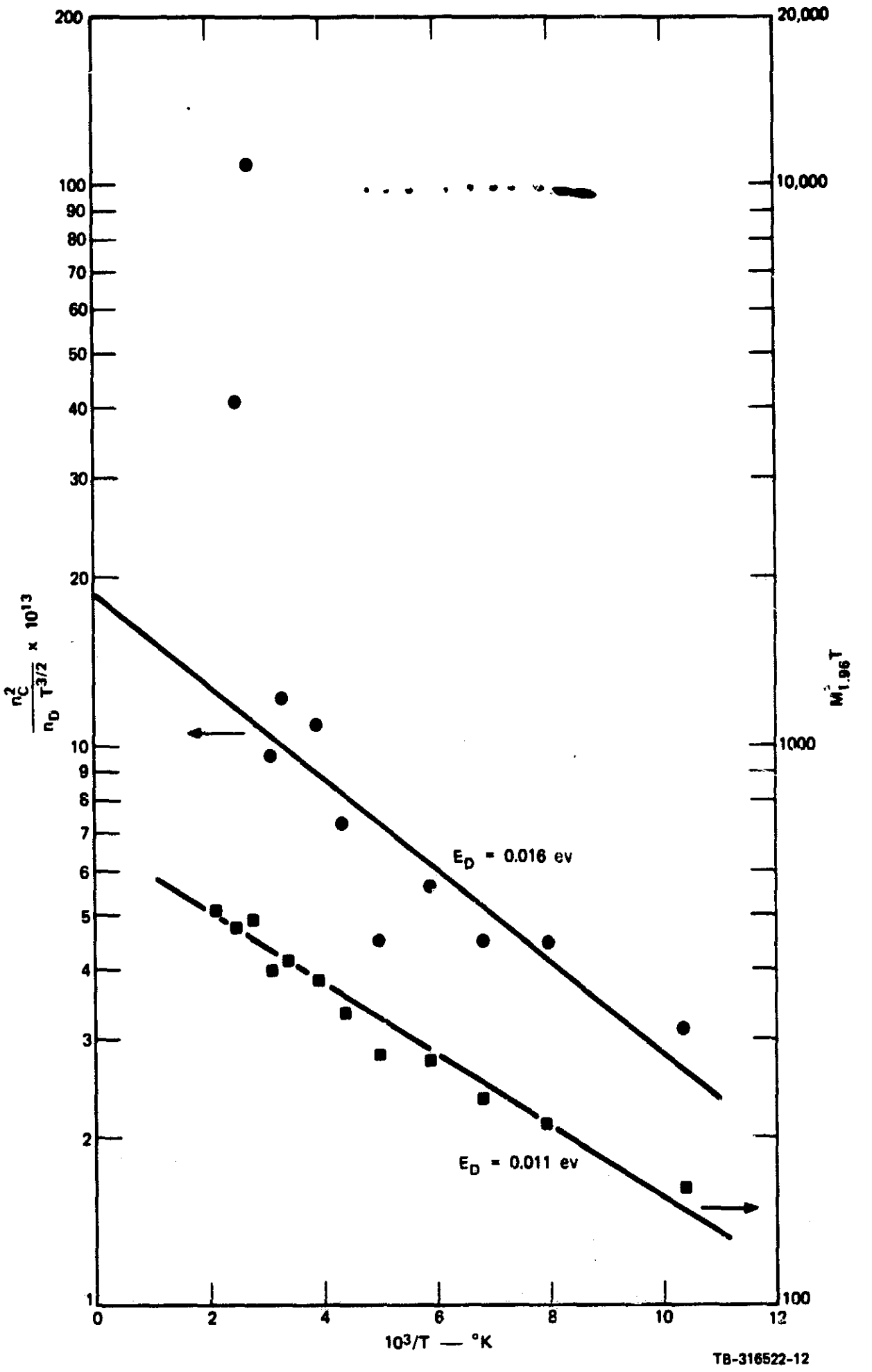

FIGURE 2 PLOT OF THE FUNCTIONS LOG $(n_c^2/n_D T^{3/2})$ AND LOG $M^*_{1.96}T$ AGAINST RECIPROCAL TEMPERATURE FOR ZnO.

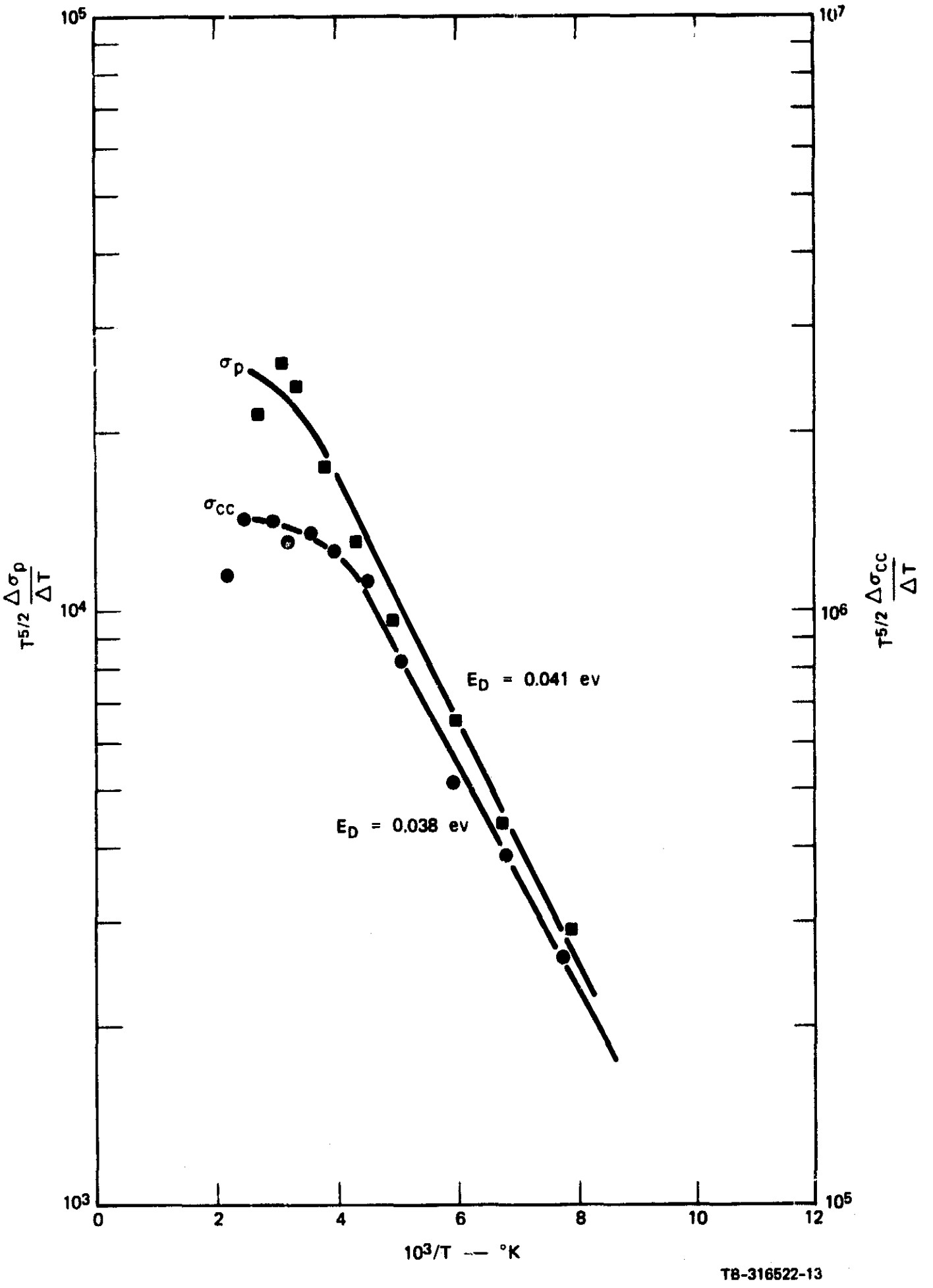

FIGURE 3 PLOT OF THE FUNCTION LOG ($T^5/^2\Delta\sigma/\Delta T$) AGAINST RECIPROCAL TEMPERATURE FOR ZnO. The notations σ_p and σ_{cc} refer to the electrical conductivity parameters $1/I_p$ and I_{cc}, respectively.

SECTION F

SELECTION OF ADDITIVES FOR MATERIALS OTHER THAN ZnO

Studies of ZrO_2 and La_2O_3 have been made to determine the position of the bottom of the conduction band edge at the surface relative to the standard redox potential series. As described in Interim Report No. 2, and in Section A of this report, measurement of the conduction band edge should permit prediction of chemical species worthy of testing as recombination centers for a given pigment.

The problem has been to develop a suitable test. We have used an electrochemical test that was satisfactory for zinc oxide. If electrons can be injected into the conduction band of the oxide from a solution, we should measure an anodic current due to this electron injection. In the case of zinc oxide, a single crystal electrode was used, and the anodic current measurement was straightforward. In the case of ZrO_2, thin anodic layers of ZrO_2 on Zr were studied. It was assumed that if these layers could be made thin enough, the injected electrons could traverse the thin anodic film to the underlying Zr, the current could then be measured, and the injection monitored. In the case of La_2O_3, thermally grown oxide films on La were studied, but the measurements were erratic because the film was not optimized. Some details of the ZrO_2 system, which was given greater attention, are presented below.

The ZrO_2 film was grown overnight in an 0.1M HNO_3 electrolyte, using a 3-volt source with a 1 meg series resistor. The samples were dried by heating to about 100°C in air, and the area to be used as an electrode was defined by black wax. During the electrochemical test, either a mercury or an aqueous solution was used. Stronger reducing agents (e.g., Na metal) are soluble in the Hg, but a greater selection of one-equivalent reducing agents is available in the aqueous solution.

Initial testing of the oxide film in aqueous solution or Hg with a constant voltage source gave erratic results, showing frequent "breakdown" with the current no longer limited by the ZrO_2 film. This

condition was avoided by use of a constant current source, usually the order of 1 to 1000 na. The potential (with respect to a Pt electrode) was then monitored and showed simple characteristics. With no additive present, the voltage rose rapidly (at any given current) at a rate apparently associated with the charging of the capacitor (Zr/ZrO_2/solution). The voltage was limited to 1.5 volts to prevent electrolytic breakdown.

Different behavior was observed with certain additives present. For example, with Hg as the solvent and sodium as the active reducing agent, it was found that the potential (versus platinum) did not reach 1.5 volts, but saturated at a low value. With ZnO as the electrode, the potential never deviated from zero independent of current, but with ZrO_2 as the electrode, the potential saturated at a few tenths of a volt.

Figure 1 shows for ZrO_2 in Hg the steady state potential V (the "saturated" value) obtained as a function of the current used. Values of V lower than 1.5 volts were obtained, as shown, with the additives Na, In, and Ga. The molar concentrations are indicated.

The results for ZrO_2 and ZnO in Hg are interpreted as follows: with the additives present, the electrochemical potential of electrons in the Hg solution was raised above the conduction band edge of the semiconductors. With ZnO, the additives lead to electron injection, and as no negative space charge could develop (no electron traps), the potential went to zero. With ZrO_2 trapping of the injected electrons occurs and a double layer forms causing a measured voltage. However, current will be able to flow at a sufficiently high potential, as the activation energy for current flow in this case is voltage sensitive. Thus the potential across the double layer will rise until the current flow equals the permitted current of the source, and the potential will saturate.

It was thus concluded that all three of these reducing agents inject into ZrO_2. However, a detailed interpretation of the current-voltage characteristics awaits further studies and may in any case be

very complex.

As these results suggested that the conduction band edge may be at a redox potential comparable to or below ZnO, the ZrO_2 was studied with an aqueous electrolyte. The motivation was that the interpretation should be much simplified using the one-equivalent ions available in aqueous solution. Erratic results were obtained, but the bulk of evidence suggests that, contrary to expectations, there is no electron injection into ZrO_2 by any species studied (CrII, FeII, IrIII, CeIII) when added to the aqueous solution.

It is possible that further studies using the Hg system would provide information interpretable in terms of the conduction band energy of ZrO_2 and other pigments, but it appears that trapping effects will complicate the approach, leading to irreproducibility and insensitivity. Other approaches are available and appear preferable.

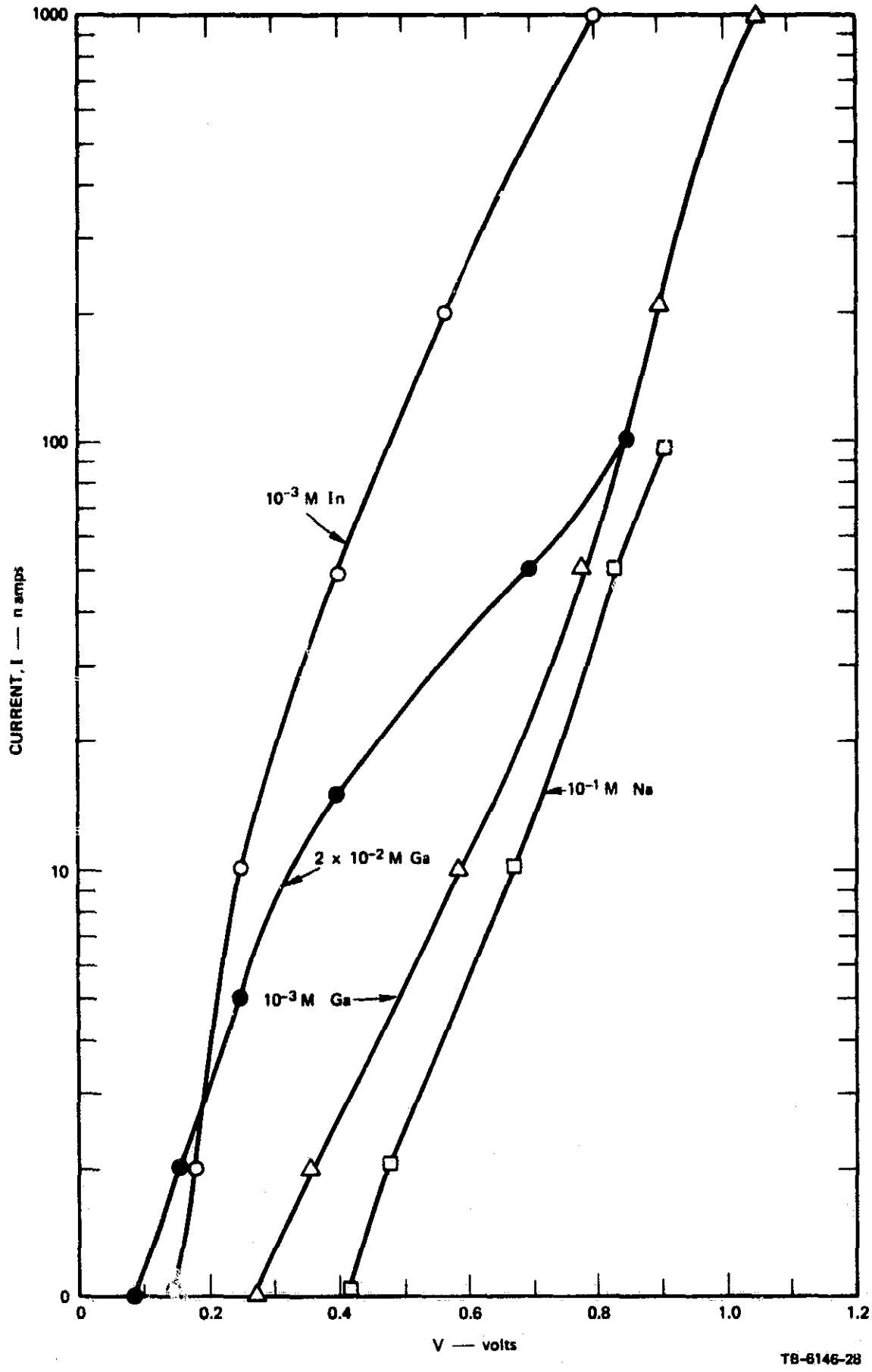

FIGURE 1 POTENTIAL (VS PT) OF A Zr/ZrO_2 ELECTRODE AT VARIOUS VALUES OF ANODIC CURRENT